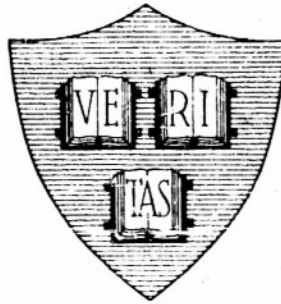


AD No. 27101
ASTIA FILE COPY

Office of Naval Research

Contract N50RI-76 • Task Order No.1 • NR-078-011

THE COLLINEAR ANTENNA ARRAY
THEORY AND MEASUREMENTS



By

Howard W. Andrews

July 15, 1953

Technical Report No. 178

Craft Laboratory
Harvard University
Cambridge, Massachusetts

Office of Naval Research

Contract N50ri-76

Task Order No. 1

NR-078-011

Technical Report

on

The Collinear Antenna Array:

Theory and Measurements

by

Howard W. Andrews

July 15, 1953

The research reported in this document was made possible through support extended Cruft Laboratory, Harvard University, jointly by the Navy Department (Office of Naval Research), the Signal Corps of the U. S. Army, and the U. S. Air Force, under ONR Contract N50ri-76, T. O. I and 28.

Technical Report No. 178

Cruft Laboratory

Harvard University

Cambridge, Massachusetts

TABLE OF CONTENTS

	Page
LIST OF FIGURES	ii
ABSTRACT	1
I. INTRODUCTION	
II. A THEORY OF THE ARRAY	
1. The Array as the Superposition of Two Separate Dipoles	7
2. The Stationary Expression for the Impedance	10
3. The Trial Current Distribution	16
4. Evaluation of the Impedance and the Current Distribution	17
5. The Single-Driven Dipole	22
III. METHOD OF IMPEDANCE MEASUREMENTS AND AUXILLIARY MEASUREMENTS	
1. Line Theory	25
2. Computation of Impedances	28
3. General Check on System using Half-Dipole Impedance Measurements	29
4. Comparison of Probes	29
5. Measurement of Gap Capacitance	30
IV. EXPERIMENTAL DATA AND COMPUTATIONS	
1. Extent of Parameter Variation	31
2. Measured Impedance Data	32
3. Computational Procedure	32
4. Conclusions	35
5. A Two-Wire Line as a Coupling Reactance between Elements	36
Appendix A: Evaluation of the Integrals	37

The Collinear Antenna Array:

Theory and Measurements

by

Howard W. Andrews

Craft Laboratory, Harvard University

Cambridge, Massachusetts

Abstract

The antenna array considered herein is an arrangement of a simple driven dipole and two parasitic elements with axes collinear to that of the driven element. A theoretical solution to the problem is obtained by considering the air gap between the elements to be a simple lumped capacitance of a size depending upon the spacing between the elements. In this way the array is considered to be a reactively-loaded center-driven dipole of overall length equal to the total length of the array. The reactances are replaced by equivalent generators and then, through superposition, the array is separated into the sum of two dipoles, one driven at its center and the other by two off-center generators.

The current distribution and the driving point impedance are computed for a variety of length as a function of the gap spacing. Measurements are given to check the validity of the theory and its range of practical application.

I

INTRODUCTION

The collinear antenna array is an arrangement of driven and parasitic elements all of whose axes are located on the same straight line. The parameters needed to describe the array are the number and spacing of the elements, their diameters and lengths, and the nature of the driving voltages. The coupling between the elements may be the free-space coupling, a lumped reactance, or a two-wire line. It is, of course, necessary to limit the parameters to be varied since, even in the simplest case of a three-element array, there are about twelve such variables. The use of an image screen reduces

the variable parameters considerably since the array must then be symmetrical. The configuration actually discussed here is a three element array with a slice generator in the center element at the plane of symmetry of the array. The elements are all of the same radius. The parameters to be varied are the lengths of the central and outer elements and the air-gap spacing between them. The quantities measured in the array are the current distribution and the driving-point impedance as a function of the three variable parameters.

This array has been previously investigated by a number of people.¹⁻⁴ Carter¹ in 1932 included it in a paper considering the impedance characteristics of several types of pairs of linear radiators. He determined the self and mutual impedances after assuming a sinusoidal current distribution on radiators of length equal to multiples of half-wavelengths. The expressions consisted of sums of sine and cosine integrals and natural logarithms. The computed results were fairly good since he had restricted himself to arrays in which the even current distributions were resonant.

Harrison² in 1945 considered an array of two identical elements driven by identical slice generators at their centers. This is the configuration that results from a vertically polarized dipole erected over a conducting earth. His procedure was entirely different from that of Carter's in that an expression is derived in which the current is the unknown quantity satisfying an integral equation; that is, the current distribution is defined implicitly by the expression and must be obtained from it. The mathematical technique used is that of Hallén⁵ for solving a similar integral equation for the current on a simple dipole. The integral equation is obtained by first writing the trigonometric solution of the simple differential equation for the vector potential on the antenna surface. The vector potential is also available in the form of the Helmholtz integral of the current distribution on the antenna. Equating this integral to the solutions of the differential equation results in an integral equation for the current. Two of these are obtained, one on each half of one of the identical elements. Hallén's method of successive approximations is then used to arrive at an expression for the current distribution for both symmetrical and antisymmetrical driving generators. The two integral equations are not immediately solvable. The boundary conditions are introduced as well as some assumptions and approximations concerning the current.

Finally explicit expressions for the currents are obtained in the form of a complicated infinite series. The computation of this series would be difficult and Harrison in the same paper presented a more approximate, but more tractable, procedure for handling the integral equation. He assumed some additional symmetries in the current distributions that led to computationally more convenient results.

R. W. P. King³ in 1950 chose to consider the three element case with only the center element driven on the basis that this array, symmetrical about the generator, is the only practically useful arrangement. His procedure was similar to Hallén's in that solutions to differential equations for the vector potential were equated to integrals of the current. A series of assumptions was then made concerning the current distribution among which was neglecting the charging current at the ends of the elements. Considerable use was made of the fact that the vector potential at a point is primarily determined by the current in the immediate vicinity of that point. The distribution on the center element was obtained by driving the outer elements so that the currents at the centers of all elements were the same; this was done for symmetrical and antisymmetrical currents. The distribution on the outer elements was obtained by considering even and odd distributions as well as symmetrical and antisymmetrical currents. With these various conditions, a series solution to the integral equation was obtained using successive approximations. From this followed expressions for the self- and mutual impedances of the various elements.

The major limitations in this theory are two. The first is that the effect of chargeable end surfaces is not considered; that is, the model best representing the theory is one that has ends upon which no charge may accumulate and has, as chargeable areas, only the longitudinal surfaces of the conductor. The second limitation is that no large odd currents should exist in the parasite; that is the parasite should not be of such length that odd currents are resonant.

At the beginning of the present study a series of preliminary measurements were taken to check the impedances computed by King. The driving point impedance of several combinations of length was measured as a function of the spacing between the elements. The spacing was varied between zero--

that is, actual contact between the elements -- and a large fraction of a wavelength. For this case of contact between the elements, or of zero gap distance, the array degenerates into a simple center driven dipole of length equal to that of the array. At the other end point of infinite spacing the array is only the driven element by itself. The plot of the driving-point impedance is often an arc of a circle between these two points. It may also be a spiral.

It was immediately noticed that the driving-point impedance changed very rapidly with gap spacing, in fact the complete variation in impedance often took place in less than $1/100$ of a wavelength and always in less than $1/10$ of a wavelength. The most rapid, and also the greatest, change occurs when the gap is at a high current point for the dipole that results when the elements are in actual contact. The action of the gap is to reduce very rapidly this current at the gap position to a comparatively low value. This large change with gap size of the magnitude of the current at this point is reflected as a correspondingly rapid change in the driving-point impedance as well as a similarly rapid change in the magnitude and shape of the current distribution. A comparatively slow and small change in the driving-point impedance occurs when the gap is at a low current point of the dipole resulting from direct contact of the elements. Then the current is already comparatively small and reducing it to zero does not have a profound effect on the driving-point impedance or on the current distribution. For this case, that is a minimum in the current distribution at the gap point, a spacing of as much as $1/10$ of a wavelength is necessary for a complete variation in the driving-point impedance.

A comparison of these experimental results with the zero-order case computed by King is plotted in Fig. 18. It may be noted that the shapes of the curves are essentially similar over the sections for the larger spacings. The displacement of the curves is no doubt due to the fact that only the zeroth-order computation has been carried out. The agreement and trend is quite poor for the small (less than $1/20\lambda$) spacings. This disagreement is probably due to the presence, in the physically existing array, of end surface upon which charge may accumulate in addition to the chargeable cylindrical surfaces of the antenna elements. The existence of such end conditions is not considered in the quasi-one-dimensional theory which determines the surface effects using a line current distribution at the center of the antenna cylinders and considers

only the coupling between the cylindrical surfaces. For small spacings in the actual array, the chargeable end areas are sufficiently close that there is an appreciable capacitive coupling between them as well as between the cylindrical surfaces. Hence such a configuration requires that in addition to the coupling between the cylindrical surfaces adequately treated by King, there be further introduced the effects due to the end coupling.

The above two effects, namely, the very rapid variation of driving-point impedance with spacing and the poor agreement of the King theory for small spacing, supposedly due to end capacitance, leads to the thought that a theory for the collinear array should include capacitive effects in the region of the gaps as an essential part of its character. For close spacings the gap is actually so small that the end coupling not included in the King theory could be well approximated by an additional near-zone lumped capacitance. This would then permit the charging current of the lumped capacitance to be treated as a displacement current across the gap. It would attempt to explain the poor agreement for small spacing as being due to neglecting the end capacitances.

With the premise that the gap is a simple lumped capacitance, the collinear array then becomes a simple dipole with a capacitance of variable size in series with its current at the appropriate point. The half length of the dipole is equal to the overall length of the array; the points of insertion of the lumped capacitance are at the positions of the gaps in the array. This configuration will be assumed to represent completely the collinear array. See Fig. 1 for this and the following succession of events.

The use of a capacitance in the array introduces the possibility of using the compensation theorem of network theory. This states that an impedance in which a current I is flowing may be replaced by a constant-voltage generator with an external potential difference equal to $-IZ$ without changing the current conditions in the network. Performing such a substitution as this causes the array to become a triply driven dipole. The generator at its plane of symmetry still exists and there are, in addition, two generators to replace the two gap capacitances. The array is otherwise a continuous dipole and the problem could be solved as such. The generators would be introduced as the energy producing boundary conditions on the scalar

potential in an approach similar to Hallén's iteration technique or as done by Storer using a variational principle. The linearity of Maxwell's equations, however, allows the use of the superposition theorem and poses the possibility of solving the problem by using at one time only those of the three generators that are found to be convenient. The results are then superimposed to give the final results.

The choice of solutions found to be most convenient is to break the triply driven dipole into two symmetrical arrangements. One of these is the doubly driven one of Fig. 2, in which the dipole is excited by two identical generators equidistant from the center. The other is the classic singly driven case with a slice generator at the dipole center. The first of these has been considered by Taylor⁶ in an extension of Storer's⁷ variational technique and by King⁶ using the iteration of an integral equation. The singly driven case is a degenerate form of the other and is obtained when the spacing between the two generators becomes zero. It has been considered by Taylor⁶ and Storer⁷ in a variational approach, and King and others using various techniques. The approach used in this thesis will be that of the variational principle in which the driving-point impedance is an extremized function of the parameters of a trial current distribution. Having the two solutions, they will be combined in such phase and amplitude that the doubly driving generators will appear to be a capacitive reactance of the proper magnitude.

In conclusion, the purpose of this research is to develop a theory of the collinear array based on the series loading of a simple dipole by lumped capacitances. Computations will be then made of the results and measurements taken to verify them. The use of a two-wire line as a coupling between driver and parasite will be investigated experimentally. This coupling is not simply represented by a lumped reactance and its corresponding voltage generator, but rather, because of its ability to support an unbalanced mode, a current generator is also required.

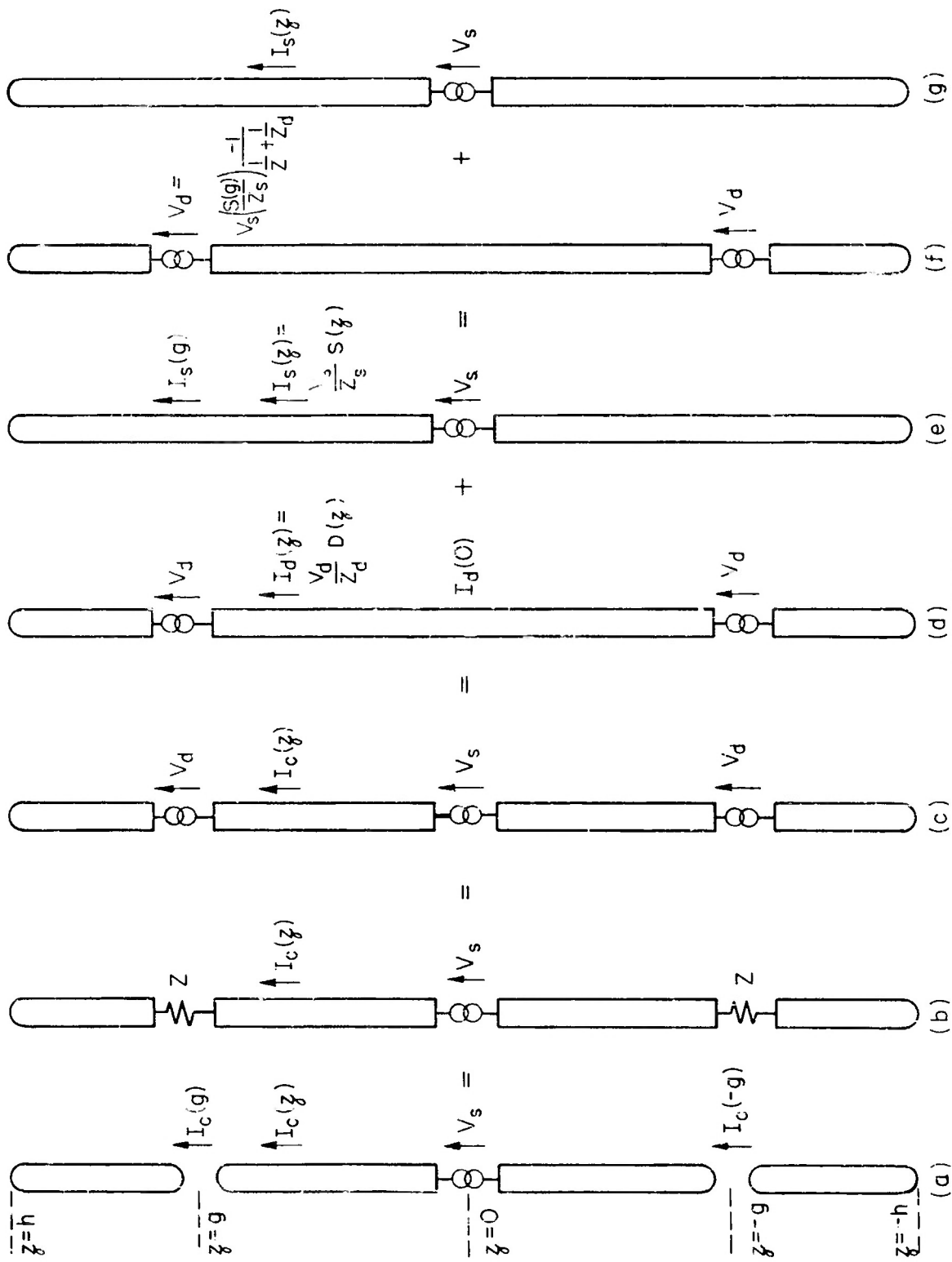


FIG. 1 THE COLLINEAR ARRAY AS THE SUPERPOSITION OF A DOUBLY DRIVEN DIPOLE AND A SINGLY DRIVEN DIPOLE

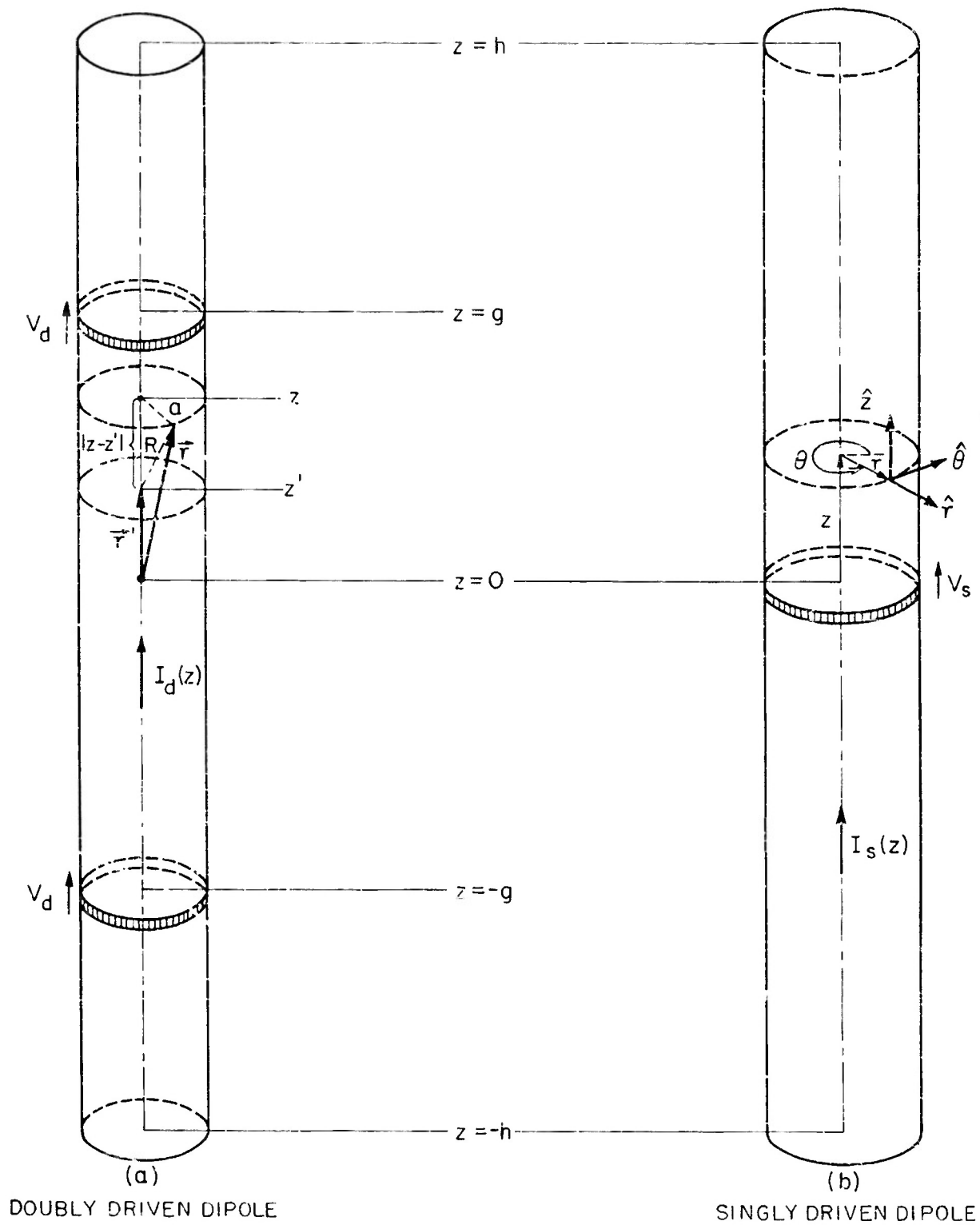


FIG. 2 MATHEMATICAL MODELS FOR DIPOLES

Chapter II

A THEORY OF THE ARRAY

1. The Array as the Superposition of Two Separate Dipoles

The closely spaced three-element collinear array will now be investigated on the basis that it is well approximated by a cylindrical dipole series loaded by a purely reactive impedance. The reactance will be that associated with the capacitive coupling between the ends of the driven and parasitic elements. The reasons for considering this approach have been presented in the previous chapter. Only the center element will be driven and the spacing between the center element and the two parasites will be the same.

It will first be necessary to discuss in more detail the transition from the array itself to its representation as the superposition of a doubly and a singly driven dipole. The series of steps are shown graphically in Fig. 1. In Fig. 1a is the array itself. From this follows (Fig. 1b) the use of a lumped capacitance as the complete gap effect, then the substitution of an equivalent generator for the lumped capacitance, next the separation (Fig. 1d and Fig. 1e) into the two dipoles, and finally (Figs. 1f and 1g) the phasing and amplitude adjustment of the generators so that the desired equivalence is obtained.

The voltage generator substituted for the reactance has a potential V_d equal to $-IZ$ where I is the current in the impedance Z and V_d is the potential rise of the generator in the direction of the current flow. The separation of the triply driven dipole into one that is singly driven and another that is doubly driven is possible because of the linearity of the applicable field equations.

Now consider the phasing and amplitude adjustment of the doubly-driving generators so that they will, when superimposed with the singly driving generator, be ninety degrees out of phase with the total current through them. The symbolism will follow that used in Fig. 1. $I_c(z)$ is the total current on the collinear array; its value at the gap position $z = \pm g$ is $I_c(\pm g)$ and, as is true of all currents used here, $I_c(-z) = I_c(z)$. The current distribution on the simple dipole of height h due to the single generator V_s at its center (Fig. 1e) is $I_s(z)$; its value at the gap is $I_s(\pm g)$. The current distribution on the dipole

of height h due to the doubly-driving off-center generators V_d (Fig. 1d) at $z = \pm g$ is $I_d(z)$; its value at the center is $I_d(0)$.

It will be found useful later to use current distributions that have been normalized to a unity driving current at the generator. For such a unity current at the center of the singly driven dipole, $S(z)$ is the resulting current distribution. Then $S(0) = 1$ and

$$I_s(z) = \frac{V_s}{Z_s} S(z) \quad (2-1)$$

where Z_s is the driving-point impedance for the center slice generator by itself. Similarly for the off-center generator of Fig. 1d the normalized current distribution is denoted by $D(z)$; then $D(\pm g) = 1$ and

$$I_d(z) = \frac{V_d}{Z_d} D(z)$$

where Z_d is the driving-point impedance presented to the off-center generators. The desired phase and amplitude relation at $z = \pm g$ when the two are superimposed is

$$-I_c(\pm g)Z = V_d$$

or

$$I_c(\pm g) = -V_d/Z \quad (2-2)$$

where Z is the impedance placed in series with the current on the loaded dipole and, in this problem, will be the apparent reactance of the gap. At the gap position (the + and - signs will be omitted from this point on)

$$I_c(g) = I_d(g) + I_s(g)$$

$$I_s(g) = I_c(g) - I_d(g)$$

Substituting (2-1) and (2-2) above

$$\begin{aligned} V_s \frac{S(g)}{Z_s} &= -\frac{V_d}{Z} - \frac{V_d}{Z_d} \\ &= V_d \left(-\frac{1}{Z} - \frac{1}{Z_d} \right) \end{aligned}$$

Solving for V_d

$$V_d = V_s \left(\frac{S(g)}{Z_s} \right) \left(\frac{-1}{\frac{1}{Z} + \frac{1}{Z_d}} \right)$$

and for a unity driving voltage V_s

$$V_d = \frac{S(g)}{Z_s} \frac{-1}{\frac{1}{Z} + \frac{1}{Z_d}}$$

Now with this value of V_d the total current $I_c(z)$ at any point on the array is

$$\begin{aligned} I_c(z) &= I_s(z) + I_d(z) \\ &= I_s(0)S(z) + I_d(g)D(z) \\ &= \frac{V_s}{Z_s} S(z) + \frac{V_d}{Z_d} D(z) \\ &= \frac{V_s}{Z_s} S(z) + \frac{V_s}{Z_d} D(z) \frac{S(g)}{Z_s} \left(\frac{-1}{\frac{1}{Z} + \frac{1}{Z_d}} \right) \end{aligned}$$

$$I_c(z) = \frac{V_s}{Z_s} \left[S(z) - \frac{D(z)S(g)}{1 + Z_d/Z} \right]$$

for $V_s = 1/0^0$

$$I_c(z) = \frac{1}{Z_s} \left[S(z) - \frac{D(z)S(g)}{1 + Z_d/Z} \right] \quad (2-3)$$

The driving-point impedance is the reciprocal of this evaluated at the driving point of $z = 0$, thus

$$\begin{aligned} Z_c &= \frac{1}{I_c(z=0)} \\ &= Z_s \left/ \left[S(0) - \frac{D(0)S(g)}{1 + Z_d/Z} \right] \right. \end{aligned}$$

But $S(0) = 1$ so that

$$Z_c = Z_s \left/ \left[1 - \frac{D(0)S(g)}{1 + Z_d/Z} \right] \right. \quad (2-4)$$

There remains now the evaluation of the current distribution $D(z)$ on a dipole of height h driven by identical voltage slice generators at $z = \pm g$ such that unity current flows in them. The arrangement of the single slice generator at the center will be obtained by setting g equal to 0. The above algebra will be used to superimpose the two currents in order to obtain the total current distribution and the driving-point impedance of the array.

2. The Stationary Expression for the Impedance

The technique to be used to determine the driving-point impedance and the current distribution will employ a variational principle⁶ for the impedance. From this will be obtained the current distribution by means of the Ritz method applied to the stationary integral.

In general, the variational method depends upon obtaining a functional expression for the driving-point impedance. This functional expression of a trial current distribution is so formulated that its value, the impedance, is stationary with respect to small deviations of the trial current from the true current distribution. The dependence of the impedance on the trial current is, in fact, only of second-order; that is, errors in the impedance vary as the square of errors in the assumed current distribution. This can be shown by introducing into the expression for the impedance a small deviation δI in the current distribution. It is found that the coefficient of the resulting error δZ in the impedance is zero but that the coefficient of $(\delta Z)^2$ is not. Alternatively, the Euler-Lagrange equations for the expression could be evaluated and it would be found that they would be satisfied by known expressions containing the Helmholtz integral for the vector potential and the definition of the impedance.

Once a stationary expression for the impedance has been found, a trial current distribution containing a number of parameters is substituted into it. Since the expression for Z is stationary, the Ritz method for evaluating the parameters may be used to obtain an expression for the current.

Throughout the following discussion all instantaneous electromagnetic quantities that vary in time are understood to be the real parts of complex quantities; for example, H is the real part of $\bar{H}e^{j\omega t}$. The time dependence $e^{j\omega t}$ and the superscript bar denoting a complex quantity are omitted throughout.

To obtain the physically existing quantity corresponding to any equation or expression, multiply through by $e^{j\omega t}$ and take the real part of the result. Rationalized MKS units will be used throughout this discussion.

The mathematical model to be considered is that drawn in Fig. 2a. The antenna is assumed to possess infinite conductivity and to have only currents in the z direction. This treatment will assume no currents on the end caps; this condition arises from the approximate one-dimensional manner in which the vector potential is calculated on the longitudinal surfaces of the antenna. Such an approach is justified since the experimental realization is an antenna of identical axial length but with hemispherical end caps of the same total chargeable area as the corresponding region of the mathematical model. In the experimental model, as in the mathematical one, the currents at $z = \pm h$ are zero. If the desired boundary condition is approximated experimentally in this way, the effective height can differ from h by, at most, a distance of the order of the conductor radius and probably only by something much less than this.

The boundary conditions resulting from the application of Maxwell's equations to the surface between a perfect conductor and free space are

$$\hat{n} \times \vec{H} = -\vec{\ell} \quad (2-5)$$

$$\hat{n} \times \vec{E} = 0 \quad (2-6)$$

The first equation (25) with $\hat{n} = -\hat{r}$ for the free space region gives

$$H_{\theta} = \ell_z(a, z)$$

where $\ell_z(a, z)$ is the surface current density in the \hat{z} direction. Note that

$$\begin{aligned} \hat{z} I_d(z) &= \int_0^a \int_0^{2\pi} \hat{z} \ell_z(r, \theta, z) r dr d\theta \\ &= \hat{z} 2\pi a \ell_z(a, z) \end{aligned} \quad (2-7)$$

and hence

$$I_d(z) = 2\pi a H_{\theta}(a, z) \quad -h \leq z \leq h$$

The second boundary condition (2-6) yields

$$E_z(a, z) = E_{\theta}(a, z) = 0 \quad (2-8)$$

Equation (2-8) does not hold at the slice generators assumed to drive the antenna. At these points there are discontinuities in the slope of the scalar potentials. These slopes will be assumed to give a delta-function discontinuity in the electric field such that in the limit of a discontinuity of infinitesimal thickness

$$\int_{g-\epsilon}^{g+\epsilon} E_z(a,z) dz = \int_{-g-\epsilon}^{-g+\epsilon} E_z(a,z) dz = -V_d \quad (2-9)$$

Let the following integral definition of the delta function, which is zero everywhere except at $z = g$ and there takes on a value such that

$$\int_{g-}^{g+} f(z) \delta(z-g) dz = f(g) \quad , \quad (2-10)$$

be introduced. Then

$$E_z(a,z) = -V_d \delta(z \pm g) \quad -h \leq z \leq h \quad (2-11)$$

Note that (2-9) has $E_z(a,z) = 0$ along the conductor as it should and has localized the generator at slices at $z = \pm g$.

The free-space equation for the electric field in terms of the scalar and vector potential is

$$\vec{E} = -\frac{\partial \vec{A}}{\partial t} - \nabla \cdot \phi \quad (2-12)$$

Using a periodic time dependence and considering only the \hat{z} -component of \vec{E} at a distance from the axis equal to the radius a of the conductor (2-12) becomes

$$E_z(a,z) = -j\omega A_z(a,z) - \frac{\partial \phi(a,z)}{\partial z} \quad (2-13)$$

The vector potential \vec{A} is defined by

$$\nabla \times \vec{A} = \vec{B}$$

the Lorentz condition

$$\nabla \cdot \vec{A} + \frac{j\omega}{c} \phi = 0 \quad (2-14)$$

and the Helmholtz integral

$$\vec{A}(a, \theta, z) = \frac{\mu}{4\pi} \int_{-h}^h \int_0^{2\pi} \vec{\ell}_z(a, \theta', z') \frac{e^{-j\beta|\vec{r}-\vec{r}'|}}{|\vec{r}-\vec{r}'|} a d\theta' dz', \quad (2-15)$$

where

$$|\vec{r}-\vec{r}'| = \sqrt{(z-z')^2 + r^2 + a^2 - 2ra \cos(\theta - \theta')},$$

$$\vec{\ell}_z(a, \theta', z') = \hat{z} \ell_z(a, \theta', z').$$

For the case considered here, where the antenna is cylindrically symmetrical and of sufficiently small radius that $\beta a \ll 1$, it has been shown¹²⁻¹⁴ that a good approximation for \vec{A} , even at the radius a and z near to z' , is obtained by assuming all of the current to be located at the axis of the conductor. Then, using (2-7), \vec{A} at the radius a is

$$\begin{aligned} \vec{A}(a, z) &= \hat{z} \frac{\mu}{4\pi} \int_{-h}^h I_d(z') \frac{e^{-j\beta R}}{R} dz' & (2-16) \\ &= \hat{z} \frac{\mu}{4\pi} \int_{-h}^h I_d(z') K(z, z') dz' \end{aligned}$$

where

$$R = \sqrt{(z-z')^2 + a^2}$$

$$K(z, z') = e^{-j\beta R} / R.$$

Note what has taken place in this last step. In (2-15) the vector potential was defined exactly as the integral over a tube of current on the antenna surface. In (2-16) this was replaced by an approximation using a one-dimensional current at the center as has been shown reasonable by King and Oseen. As a result, the electric field (which is given by (2-18) and (2-19) below) is precisely that at a radius a due to a current at $r = 0$.

Since \vec{A} has only a \hat{z} component (as seen from the integral) then

$$\nabla \cdot \vec{A}(a, z) = \frac{\partial A_z(a, z)}{\partial z}$$

Substituting this in the Lorentz condition (2-14) gives

$$\frac{\partial A_z(a, z)}{\partial z} + \frac{j\omega}{c} \phi(a, z) = 0$$

and hence,

$$\frac{\partial \phi(a, z)}{\partial z} = -\frac{j\omega}{c} \frac{\partial^2 A_z(a, z)}{\partial z^2}$$

Then (2-12) for the electric field at the radius a becomes

$$E_z(a, z) = -j\omega A_z(a, z) - \frac{j\omega}{\beta^2} \frac{\partial^2 A_z(a, z)}{\partial z^2} \quad (2-17)$$

where $\beta = \omega/c$. Rearranging (2-17) leads to

$$E_z(a, z) = \left(\frac{-j\omega}{\beta^2} \left(\frac{\partial^2}{\partial z^2} + \beta^2 \right) A_z(a, z) \right) \quad (2-18)$$

$$= L(z) A_z(a, z) \quad (2-19)$$

By equating (2-19) for the electric field at a distance a from the one dimensional current $I_d(z)$ and (2-11) for the field on the surface of a perfect conductor, there is obtained

$$-V_d \delta(z \pm g) = L(z) A_z(a, z) \quad (2-20)$$

Multiplying (2-20) through by $I_d(z)$ and integrating from $-h$ to h gives an equality relating the complex power supplied by the generator to the complex power radiated by the current $I_d(z)$ as evaluated at $r = a$.

$$-\int_{-h}^h I_d(z) V_d \delta(z \pm g) dz = \int_{-h}^h I_d(z) L(z) A_z(a, z) dz$$

Performing the integration on the left using (2-10) and substituting (2-16) on the right gives

$$-I_d(-g) V_d - I_d(g) V_d = \frac{\mu}{4\pi} \int_{-h}^h dz I_d(z) L(z) \int_{-h}^h I_d(z') K(z, z') dz' \quad (2-21)$$

Substituting the definition of the impedance,

$$V_d = I_d(\pm g)Z_d ,$$

into (2-21) and making use of the symmetry of the current, $I_z(-g) = I_z(g)$, leads to

$$- 2I_z^2(g)Z_d = \frac{\mu}{4\pi} \int_{-h}^h dz I_d(z)L(z) \int_{-h}^h I_d(z')K(z,z')dz' \quad (2-22)$$

The presence of a minus sign on the left locates the power source in the generator; the right side is the power radiated. The solution of (2-22) for Z_d is

$$Z_d = - \frac{\mu}{8\pi I_d^2(g)} \int_{-h}^h dz I_d(z)L(z) \int_{-h}^h I_d(z')K(z,z')dz' \quad (2-23)$$

This expression for Z_d is stationary; that is, small deviations of the values of $I_d(z)$ from the true value will result in only second-order variations in Z_d . This can be shown by obtaining the first variation δZ_d of Z_d due to a small variation δI in $I_d(z)$. The value of δZ_d is found to be zero.

The expression (2-23) can be simplified using the symmetry of $I_d(z)$ and $L(z)A_z(a,z)$. Using these properties (2-23) becomes

$$Z_d = - \frac{\mu}{4\pi I_d^2(g)} \int_0^h dz I_d(z)L(z) \int_{-h}^h I_d(z')K(z,z')dz' \quad (2-24)$$

In (2-24) $L(z)$ operates on the kernel of the integral. Since

$$\frac{\partial^2}{\partial z^2} K(z,z') = \frac{\partial^2}{\partial z'^2} K(z,z') ,$$

$$I_d(h) = 0 = I_d(-h) ,$$

and $I_d(z)$ and $L(z)I_d(z)$ are even functions about $z = 0$, it is possible to simplify the $L(z)A(z)$ part of (2-24). The result is

$$Z_d = -\frac{\mu}{4\pi I_d^2(g)} \left[\int_0^h dz I_d(z) \int_0^h [K(z, z') + K(z, -z')] L(z') I_d(z') dz' \right. \\ \left. + \frac{j\omega}{\beta^2} \left(\frac{dI_d(z)}{dz} \right)_{z=h} \int_0^h I_d(z) [K(z, h) + K(z, -h)] dz \right] \quad (2-25)$$

3. The Trial Current Distribution

The selection of a trial function to be used in (2-25) is governed as much by the necessity of obtaining results in terms of tabulated functions as by employing an excellent approximation to the current distribution. With a kernel of the type occurring in (2-25), trial functions including $\sin \beta z$, $\cos \beta z$, $z \sin \beta z$, $z \cos \beta z$ and constants yield the tabulated generalized sine and cosine integrals. The distribution is known to be continuous, even about $z = 0$, zero at $\pm h$, and to have a discontinuous slope at $z = \pm g$. All of these conditions should be approximated as closely as possible. Storer⁷ found that a combination of $\sin \beta z$, $\cos \beta z$, and a constant quite accurately represented the simple dipole current. Such functions should also be suitable for section of the antenna defined by $|z| \geq g$. A constant and $\cos \beta z$ should be satisfactory for $|z| \leq g$. With these conditions in mind suitable trial currents are

$$I_d(z) = C_1 + C_2 \cos \beta z \quad |z| \leq g$$

$$I_d(z) = D_1 \sin \beta(h-z) + D_2 [1 - \cos \beta(h-z)] \quad |z| \geq g$$

where the C's and D's are complex coefficients. Note that Z in (2-23) is independent of the absolute value of the current levels. Hence, let $I_d(\pm g) = 1$. The trial currents then become

$$I_d(z) = 1 + C [1 + \cos \beta z] \quad |z| \leq g \quad (2-26)$$

$$I_d(z) = \delta [1 - \cos \beta(h-z)] + D \left\{ \sin \beta(h-z) + \epsilon [1 - \cos \beta(h-z)] \right\} \quad |z| \geq g \quad (2-27)$$

where

$$a = -\cos \beta g$$

$$\delta = \frac{1}{1 - \cos \beta(h-g)}$$

$$\epsilon = -\frac{\sin \beta(h-g)}{1 - \cos \beta(h-g)}$$

The lengths for which these may be considered reasonable are $\beta g < \pi$ for (2-26) and $\beta(h-g) < 2\pi$ for (2-27). Equation (2-26) with a constant term would be expected to fail for g near a half-wavelength. Equation (2-27) actually has a singularity at $(h-g)$ equal to a wavelength and probably is not too accurate for $(h-g)$ larger than about three-quarters of a wavelength.

4. Evaluation of the Impedance and the Current Distribution

Substituting (2-26) and (2-27) into (2-25) yields⁶

$$Z_d = \frac{j\zeta}{4\pi} [\gamma_o + \gamma_C C + \gamma_D D + \gamma_{CC} C^2 + \gamma_{DD} D^2 + \gamma_{CD} CD] \quad (2-28)$$

where

$$\begin{aligned} \gamma_o &= \frac{1}{[1 - \cos \beta(h-g)]^2} \left\{ [1 + \cos^2 \beta(h-g)] \sin \beta a - \cos^2 \beta(h-g) \sin \beta \sqrt{(2g)^2 + a^2} \right. \\ &\quad - 2 \cos \beta(h-g) [\sin \beta \sqrt{(h-g)^2 + a^2} - \sin \beta \sqrt{(h+g)^2 + a^2}] - \sin \beta \sqrt{(2h)^2 + a^2} \\ &\quad + [2\beta g \cos^2 \beta(h-g) + \sin 2\beta(h-g)] \bar{C}(\beta a, 2\beta g) \\ &\quad + [2\beta(h-g) \cos \beta(h-g) - 2 \sin \beta(h-g)] \bar{C}(\beta a, \beta(h-g)) + 2\beta h \bar{C}(\beta a, 2\beta h) \\ &\quad - [2\beta(h+g) \cos \beta(h-g) + 2 \sin \beta(h-g)] \bar{C}(\beta a, \beta(h+g)) + 2C_s(\beta a, \beta(h-g)) \\ &\quad \left. + \sin 2\beta h [2\bar{C}_c(\beta a, \beta(h+g)) - \bar{C}_c(\beta a, 2\beta h) - \bar{C}_c(\beta a, 2\beta g)] \right\} \end{aligned}$$

$$\begin{aligned}
& - \cos 2\beta h [2C_s(\beta a, \beta(h+g)) - C_s(\beta a, 2\beta h) - C_s(\beta a, 2\beta g)] \\
& - j(\cos^2 \beta(h-g) \cos \beta \sqrt{(2g)^2 + a^2} - [1 + \cos^2 \beta(h-g)] \cos \beta a \\
& + 2 \cos \beta(h-g) [\cos \beta \sqrt{(h-g)^2 + a^2} - \cos \beta \sqrt{(h+g)^2 + a^2}] + \cos \beta \sqrt{(2h)^2 + a^2} \\
& + [2\beta \cos^2 \beta(h-g) + \sin 2\beta(h-g)] S(\beta a, 2\beta g) \\
& + [2\beta(h-g) \cos \beta(h-g) - 2 \sin \beta(h-g) S(\beta a, \beta(h-g)) + 2\beta h S(\beta a, 2\beta h) \\
& - [2\beta(h+g) \cos \beta(h-g) + 2 \sin \beta(h-g)] S(\beta a, \beta(h+g)) + 2S_s(\beta a, \beta(h-g)) \\
& + \sin 2\beta h [2S_c(\beta a, \beta(h+g)) - S_c(\beta a, 2\beta h) - S_c(\beta a, 2\beta g)] \\
& - \cos 2\beta h [2S_s(\beta a, \beta(h+g)) - S_s(\beta a, 2\beta h) - S_s(\beta a, 2\beta g)] \} , \\
Y_C & = \frac{2}{1 - \cos \beta(h-g)} \left\{ \cos \beta g \cos \beta(h-g) [\sin \beta a - \sin \beta \sqrt{(2g)^2 + a^2}] \right. \\
& - \cos \beta g [\sin \beta \sqrt{(h-g)^2 + a^2} - \sin \beta \sqrt{(h+g)^2 + a^2}] \\
& + [2\beta g \cos \beta g \cos \beta(h-g) + \sin \beta (h-2g)] \bar{C}(\beta a, 2\beta g) \\
& + [\sin \beta g + \beta(h-g) \cos \beta g] \bar{C}(\beta a, \beta(h-g)) \\
& + [\sin \beta g - \beta(h+g) \cos \beta g] \bar{C}(\beta a, \beta(h+g)) \\
& + \sin \beta h [\bar{C}_c(\beta a, \beta(h+g)) - \bar{C}_c(\beta a, \beta(h-g)) - \bar{C}_c(\beta a, 2\beta g)] \\
& - \cos \beta h [C_s(\beta a, \beta(h+g)) - C_s(\beta a, \beta(h-g)) - C_s(\beta a, 2\beta g)] \\
& - j(\cos \beta g \cos \beta(h-g) [\cos \beta \sqrt{(2g)^2 + a^2} - \cos \beta a] \\
& - \cos \beta g [\cos \beta \sqrt{(h+g)^2 + a^2} - \cos \beta \sqrt{(h-g)^2 + a^2}]
\end{aligned}$$

$$\begin{aligned}
& + [2\beta g \cos \beta g \cos \beta(h-g) + \sin \beta(h-2g)] S(\beta a, 2\beta s) \\
& + [\sin \beta g + \beta(h-g) \cos \beta g] S(\beta a, \beta(h-g)) \\
& + [\sin \beta g - \beta(h+g) \cos \beta g] S(\beta a, \beta(h+g)) \\
& + \sin \beta h [S_c(\beta a, \beta(h+g)) - S_c(\beta a, \beta(h-g)) - S_c(\beta a, 2\beta g)] \\
& - \cos \beta h [S_s(\beta a, \beta(h+g)) - S_s(\beta a, \beta(h-g)) - S_s(\beta a, 2\beta g)] \} , \\
Y_D = & \frac{2}{[1 - \cos \beta(h-g)]^2} \left\{ \frac{1}{2} \sin 2\beta(h-g) \sin \beta \sqrt{(2g)^2 + a^2} + \sin \beta(h-g) \sin \beta \sqrt{(2h)^2 + a^2} \right. \\
& + [\sin \beta(h-g) + \frac{1}{2} \sin 2\beta(h-g)] [\sin \beta \sqrt{(h-g)^2 + a^2} - \sin \beta \sqrt{(h+g)^2 + a^2} - \sin \beta a] \\
& - [2\beta h \sin \beta(h-g) + \cos \beta(h-g) - 1] \bar{C}(\beta a, 2\beta h) - 2 \sin \beta(h-g) C_s(\beta a, \beta(h-g)) \\
& - [\beta g \sin 2\beta(h-g) - \cos 2\beta(h-g) + \cos \beta(h-g)] \bar{C}(\beta a, 2\beta g) \\
& + [\beta(h+g)(\sin \beta(h-g) + \frac{1}{2} \sin 2\beta(h-g)) + 2 - 2 \cos \beta(h-g)] \bar{C}(\beta a, \beta(h+g)) \\
& - [\beta(h-g)(\sin \beta(h-g) + \frac{1}{2} \sin 2\beta(h-g)) - 2 \sin^2 \beta(h-g)] \bar{C}(\beta a, \beta(h-g)) \\
& - [\cos \beta(h+g) - \cos 2\beta h] [2\bar{C}_c(\beta a, \beta(h+g)) - \bar{C}_c(\beta a, 2\beta h) - \bar{C}_c(\beta a, 2\beta g)] \\
& - [\sin \beta(h+g) - \sin 2\beta h] [2C_s(\beta a, \beta(h+g)) - C_s(\beta a, 2\beta h) - C_s(\beta a, 2\beta g)] \\
& - j(-\frac{1}{2} \sin 2\beta(h-g) \cos \beta \sqrt{(2g)^2 + a^2} - \sin \beta(h-g) \cos \beta \sqrt{(2h)^2 + a^2} \\
& - [\sin \beta(h-g) + \frac{1}{2} \sin 2\beta(h-g)] [\cos \beta \sqrt{(h-g)^2 + a^2} - \cos \beta \sqrt{(h+g)^2 + a^2} - \cos \beta a] \\
& - [2\beta h \sin \beta(h-g) + \cos \beta(h-g) - 1] S(\beta a, 2\beta h) - 2 \sin \beta(h-g) S_s(\beta a, \beta(h-g)) \\
& - [\beta g \sin 2\beta(h-g) - \cos 2\beta(h-g) + \cos \beta(h-g)] S(\beta a, 2\beta g)
\end{aligned}$$

$$\begin{aligned}
& + [\beta(h+g)(\sin \beta(h-g) + \frac{1}{2} \sin 2\beta(h-g)) + 2 - 2 \cos \beta(h-g)] S(\beta a, \beta(h+g)) \\
& - [\beta(h-g)(\sin \beta(h-g) + \frac{1}{2} \sin 2\beta(h-g)) - 2 \sin^2 \beta(h-g)] S(\beta a, \beta(h-g)) \\
& - [\cos(h+g) - \cos 2\beta h] [2S_c(\beta a, \beta(h+g)) - S_c(\beta a, 2\beta h) - S_c(\beta a, 2\beta g)] \\
& - [\sin \beta(h+g) - \sin 2\beta h] [2S_s(\beta a, \beta(h+g)) - S_s(\beta a, 2\beta h) - S_s(\beta a, 2\beta g)] \} ,
\end{aligned}$$

$$\begin{aligned}
Y_{CC} & = \cos^2 \beta g [\sin \beta a - \sin \beta \sqrt{(2g)^2 + a^2}] + C_s(\beta a, 2\beta g) \\
& + 2 \cos \beta g [\beta g \cos \beta g - \sin \beta g] \bar{C}(\beta a, 2\beta g) \\
& - j(\cos^2 \beta g [\cos \beta \sqrt{(2g)^2 + a^2} - \cos \beta a] + S_s(\beta a, 2\beta g)) \\
& + 2 \cos \beta g [\beta g \cos \beta g - \sin \beta g] S(\beta a, 2\beta g) ,
\end{aligned}$$

$$\begin{aligned}
Y_{DD} & = \frac{2}{1 - \cos \beta(h-g)} \left\{ (1 + \cos \beta(h-g)) [\sin \beta a - \sin \beta \sqrt{(h-g)^2 + a^2}] \right. \\
& + \sin \beta \sqrt{(h+g)^2 + a^2} - \frac{1}{2} \sin \beta \sqrt{(2h)^2 + a^2} \\
& - \frac{1}{2} \sin \beta \sqrt{(2g)^2 + a^2} + 2C_s(\beta a, \beta(h-g)) \\
& + [\beta g(1 + \cos \beta(h-g)) + \sin \beta(h-g)] \bar{C}(\beta a, 2\beta g) \\
& + [\beta h(1 + \cos \beta(h-g)) - \sin \beta(h-g)] \bar{C}(\beta a, 2\beta h) \\
& + [\beta(h-g)(1 + \cos \beta(h-g)) - 2 \sin \beta(h-g)] \bar{C}(\beta a, \beta(h-g)) \\
& - \beta(h+g)(1 + \cos \beta(h-g)) \bar{C}(\beta a, \beta(h+g)) \\
& + \sin \beta(h+g) [2\bar{C}_c(\beta a, \beta(h+g)) - \bar{C}_c(\beta a, 2\beta h) - \bar{C}_c(\beta a, 2\beta g)] \\
& - \cos \beta(h+g) [2C_s(\beta a, \beta(h+g)) - C_s(\beta a, 2\beta h) - C_s(\beta a, 2\beta g)] \}
\end{aligned}$$

$$\begin{aligned}
& - j((1 + \cos \beta(h-g))[\cos \beta \sqrt{(h-g)^2 + a^2} - \cos \beta a - \cos \beta \sqrt{(h+g)^2 + a^2} \\
& + \frac{1}{2} \cos \beta \sqrt{(2h)^2 + a^2} + \frac{1}{2} \cos \beta \sqrt{(2g)^2 + a^2}] + 2S_s(\beta a, \beta(h-g)) \\
& + [\beta g(1 + \cos \beta(h-g)) + \sin \beta(h-g)] S(\beta a, 2\beta g) \\
& + [\beta h(1 + \cos \beta(h-g)) - \sin \beta(h-g)] S(\beta a, 2\beta h) \\
& + [\beta(h-g)(1 + \cos \beta(h-g)) - 2 \sin \beta(h-g)] S(\beta a, \beta(h-g)) \\
& - \beta(h+g)(1 + \cos \beta(h-g)) S(\beta a, \beta(h+g)) \\
& + \sin \beta(h+g)[2S_c(\beta a, \beta(h+g)) - S_c(\beta a, 2\beta h) - S_c(\beta a, 2\beta g)] \\
& - \cos \beta(h+g)[2S_s(\beta a, \beta(h+g)) - S_s(\beta a, 2\beta h) - S_s(\beta a, 2\beta g)] \} ,
\end{aligned}$$

and

$$\begin{aligned}
Y_{CD} = & \frac{2}{1 - \cos \beta(h-g)} \left\{ \cos \beta g \sin \beta(h-g) [\sin \beta \sqrt{(2g)^2 + a^2} - \sin \beta a \right. \\
& + \sin \beta \sqrt{(h-g)^2 + a^2} - \sin \beta \sqrt{(h+g)^2 + a^2}] \\
& - [2\beta g \cos \beta g \sin \beta(h-g) + \cos \beta g - \cos \beta(h-2g)] \bar{C}(\beta a, 2\beta g) \\
& + [\beta(h+g) \cos \beta g \sin \beta(h-g) + \cos \beta h - \cos \beta g] \bar{C}(\beta a, \beta(h+g)) \\
& - [\beta(h-g) \cos \beta g \sin \beta(h-g) - \cos \beta g + \cos \beta(h-2g)] \bar{C}(\beta a, \beta(h-g)) \\
& + [\cos \beta h - \cos \beta g] [\bar{C}_c(\beta a, \beta(h+g)) - \bar{C}_c(\beta a, \beta(h-g)) - \bar{C}_c(\beta a, 2\beta g)] \\
& + [\sin \beta h - \sin \beta g] [C_s(\beta a, \beta(h+g)) - C_s(\beta a, \beta(h-g)) - C_s(\beta a, 2\beta g)] \\
& - j[\cos \beta g \sin \beta(h-g) [\cos \beta a - \cos \beta \sqrt{(2g)^2 + a^2} + \cos \beta \sqrt{(h+g)^2 + a^2} \\
& \quad \left. - \cos \beta \sqrt{(h-g)^2 + a^2}] \right\}
\end{aligned}$$

$$\begin{aligned}
& - [2\beta g \cos \beta g \sin \beta(h-g) + \cos \beta g - \cos \beta(h-2g)] S(\beta a, 2\beta g) \\
& + [\beta(h+g) \cos \beta g \sin \beta(h-g) + \cos \beta h - \cos \beta g] S(\beta a, \beta(h+g)) \\
& - [\beta(h-g) \cos \beta g \sin \beta(h-g) - \cos \beta g + \cos \beta(h-2g)] S(\beta a, \beta(h-g)) \\
& + [\cos \beta h - \cos \beta g] [S_c(\beta a, \beta(h+g)) - S_c(\beta a, \beta(h-g)) - S_c(\beta a, 2\beta g)] \\
& + [\sin \beta h - \sin \beta g] [S_s(\beta a, \beta(h+g)) - S_s(\beta a, \beta(h-g)) - S_s(\beta a, 2\beta g)] \}
\end{aligned}$$

See Appendix A for the evaluation of the various γ 's.

This expression (2-28) is known to be stationary; that is, it is an extremum of the function $I_d(z)$. More exactly $\partial Z / \partial I = 0$ or

$$\frac{\partial Z}{\partial C} = \frac{\partial Z}{\partial D} = 0$$

After carrying out these operations and solving the resulting simultaneous equations for C and D the following results are obtained:

$$\begin{aligned}
C &= \frac{\gamma_D \gamma_{CD} - 2\gamma_C \gamma_{DD}}{4\gamma_{CC} \gamma_{DD} - \gamma_{CD}^2} \\
D &= \frac{\gamma_C \gamma_{CD} - 2\gamma_D \gamma_{CC}}{4\gamma_{CC} \gamma_{DD} - \gamma_{CD}^2}
\end{aligned}$$

5. The Single-Driven Dipole

The singly-driven dipole is a degenerate case of the doubly-driven one; see Fig. 2-2b. Allowing g to equal zero causes the two slice generators to become but one at $z = 0$. This causes $\gamma_C = \gamma_{CC} = \gamma_{CD} = 0$ and ⁶

$$\begin{aligned}
\gamma_0 &= \frac{1}{(1 - \cos \beta h)^2} \left\{ \sin \beta a - \sin \beta \sqrt{(2h)^2 + a^2} - 4 \sin \beta h \bar{C}(\beta a, \beta h) \right. \\
&\quad \left. + 2\beta h \bar{C}(\beta a, 2\beta h) + \sin 2\beta h [2\bar{C}_c(\beta a, \beta h) + 2\bar{C}_c(\beta a, 2\beta h)] \right\}
\end{aligned}$$

$$\begin{aligned}
& - \cos 2\beta h [2C_s(\beta a, \beta h) - C_s(\beta a, 2\beta h)] + 2C_s(\beta a, 2\beta h) \\
& - j(\cos \beta \sqrt{(2h)^2 + a^2} - \cos \beta a - 4 \sin \beta h S(\beta a, \beta h) \\
& + 2\beta h S(\beta a, 2\beta h) + \sin 2\beta h [2S_c(\beta a, \beta h) - S_c(\beta a, 2\beta h)] \\
& - \cos 2\beta h [2S_s(\beta a, \beta h) - S_s(\beta a, 2\beta h)] + 2S_s(\beta a, 2\beta h)) \} ,
\end{aligned}$$

$$\begin{aligned}
Y_D = \frac{2}{(1 - \cos \beta h)^2} & \left\{ \sin \beta h [\sin \beta \sqrt{(2h)^2 + a^2} - \sin \beta a] - 2 \sin \beta h C_s(\beta a, \beta h) \right. \\
& - [2\beta h \sin \beta h + \cos \beta h - 1] \bar{C}(\beta a, 2\beta h) + 2[1 + \sin^2 \beta h - \cos \beta h] \bar{C}(\beta a, \beta h) \\
& - [\cos \beta h - \cos 2\beta h] [2\bar{C}_c(\beta a, \beta h) - \bar{C}_c(\beta a, 2\beta h)] - [\sin \beta h - \sin 2\beta h] \\
& \quad [2C_s(\beta a, \beta h) - C_s(\beta a, 2\beta h)] \\
& - j(\sin \beta h [\cos \beta a - \cos \beta \sqrt{(2h)^2 + a^2}] - 2 \sin \beta h S_s(\beta a, \beta h) \\
& - [2\beta h \sin \beta h + \cos \beta h - 1] S(\beta a, 2\beta h) + 2[1 + \sin^2 \beta h - \cos \beta h] S(\beta a, \beta h) \\
& - [\cos \beta h - \cos 2\beta h] [2S_c(\beta a, \beta h) - S_c(\beta a, 2\beta h)] - [\sin \beta h - \sin 2\beta h] \\
& \quad [2S_s(\beta a, \beta h) - S_s(\beta a, 2\beta h)]) \} ,
\end{aligned}$$

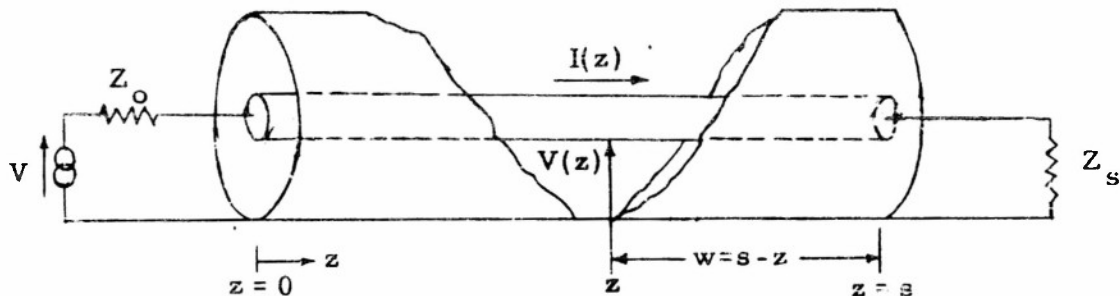
and

$$\begin{aligned}
Y_{DD} = \frac{2}{1 - \cos \beta h} & \left\{ \frac{1}{2}(1 + \cos \beta h) [\sin \beta a - \sin \beta \sqrt{(2h)^2 + a^2}] - 2 \sin \beta h \bar{C}(\beta a, \beta h) \right. \\
& \quad \left. + 2C_s(\beta a, \beta h) \right. \\
& + [\beta h(1 + \cos \beta h) - \sin \beta h] \bar{C}(\beta a, 2\beta h) + \sin \beta h [2\bar{C}_c(\beta a, \beta h) - \bar{C}_c(\beta a, 2\beta h)] \\
& \left. - \cos \beta h [2C_s(\beta a, \beta h) - C_s(\beta a, 2\beta h)] \right\}
\end{aligned}$$

Chapter III
 METHOD OF IMPEDANCE MEASUREMENTS
 AND AUXILLIARY MEASUREMENTS

1. Line Theory

The impedances presented in this paper were measured on the coaxial transmission line with a characteristic impedance Z_c equal to 123.6 ohms, a phase constant β of 12.775 radians per meter, and a theoretical attenuation constant α of 0.003 nepers/meter.



The differential equations describing the current and voltage at points remote from the ends of the line are

$$\frac{-\partial V(z)}{\partial z} = (r + j\omega l)I(z) \quad (3-1)$$

$$\frac{-\partial I(z)}{\partial z} = (g + j\omega c)V(z) \quad (3-2)$$

where r, l, g and c are the series resistance and inductance, shunt conductance and capacitance per meter of line. The time dependence and the complex nature of the current and voltage have been suppressed. A solution for the current containing the boundary conditions indicated in the diagram above is,¹⁵

$$I(z) = V \left[\frac{Z_c \sinh \gamma w + Z_0 \cosh \gamma w}{(Z_c^2 + Z_0 Z_s) \sinh \gamma s + Z_c (Z_0 + Z_s) \cosh \gamma s} \right],$$

where

$$\gamma = \alpha + j\beta = [(r+j\omega l)(g+j\omega c)]^{1/2}$$

Using the form

$$Z = Z_c \coth \theta = Z_c \coth(\rho + j\phi) \quad , \quad (3-3)$$

an expression containing only hyperbolic functions is obtained.

$$I(z) = \frac{V}{Z_c} \left[\frac{\sinh \theta_o \sinh(\gamma w + \theta_s)}{\sinh(\gamma s + \theta_o + \theta_s)} \right]$$

This formula describes the current completely, but is in complex form. A detector, sensitive only to the magnitude of this current, will measure the quantity.

$$|I(z)| = \left| \frac{V}{Z_c} \right| \left[\frac{(\sinh^2 \rho_o + \sin^2 \phi_o)(\sinh^2(\alpha w + \rho_s) + \sin^2(\beta w + \phi_s))}{\sinh^2(\alpha s + \rho_o + \rho_s) + \sin^2(\beta s + \phi_o + \phi_s)} \right]^{1/2}$$

The position of the minimum of this current distribution may be conveniently located, and for a lossless line this position is solely a function of the phase ϕ_s of the load. Taking the derivative of the square of the magnitude and equating to zero results in the equation

$$\alpha \sinh(\alpha w + \rho_s) \cosh(\alpha w + \rho_s) = -\beta \sin(\beta w + \phi_s) \cos(\beta w + \phi_s) \quad .$$

Squaring both sides and using the double angle trigonometric identities gives,

$$\frac{\alpha^2}{\beta^2} \sinh^2 2(\alpha w + \rho_s) = 1 - \cos^2 2(\beta w + \phi_s)$$

and therefore,

$$\cos 2(\beta w + \phi_s) = \pm \sqrt{1 - \frac{\alpha^2}{\beta^2} \sinh^2 2(\alpha w + \rho_s)} \quad .$$

Assuming

$$\frac{\alpha^2}{\beta^2} \sinh^2 2(\alpha w + \rho_s) \ll 1 \quad (3-4)$$

then

$$\cos 2(\beta w + \phi_s) = \pm 1$$

and hence

$$\beta w + \phi_s = \pm \frac{n\pi}{2}, \quad n = 0, 1, 2, 3, \dots$$

determines the positions of the maxima and minima. The minima occur for n even. For the first minimum from the end ($w = 0$), $n = 2$, $w = w_{\min}$ of the current distribution and

$$\phi_s = \pi - \beta w_{\min} \quad (3-5)$$

The other parameter characterizing the load impedance is ρ_s . It may be determined from the current distribution in the vicinity of the minimum normalized to the value of this minimum current. There are two points, one either side of the minimum, having the same value of current. For a lossless line ($(\alpha\delta w)^2 \ll \frac{1}{8}$) these points are located symmetrically at a distance δw either side of the minimum. In the vicinity of the minimum

$$\left| \frac{I(z)}{I(z_{\min})} \right| = p(w) = \left| \frac{\sinh(\gamma w + \rho_s \pm \alpha\delta w)}{\sinh(\gamma w_m + \theta_s)} \right|$$

The squared magnitude of this quantity is,

$$p^2(w) = \frac{\sinh^2(\alpha w_m + \rho_s \pm \alpha\delta w) + \sin^2(\beta w_m + \phi_s \pm \beta\delta w)}{\sinh^2(\alpha w_m + \rho_s) + \sin^2(\beta w_m + \phi_s)}$$

Substituting in the value $\beta w + \phi_s = \pi$ at the first minimum,

$$p^2(w) \sinh^2(\alpha w_m + \rho_s) = \sinh^2(\alpha w_m + \rho_s \pm \alpha\delta w) + \sin^2\beta\delta w$$

Assuming that $\alpha\delta w \ll \alpha w_m + \rho_s$, then $(p^2(w) - 1) \sinh^2(\alpha w_m + \rho_s) = \sin^2\beta\delta w$. The point of maximum slope of $p^2(w)$ occurs at $p^2 = 2$, and it is the point where the current squared on the line is twice that at the minimum. For $p^2(w) = 2$

$$\rho_s = \sinh^{-1}(\sin\beta\delta w) - \alpha w_m \quad (3-6)$$

Thus the two quantities needed in (3-3) to describe an arbitrary load impedance

can be determined from the position of the minimum and the width of the distribution curve at the double-power points.

Three approximations have been made here, other than those in (3-1) and (3-2), in locating the minimum; (3-5) and $w_m = (\pi - \phi_g)/\beta$ are true to the extent that (3-4) is satisfied. For the experimental line used, and for example with an unusually low standing-wave ratio of 1.1, then $(\frac{a}{\beta Z}) \sinh^2 2(a w_m + \beta_g) = 5.54 \times 10^{-6}$ and (3-4) is certainly well satisfied. Using¹⁶ the formula $Q = \beta/2a = 4580$, the condition $(a\delta w)^2 \ll \frac{1}{8}$ becomes $Q^2 \gg 1$, and $a\delta w \ll a w_m + \beta_g$ requires $Q \gg 1$. All of the conditions on the approximations are easily met and the line losses do not contribute to the error in (3-5) or (3-6).

The limiting accuracy thus rests on the accuracy with which the position of the double power points may be located. The choice of $p^2 = 2$ is optimum for a square law detector in that the points for $w_m \pm \delta w$ fall on the steepest part of the measured distribution. Attempts to average a few points about the minimum as compared to averaging the position of the two double power points resulted in no improvement in the accuracy with which the minimum was located. The error in measuring the double power width increases at lower standing-wave ratios, but will be less important since the impedance corresponding to a small standing-wave ratio is then less sensitive to errors in the determination of ρ_g . Since only a 6 db range of the detector calibration curve is used, it is possible to restrict the measurement to that portion found to have a constant slope and be nearly square law.

2. Computation of Impedances

A desk calculator used in conjunction with a large scale Smith chart provides a convenient technique for processing the data from the slotted line measurements. The sum and average of the positions of the two double-power points are quickly computed to give the positions of the minimum, and thus ϕ_g . Their difference gives δw and thus ρ_g . Tables of $\sinh^{-1}(\sin \beta \delta w)$ for $0 < \beta \delta w < 1.500$ in steps of 0.0005 radians were prepared to facilitate the computation of ρ_g . The correction due to $a w_m$ in (3-6) was of the order of 0.001 radians and usually negligible.

A 15 inch diameter Smith chart was covered with a rotatable transparent disk carrying a radial ρ_s scale. Knowing ρ_s and ϕ_s , the normalized impedance on the line was calculated with about 1 percent accuracy.

Some of the data were corrected for the end effect¹⁷ on a coaxial line. The admittance corresponding to the measured impedance was obtained graphically from the Smith chart by rotating the measured ρ_s, ϕ_s point by 180 degrees about the center of the chart. The end-correction, a negative capacitive susceptance, of 0.144 mhos, normalized at 600 MC on this line, is added and the new ρ and ϕ point rotated another 180 degrees to give the corrected measured load impedance. See Fig. 3 and Figs. 15 to 18 for examples of the importance of this correction. A more complicated correction has been considered by Whinnery¹⁸ and also by Zeoli,¹⁹ but it was decided that the general accuracy of the problem is not great enough to make such correction necessary. The total capacity of their π network is nearly equal to that of the Hartig correction if the inductance is neglected.

3. General Check on System using Half-Dipole Impedance Measurements.

The general accuracy of the measurements was checked by measuring the impedance of the simple half dipole of constant radius as a function of length, correcting it for end effects and then comparing the results with the King-Middleton second-order impedance for a constant radius dipole, obtained recently by cross plotting from constant Ω data.²⁰ See Fig. 3 for a comparison of these results.

4. Comparison of Probes.

The accuracy of the auxiliary probe as used on the polyfoam supporting column was investigated by measuring the current distribution on a half-wavelength dipole with both probes. The resulting curves were plotted and normalized to have the same maximum. (See Fig. 4 Also plotted in this diagram are the King-Middleton²¹ first-order distribution and the current obtained using the equation for $I_g(z)$ on page 2-24.

5. Measurement of Gap Capacitance.

Experimentally, the gap between the end of the driven antenna and its parasite is the parameter varied in any particular array. A varying capacitive reactance is assumed to be the equivalent of this in the theory of the array. Hence the magnitude of the lumped capacitance between the hemispherical end caps is needed in order to compare the theory with data using the gap reactance as a parameter.

Since the theory applies precisely only for small ($0 < \text{gap} < \lambda/10$) gaps, it seems reasonable that the capacitance of such a gap could be measured by constructing it in the center conductor of a shorted coaxial line. Such a measurement was set up with a variable gap placed a half wavelength from the shorted end of the line. The apparent series reactance and capacitance of the gap was so determined and plotted in Fig. 5. For spacings less than 0.01 cm the curve was extrapolated linearly from its measured values at larger spacings. The results agree qualitatively with those found by Jeans²² for the capacitance between two identical spheres. For very small gaps in the actual array, a small piece of dielectric tape was used to separate the ends of the antenna elements. The tape was 0.006 cm thick, and, assuming a dielectric constant of 2 or 3, the equivalent air gap is about 0.003 cm with a corresponding gap reactance of approximately 250 ohms.

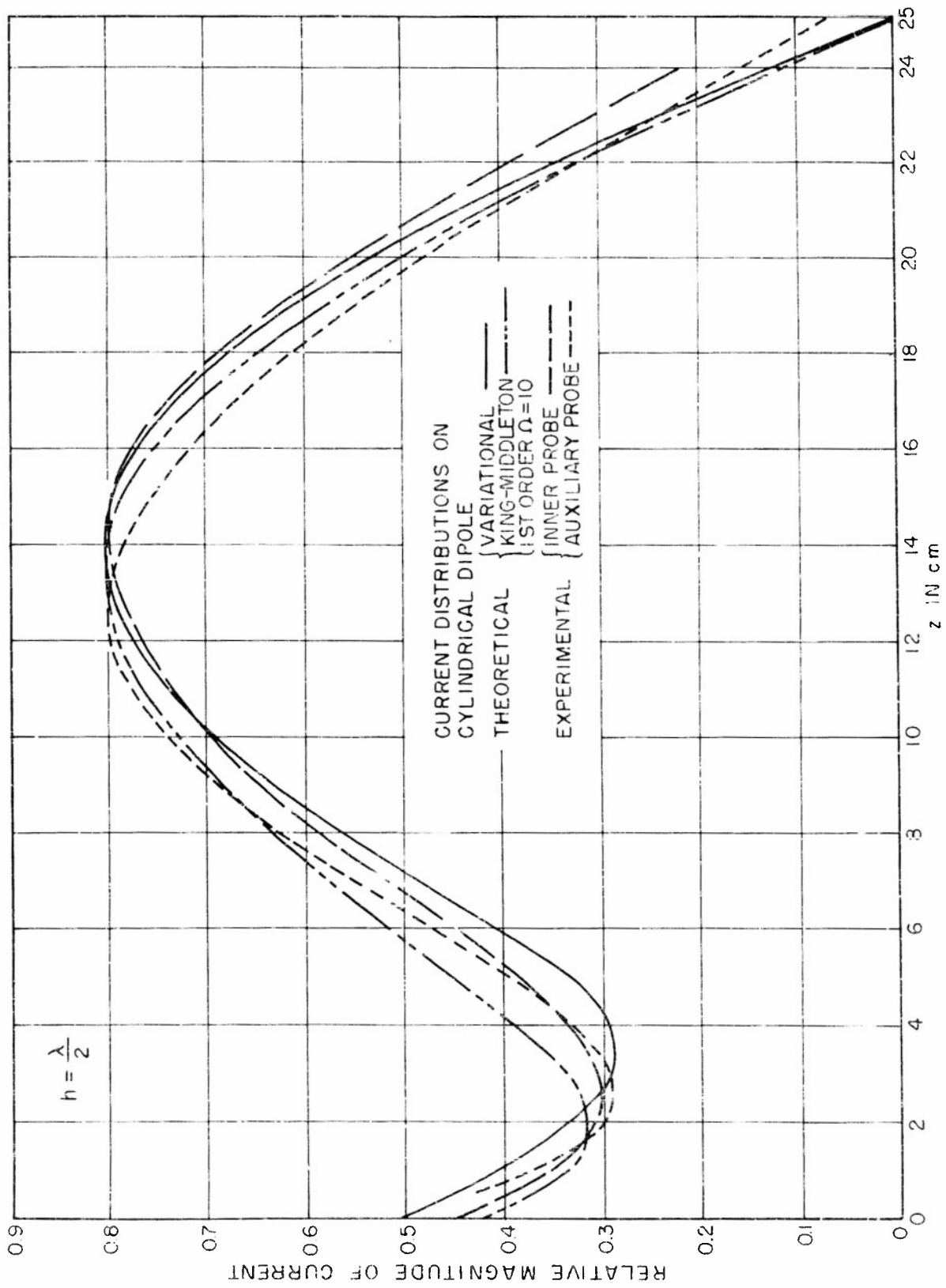


FIG. 4 COMPARISON OF EQUIPMENT PROBES WITH DIPOLE ANTENNA THEORIES

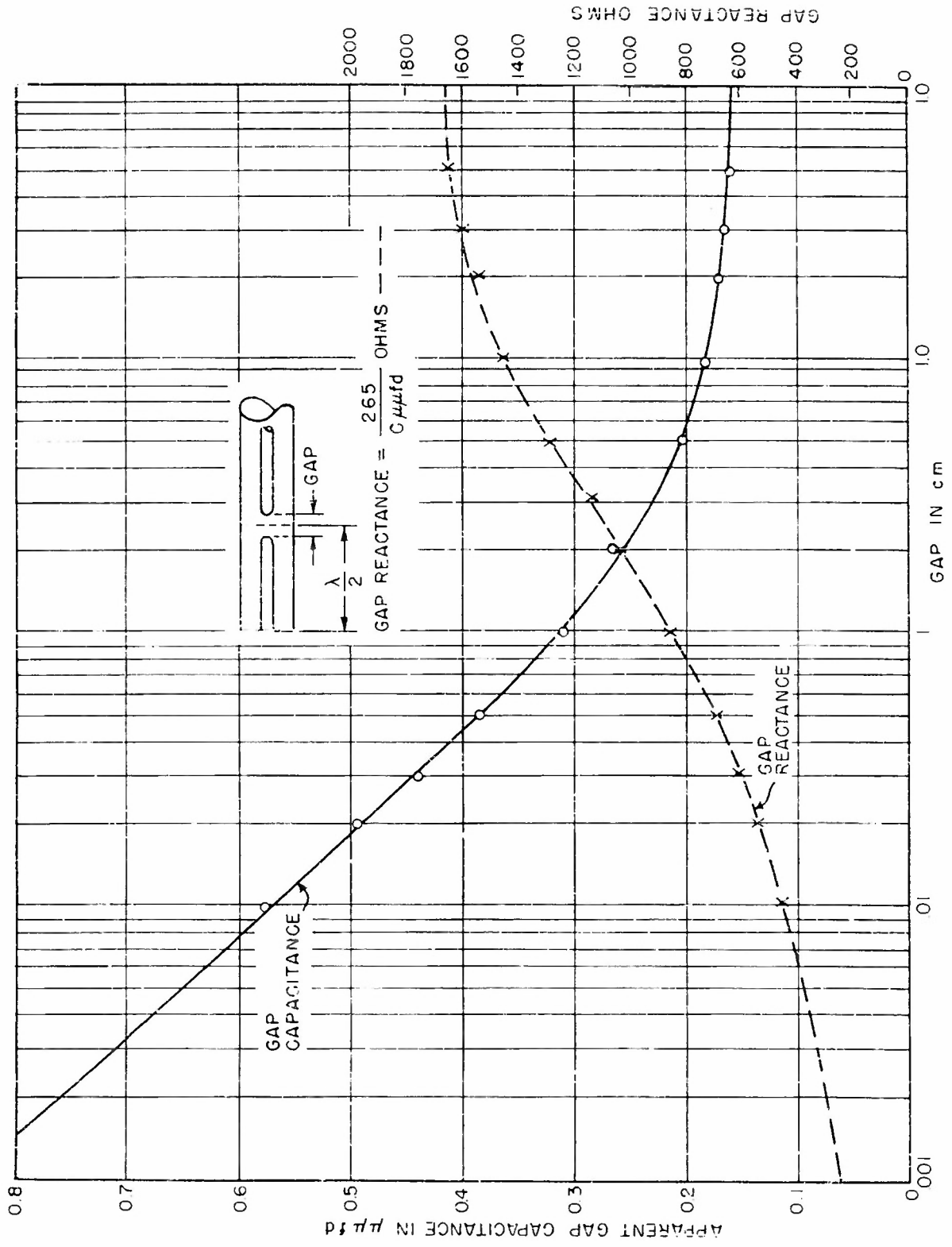


FIG. 5 APPARENT CAPACITANCE AND REACTANCE OF THE GAP

Chapter IV

EXPERIMENTAL DATA AND COMPUTATIONS

1. Extent of Parameter Variation

The parameters selected to be varied in the measurements are the lengths of the driven and parasitic elements and the spacing between them. Since one of the purposes for making the measurements is to check the theory over its complete range of applicability, these parameters must be varied over a range which includes poor as well as good agreement between theory and experiment. The trial functions used are such that the current distribution is well represented on the portion of the antenna for which $|z| < g$ where g is less than $\lambda/2$. Likewise the trial current on the section with $|z| > g$ is a good approximation for $h-g$ less than about $3\lambda/4$. Hence half lengths ranging up to a half wavelength for the driven antenna and overall lengths up to $3\lambda/4$ for the parasite should be investigated experimentally. The impedance and current distribution for similar lengths should be calculated from the theory. Longer lengths should be investigated experimentally, but there is little point to computing theory for them. The theory should be in good agreement with measurements for short lengths, $g < \lambda/4$ and $h-g$ less than $\lambda/2$, and should become progressively less applicable at greater lengths. The theoretical impedance should be in better agreement with the measured impedance over a greater range of lengths than that over which the theoretical current distribution is in agreement with the experimental distribution. This is a consequence of the use of a variational principle to improve the impedance approximation.

The gap should be varied experimentally from zero (i.e. actual contact of the elements) to as large a spacing as is possible in the existing experimental equipment. The theory however, considers the gap to be well represented by a variable lumped capacitance and assumes the coupling between the cylindrical surfaces of the array elements to be constant. Hence the limit of applicability of the theory is at the point where the coupling between the cylindrical surfaces has

changed appreciably. Note also that the coupling between the end surfaces changes very rapidly with spacing, and as soon as this change is essentially complete, then there will be no further appreciable effects due to actually reducing it to zero. With this in mind, the theory is limited to the maximum gap size required to reduce the end cap coupling effect to essentially zero. As the gap is increased beyond either of the above limits, whatever effects result will not be predicted by theory.

The importance of these limits and the rapidity with which they occur are difficult to predict. A $1/10$ wavelength gap should make a very large change in the coupling between the cylindrical surfaces, so the theory should certainly not be used beyond this point. Probably $1/20$ to $1/50$ wavelength would be a reasonable limit. As far as the gap coupling is concerned, consideration of Fig. 5 shows that the gap capacitance varies only very slowly for gaps greater than 1 cm, or about $1/50$ of a wavelength. Beyond this point the gap reactance does not change appreciably and the theory is no longer applicable. Hence the gaps to be investigated by computation from the theory, and experimentally, should range at least over separations of zero to 1 cm. Larger gaps may be investigated experimentally as far beyond as is convenient.

2. Measured Impedance Data.

The impedances measured are shown in Figs 6 through 18 along with the corresponding arrays on which the measurements were made. Smith charts were chosen, in Figs. 6 through 11 for example, rather than rectangular plots since the curve of the collinear impedance between the two end points would be more obvious. When the circle was too small to be convenient the impedances were denormalized and plotted in rectangular resistance and reactance coordinates.

3. Computational Procedure.

The choosing of cases for computation must be done with care, for the calculations are complicated and time consuming. On this basis, it is convenient to consider cases for which as many terms as possible

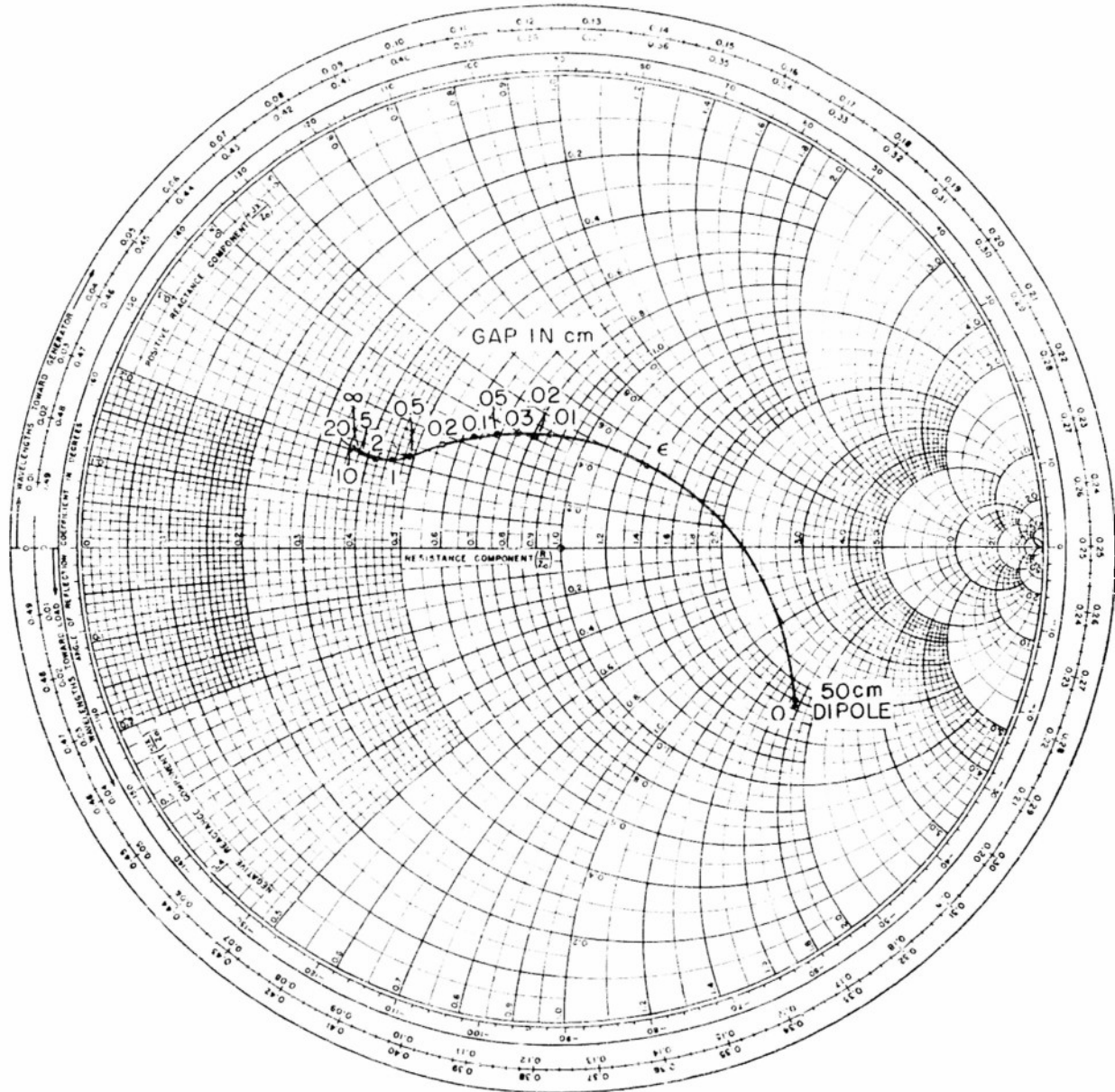
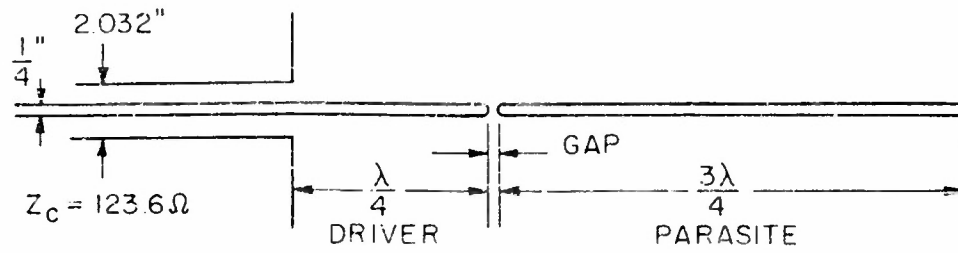


FIG. 6 MEASURED IMPEDANCE OF COLLINEAR ARRAY

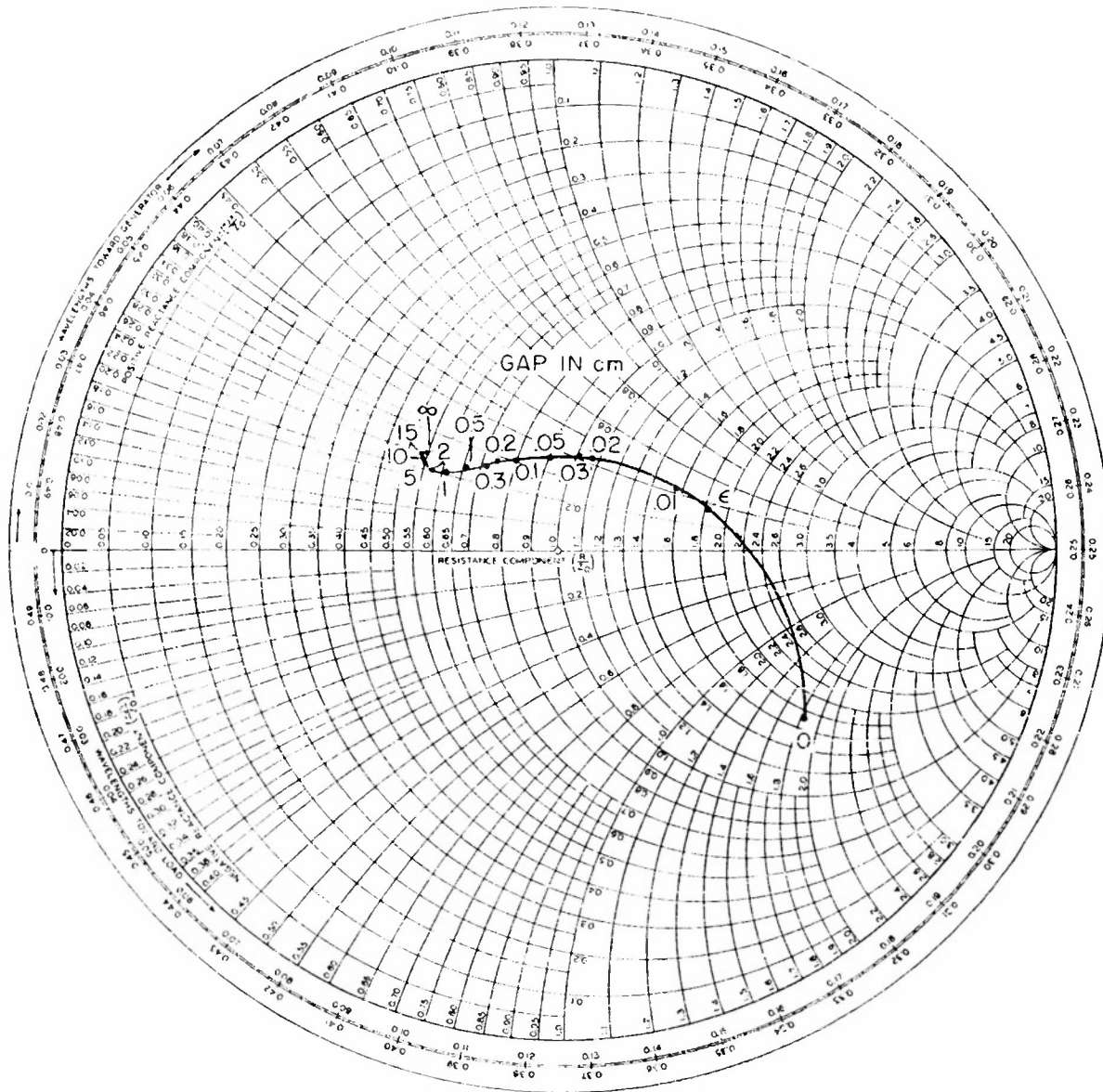
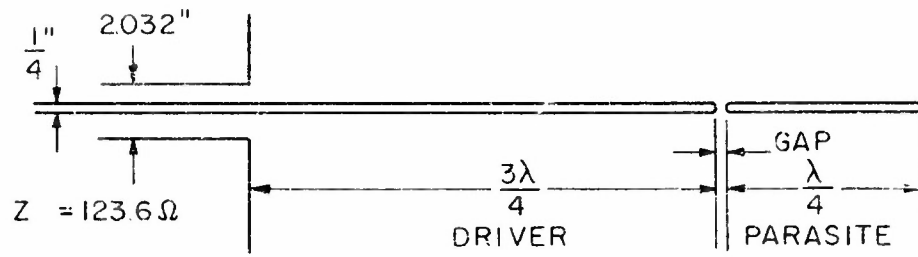


FIG. 8 MEASURED IMPEDANCE OF COLLINEAR ARRAY

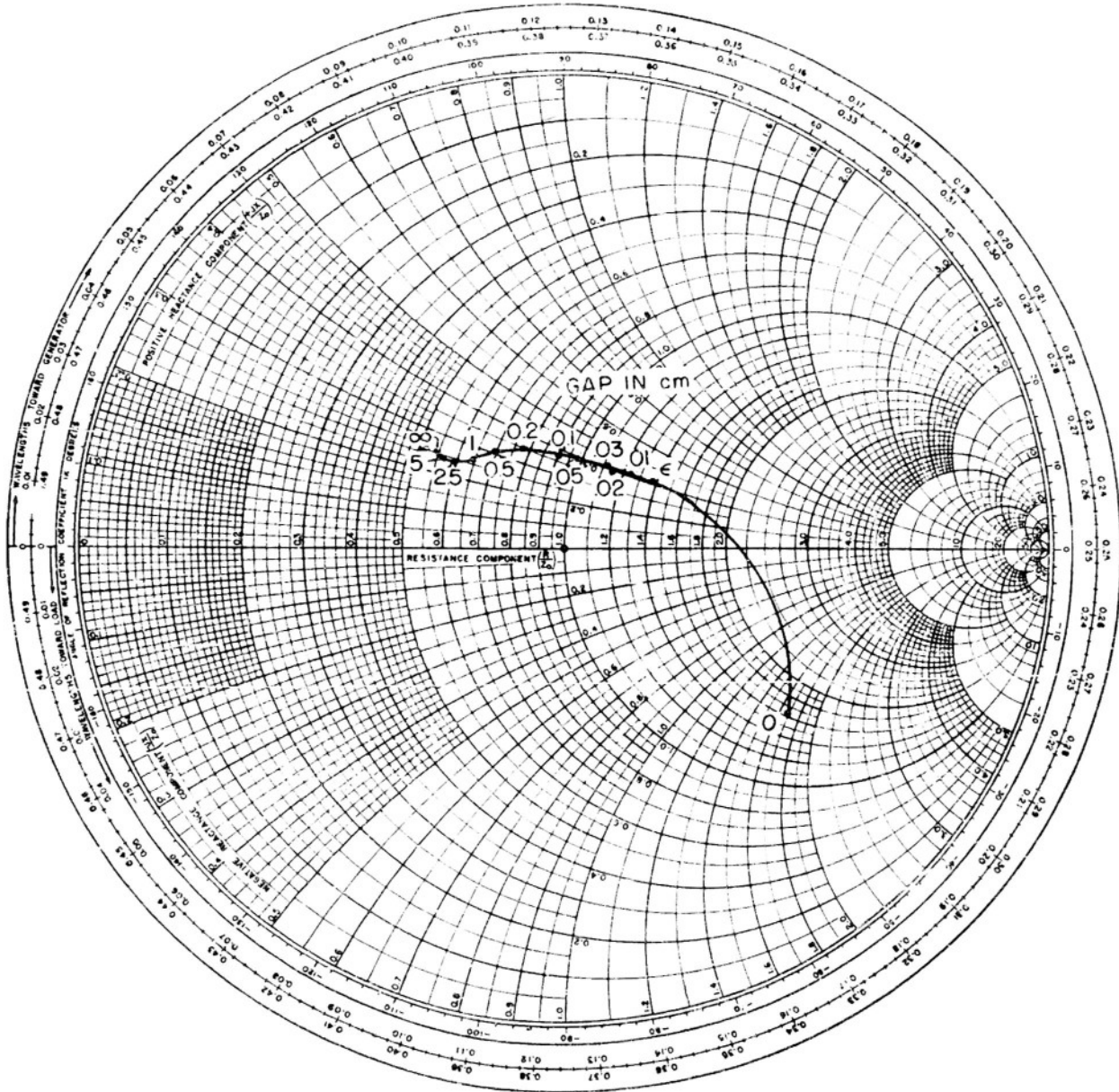
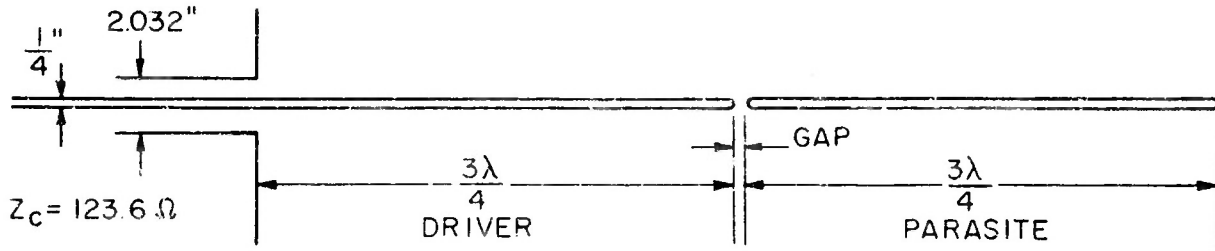


FIG 9 MEASURED IMPEDANCE OF COLLINEAR ARRAY

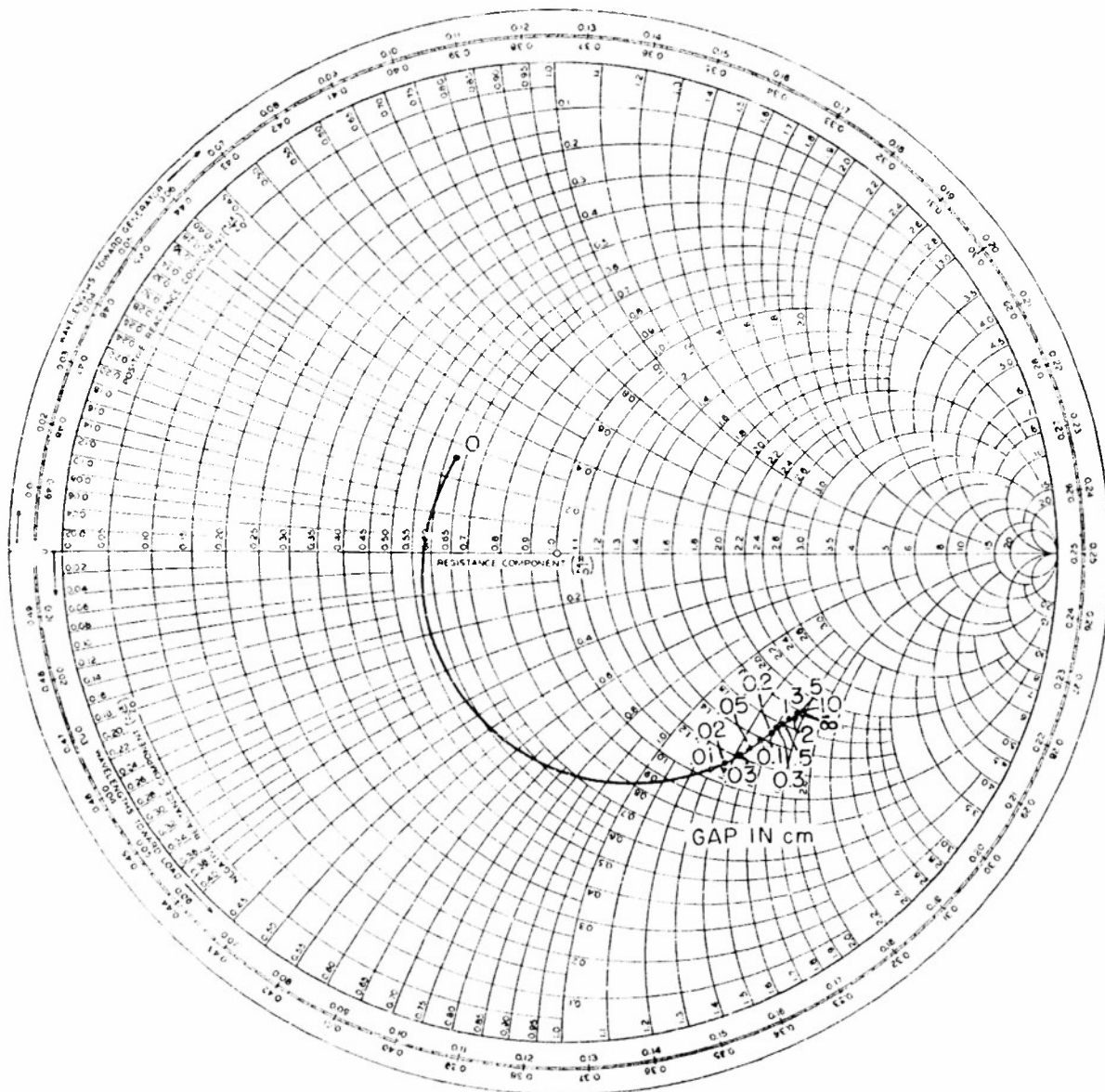
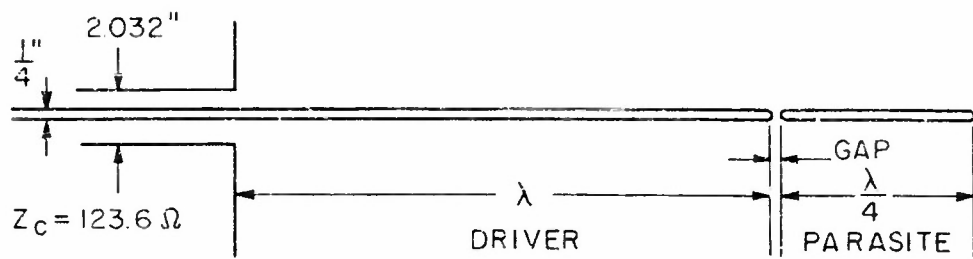


FIG. 10 MEASURED IMPEDANCE OF COLLINEAR ARRAY

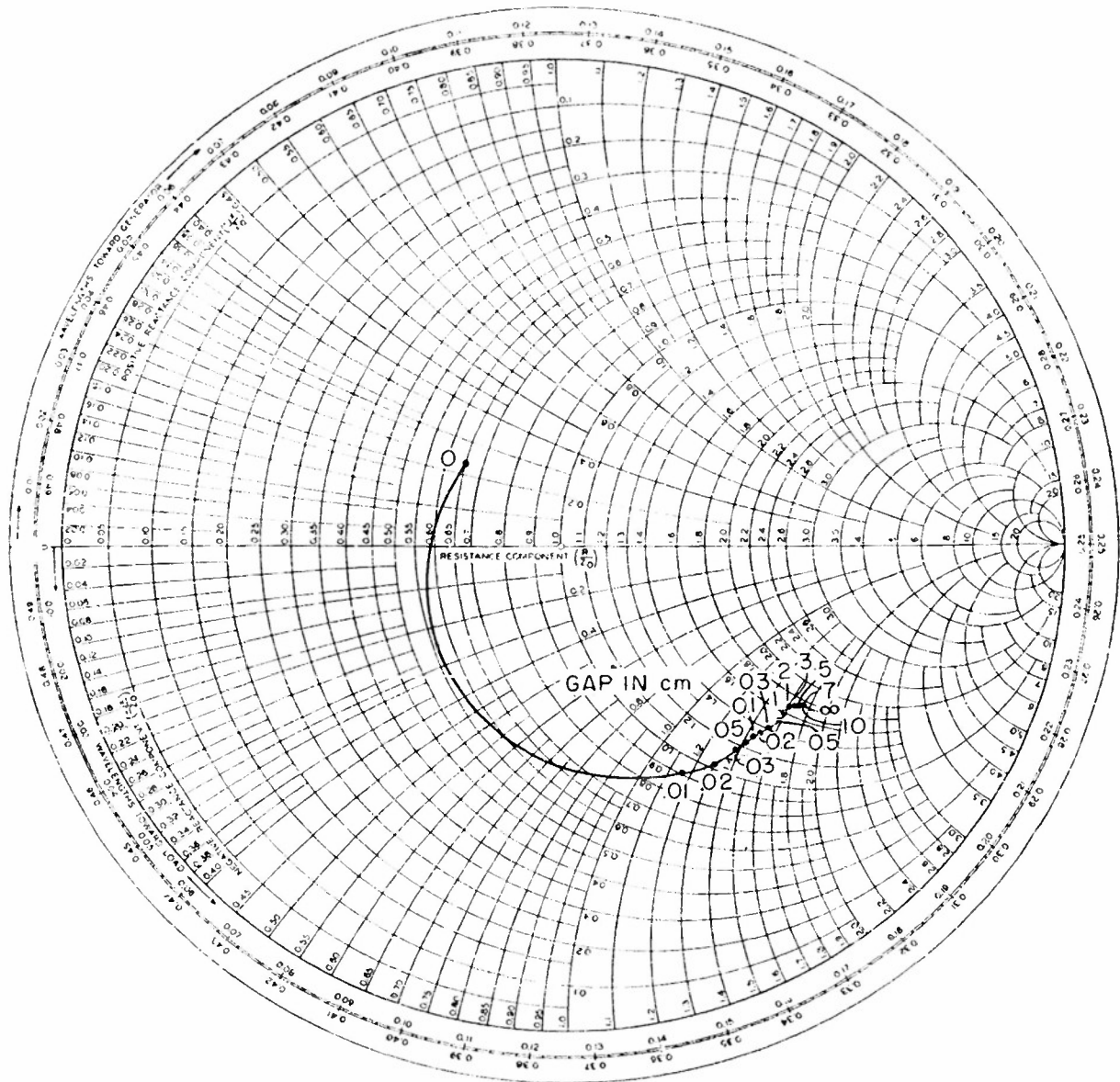
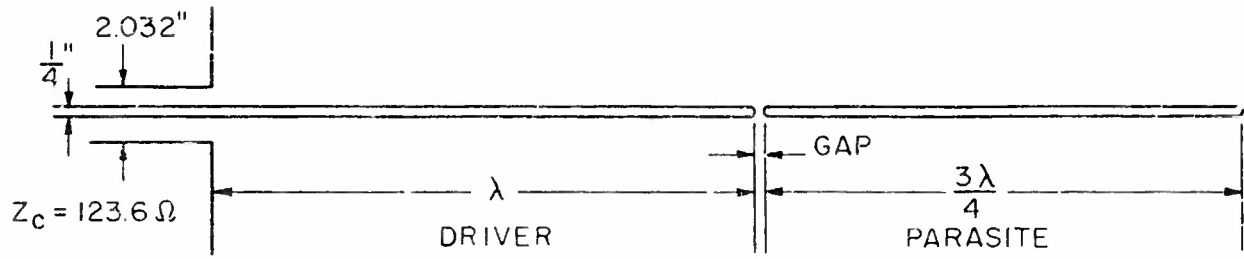


FIG. 11 MEASURED IMPEDANCE OF COLLINEAR ARRAY

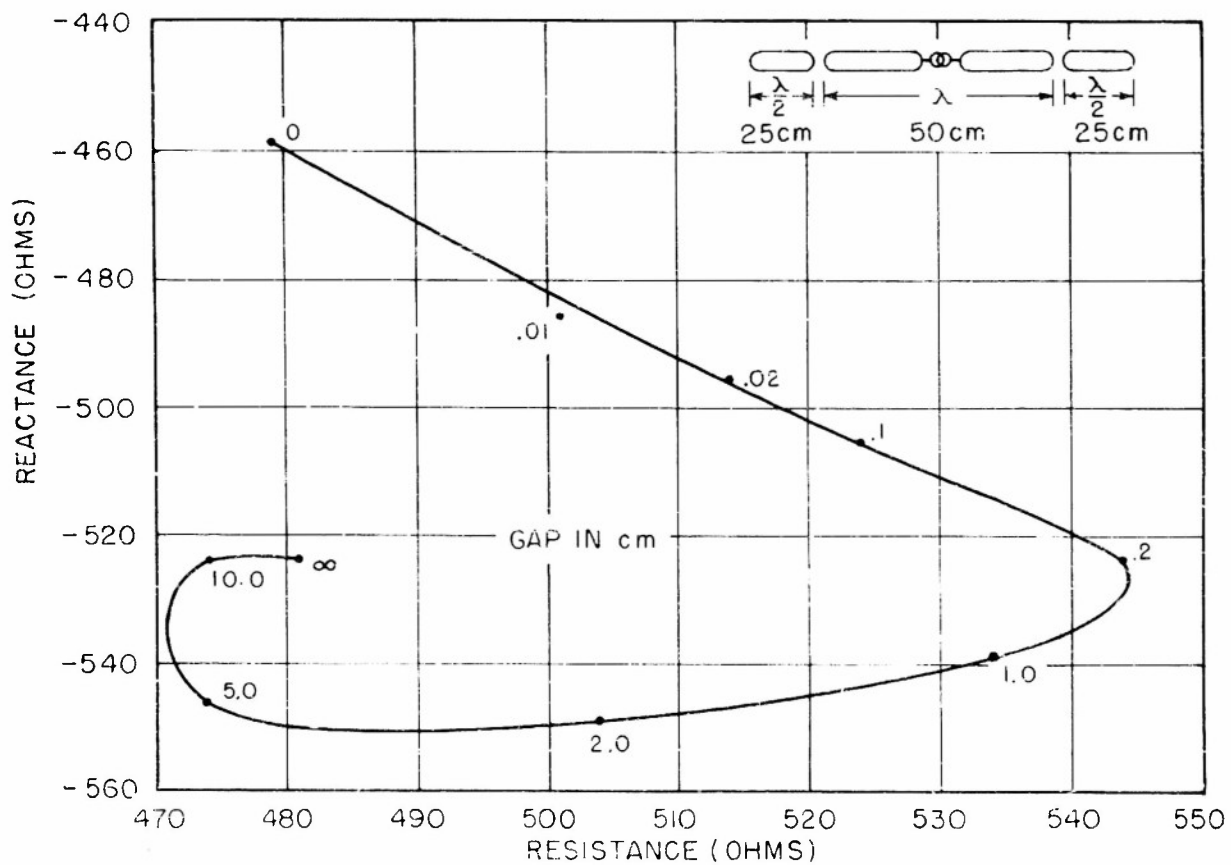
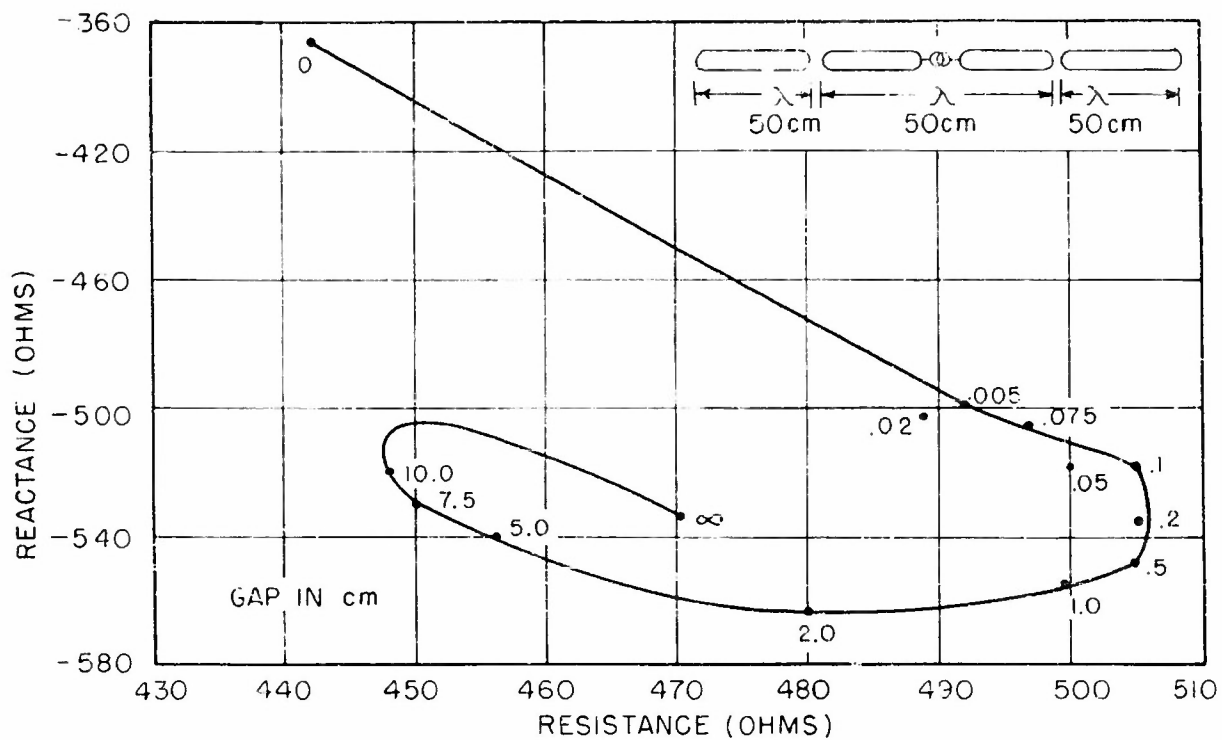


FIG. 12 MEASURED IMPEDANCE OF COLLINEAR ARRAY

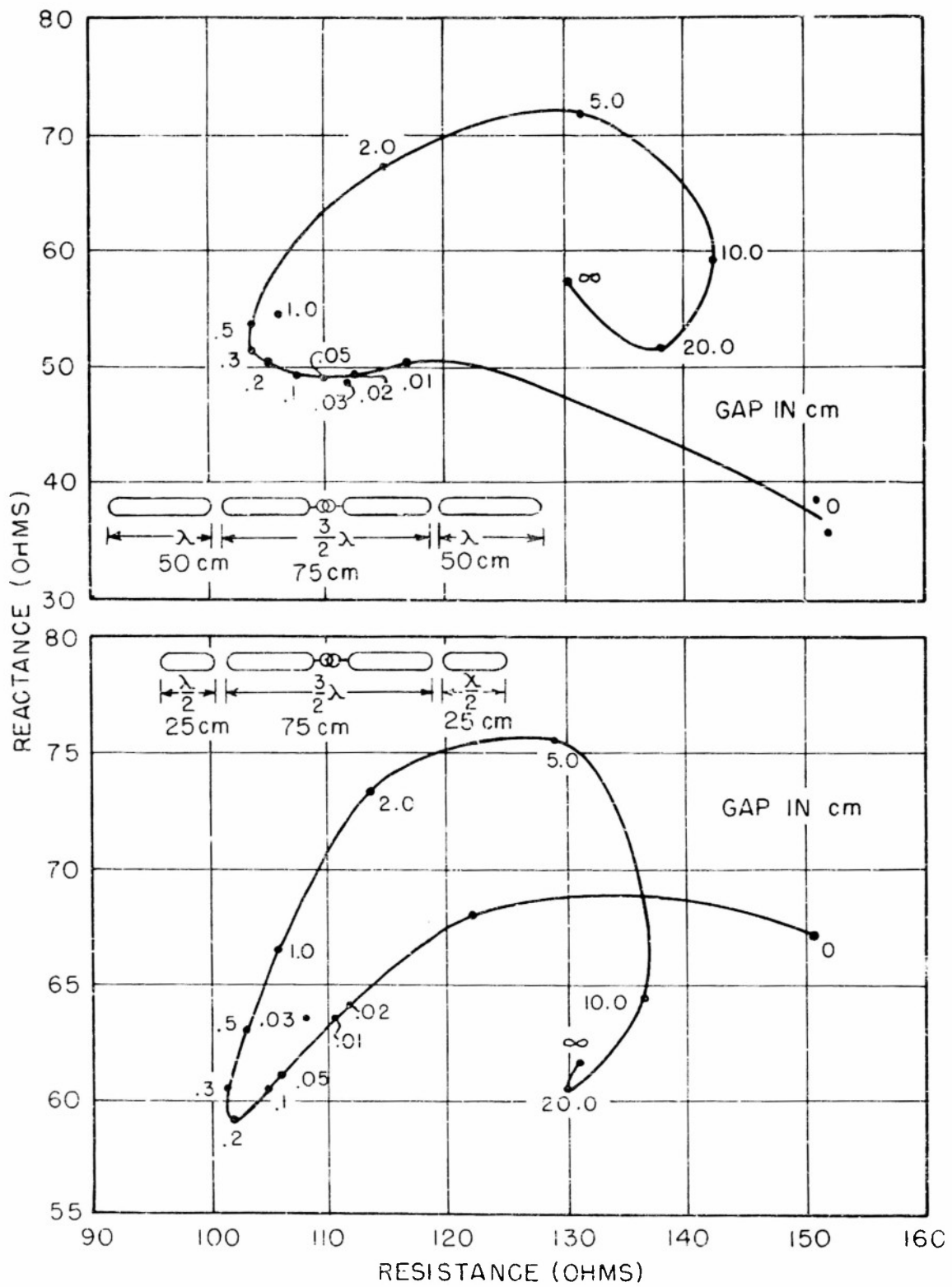


FIG. 13 MEASURED IMPEDANCE OF COLLINEAR ARRAY

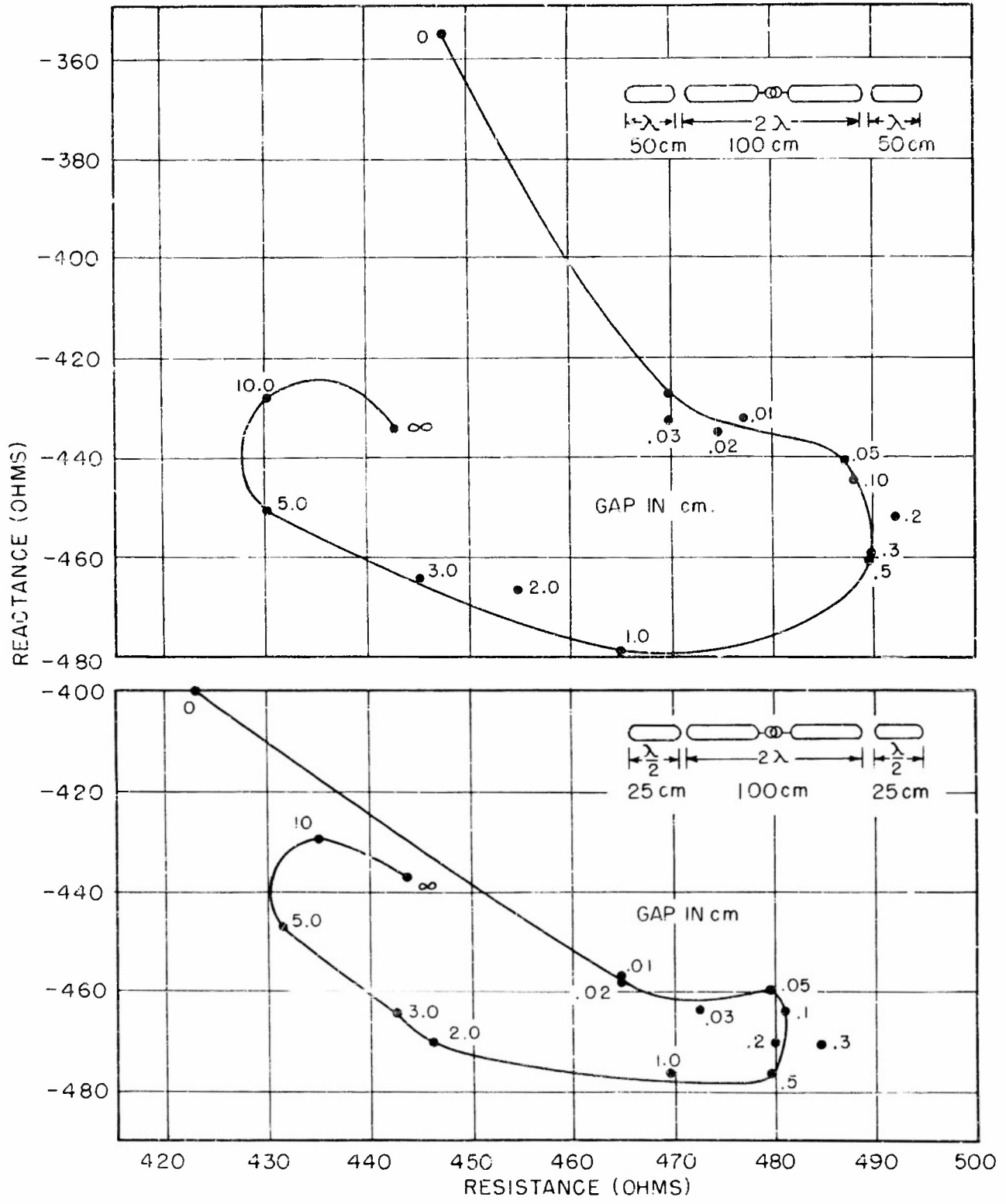


FIG. 14 MEASURED IMPEDANCE OF COLLINER ARRAY

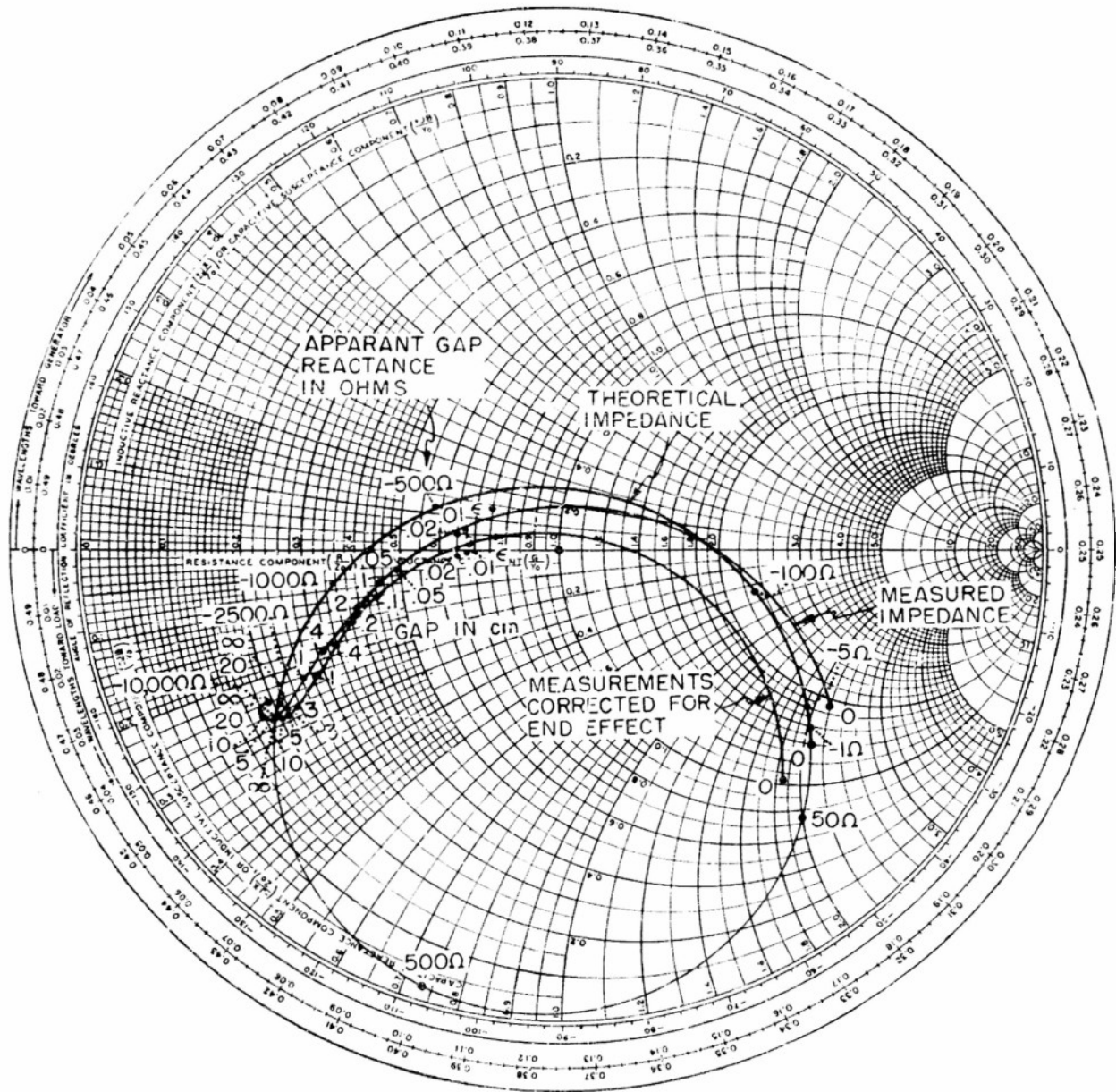
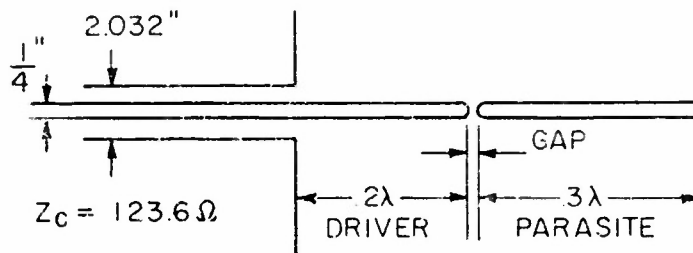


FIG. 15 COMPARISON OF THEORY AND MEASUREMENTS OF COLLINEAR ARRAY

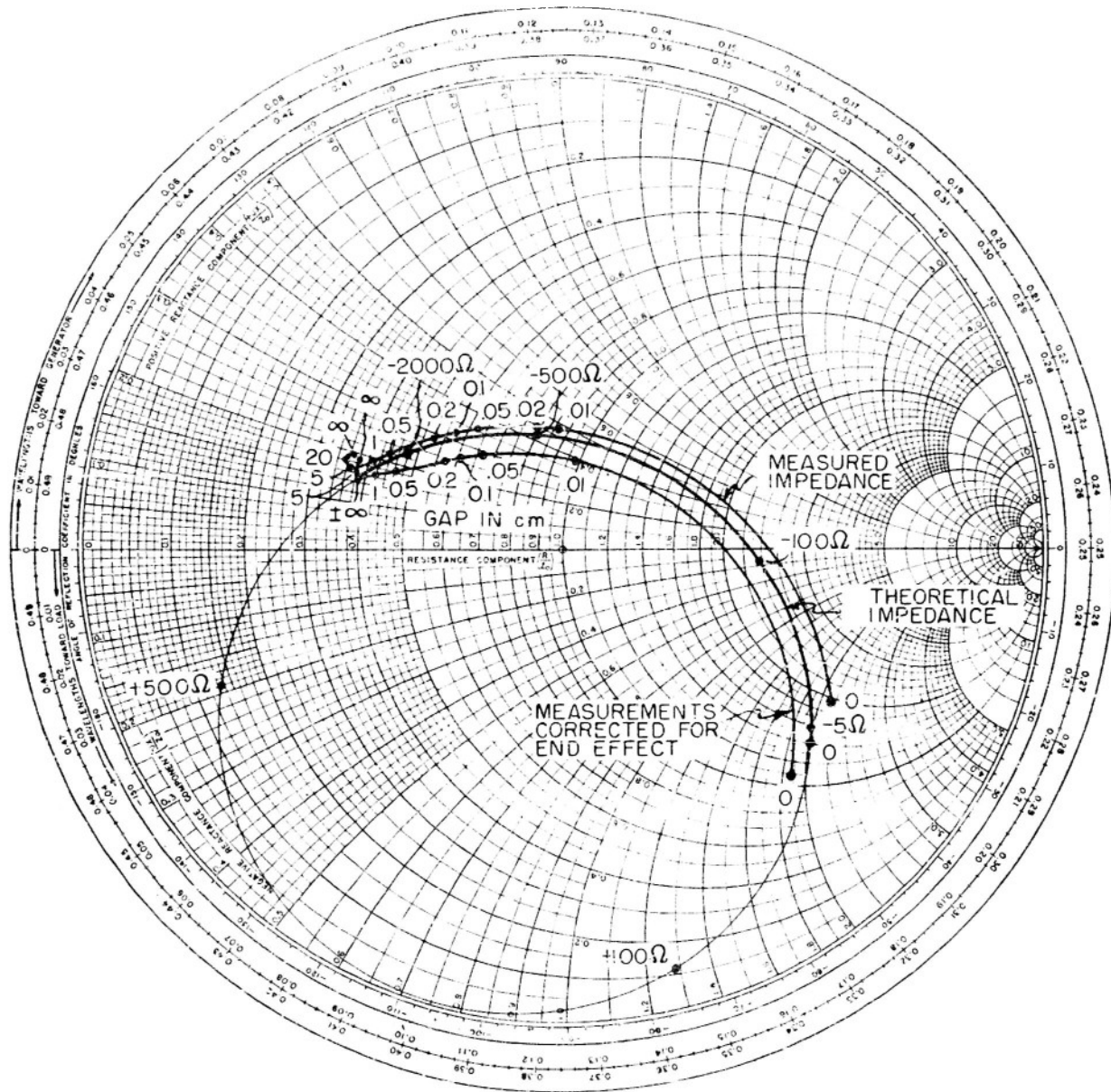
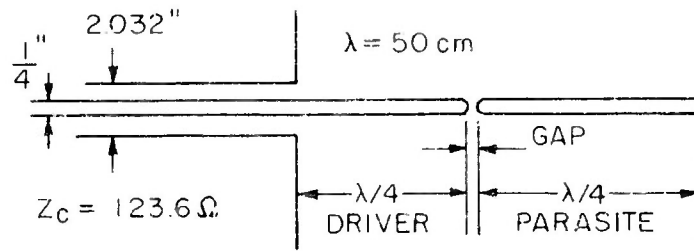


FIG. 16 COMPARISON OF THEORY AND MEASUREMENTS OF COLLINEAR ARRAY

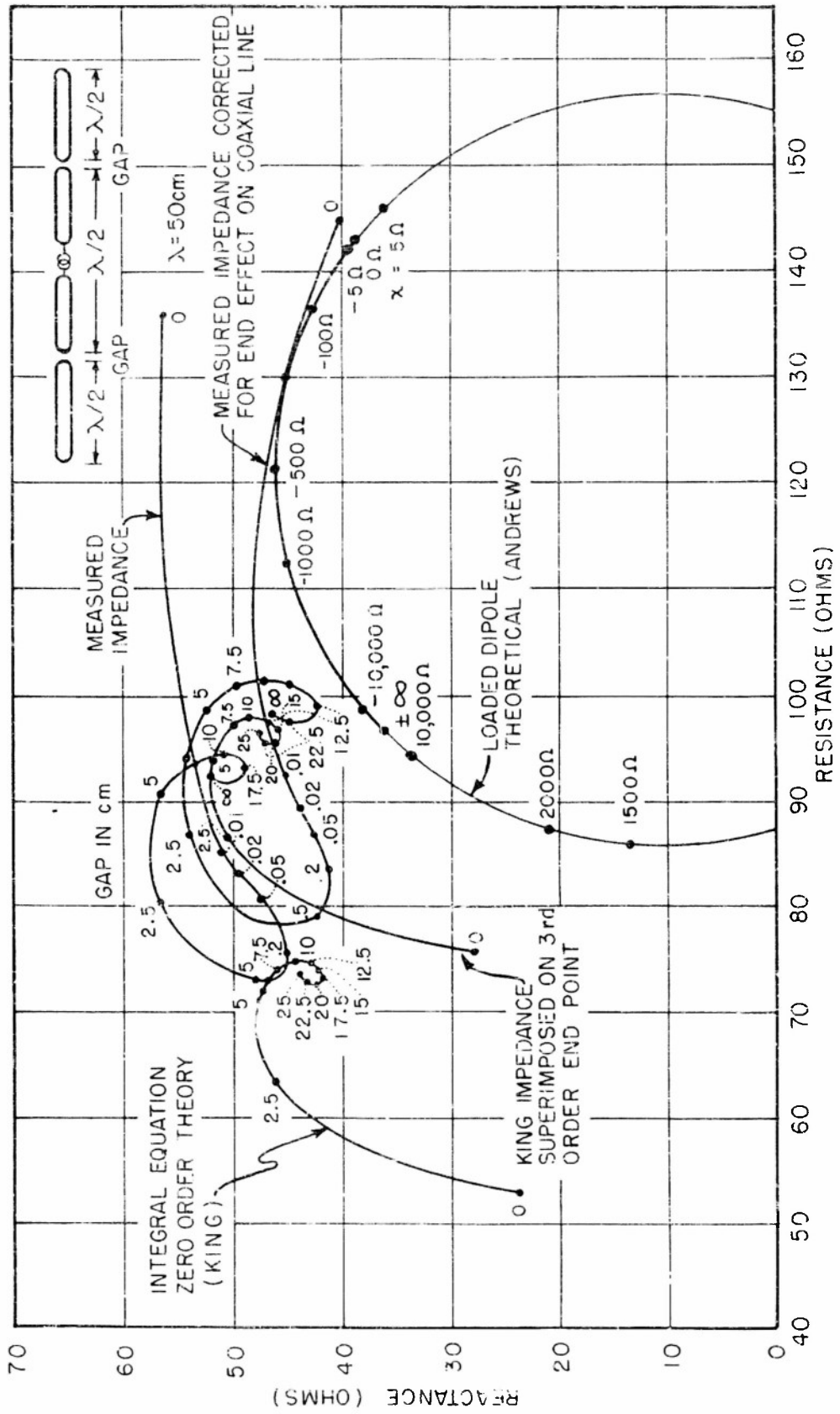


FIG. 18 COMPARISON OF THEORIES AND MEASUREMENTS

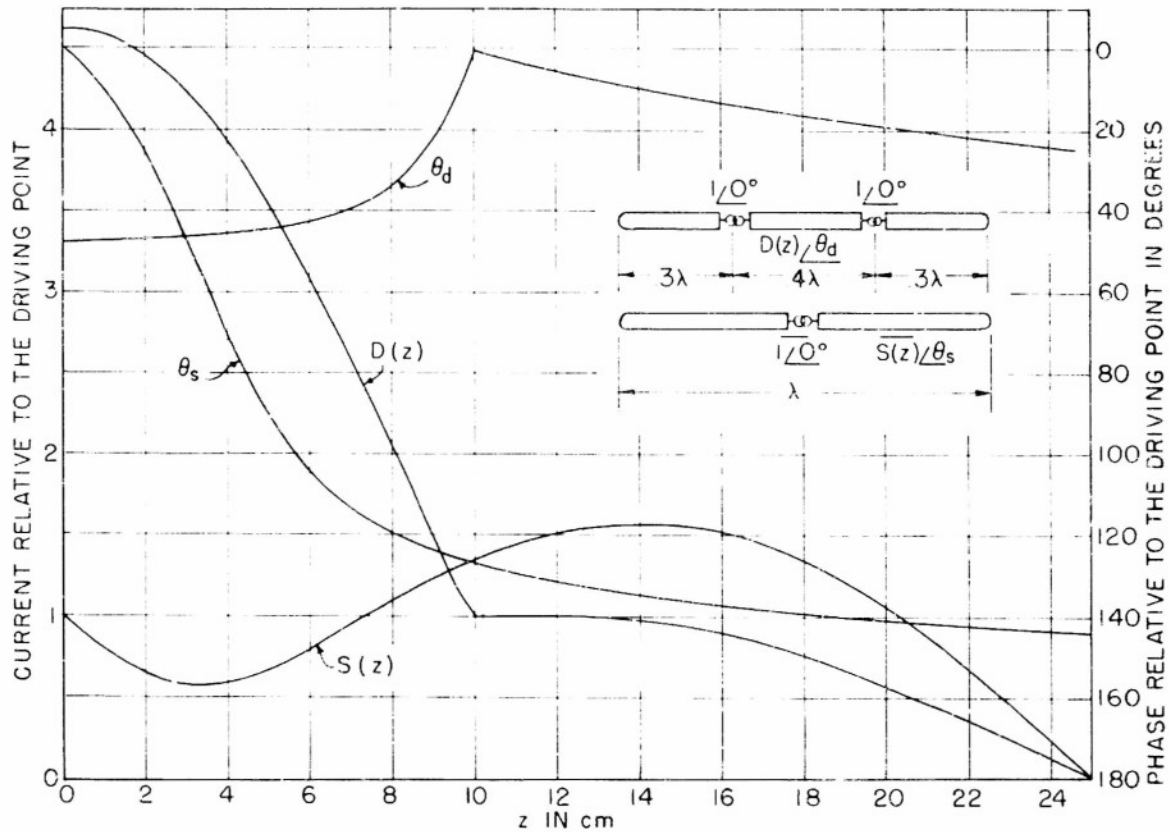


FIG. 19 THEORETICAL CURRENT DISTRIBUTION ON SINGLY AND DOUBLY DRIVEN DIPOLES

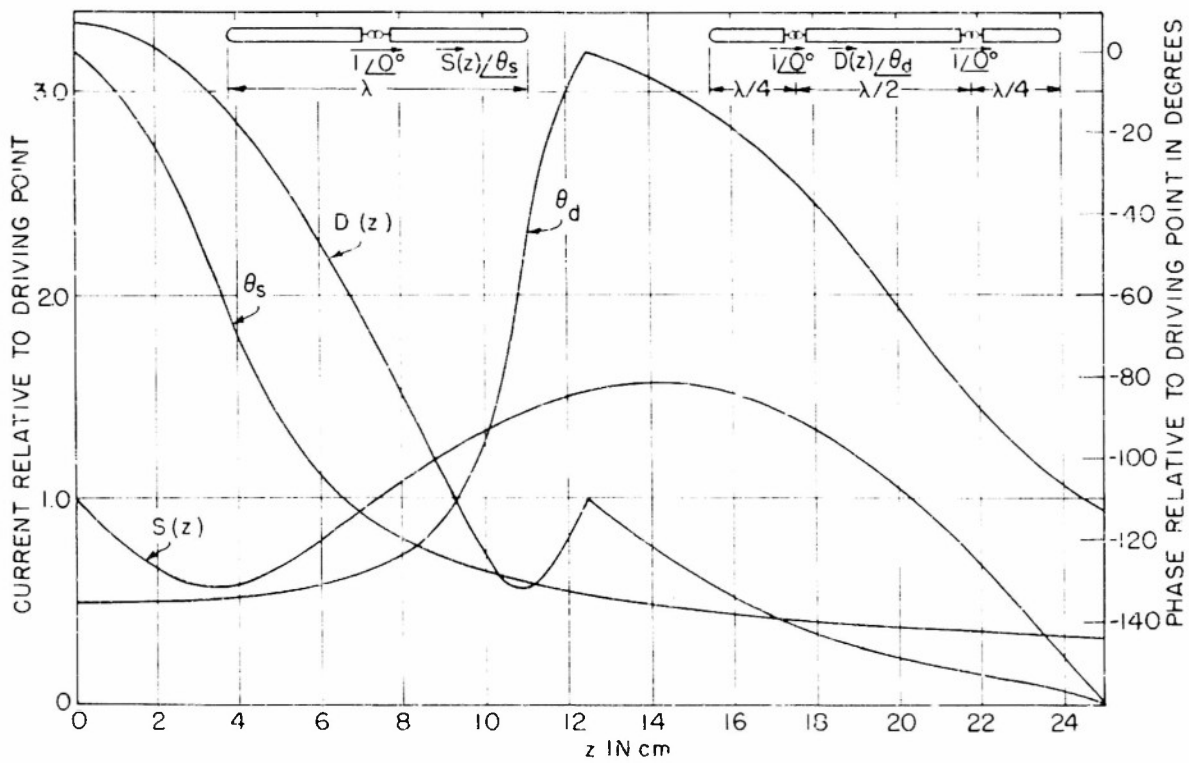


FIG. 20 THEORETICAL CURRENT DISTRIBUTION ON SINGLY AND DOUBLY DRIVEN DIPOLES

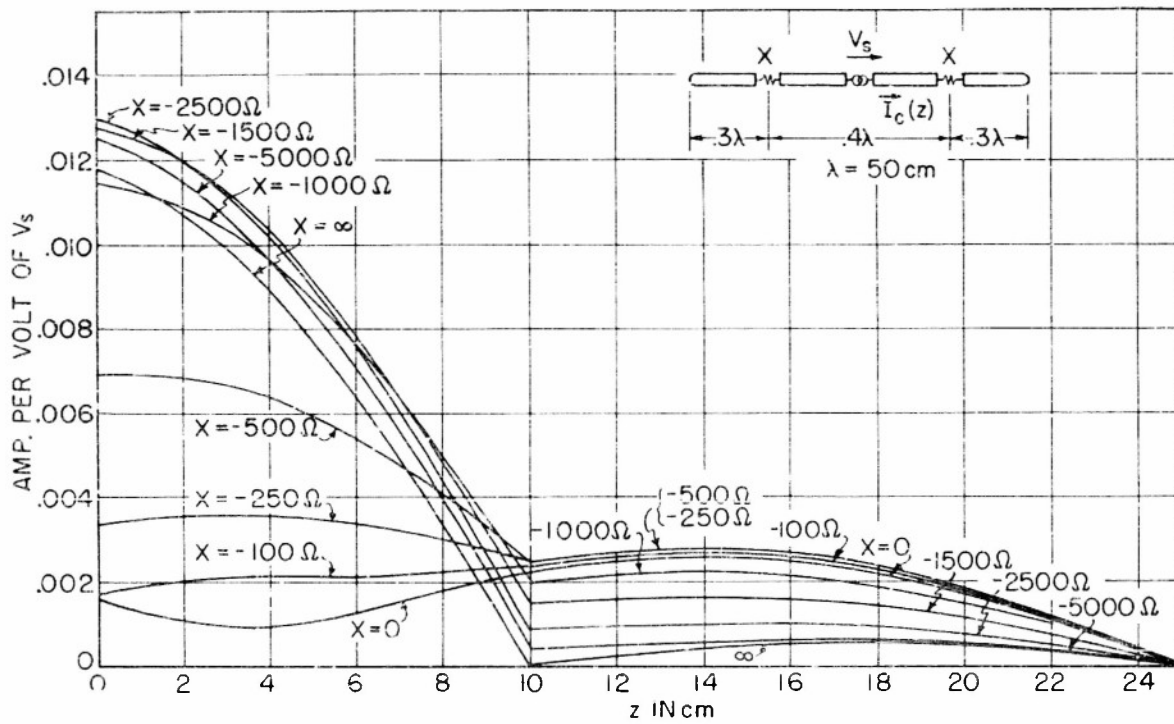


FIG. 21 THEORETICAL CURRENT DISTRIBUTION ON COLLINEAR ARRAY

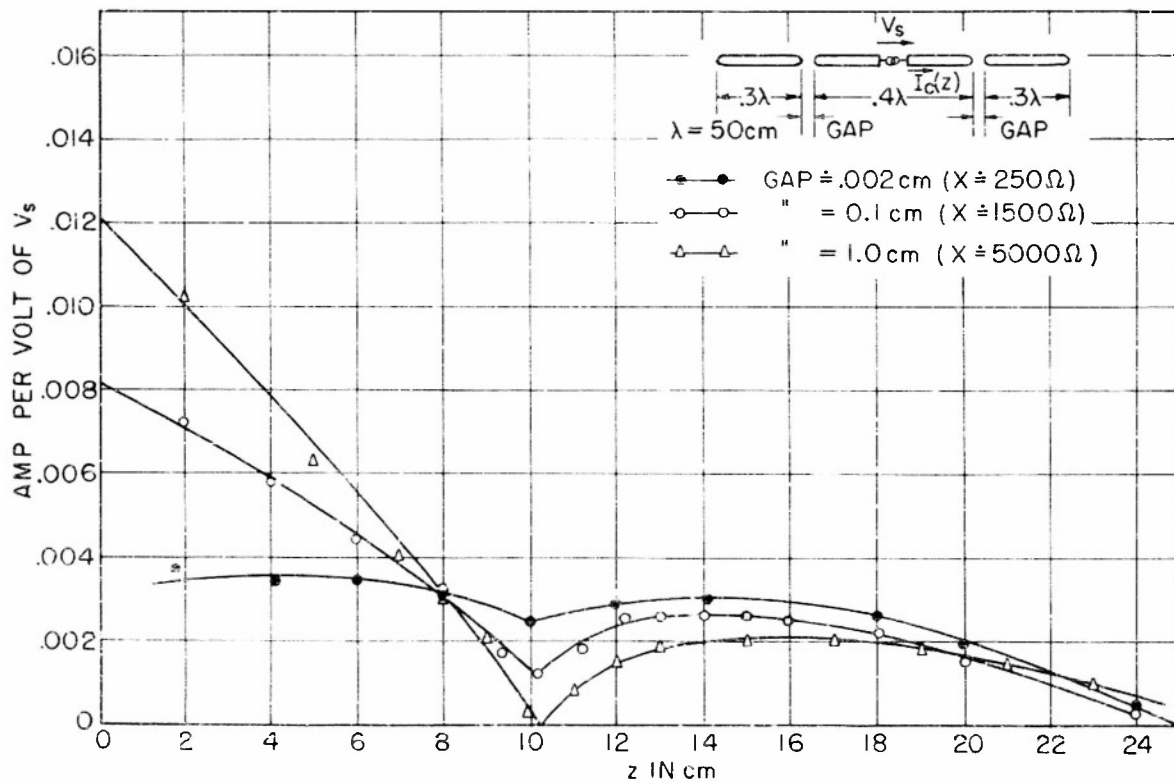


FIG. 22 MEASURED CURRENT DISTRIBUTION ON COLLINEAR ARRAY

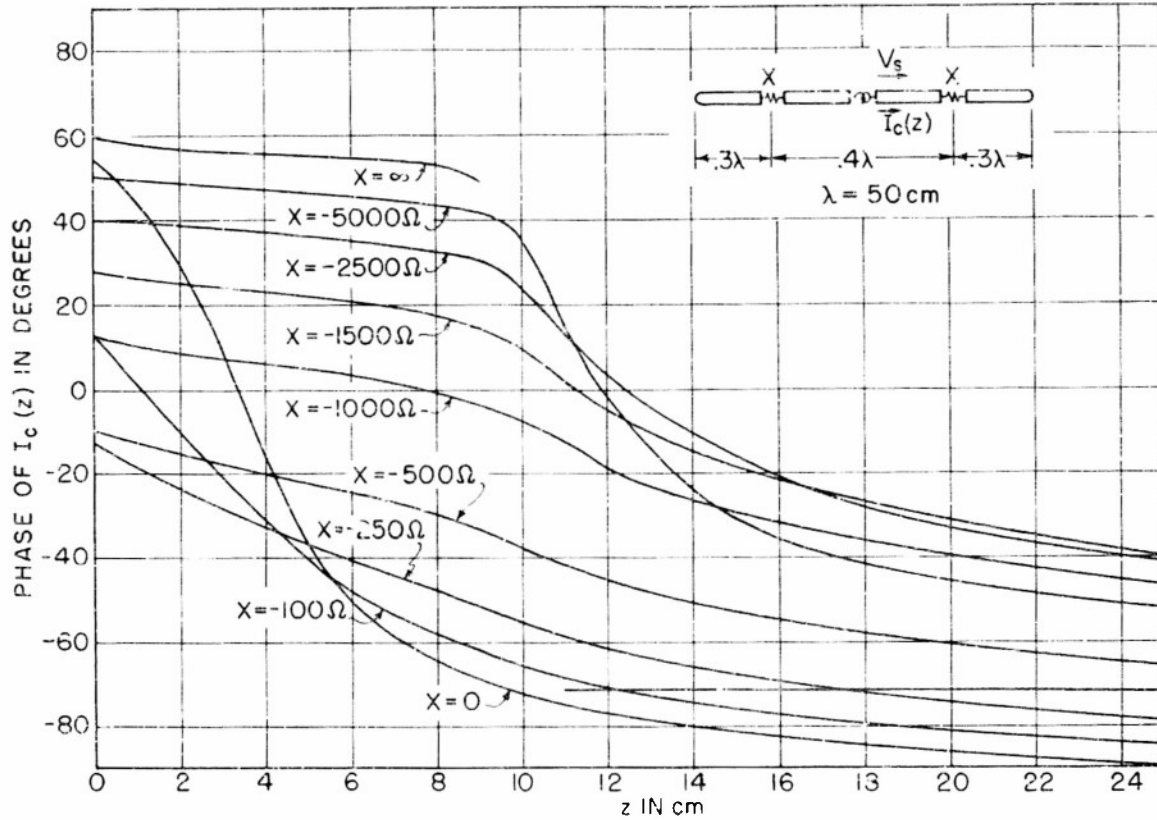


FIG. 23 PHASE OF THEORETICAL CURRENT DISTRIBUTION ON COLLINEAR ARRAY

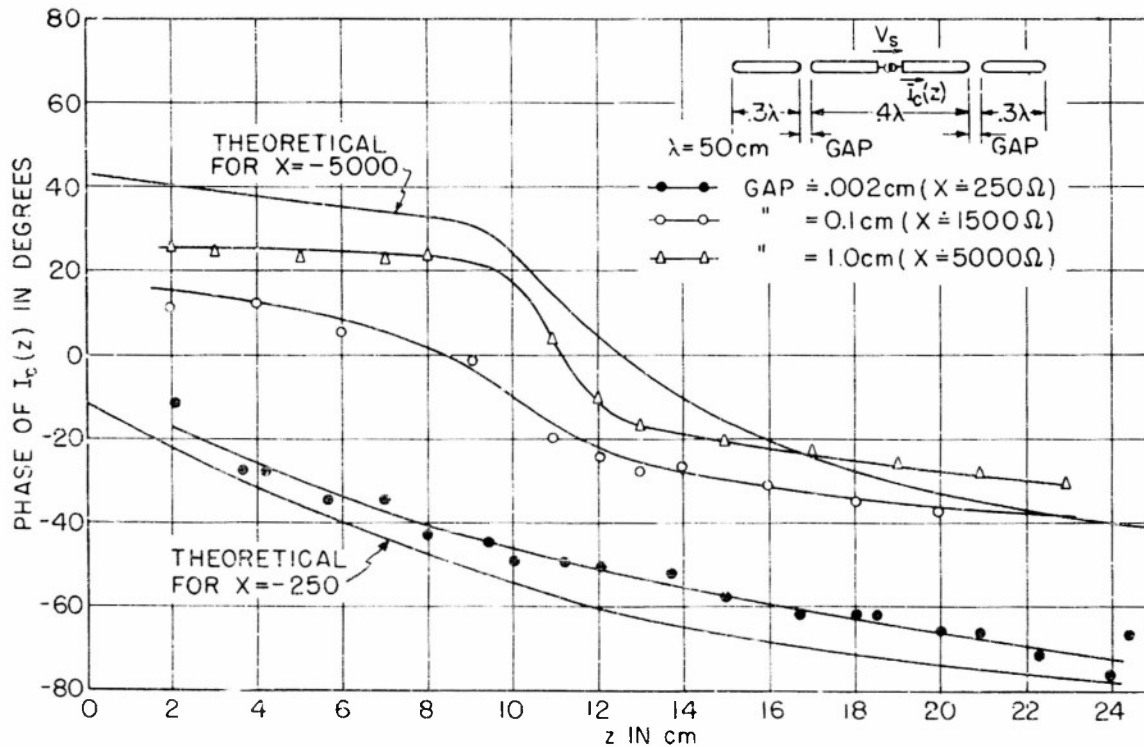


FIG. 24 MEASURED PHASE OF CURRENT DISTRIBUTION ON COLLINEAR ARRAY

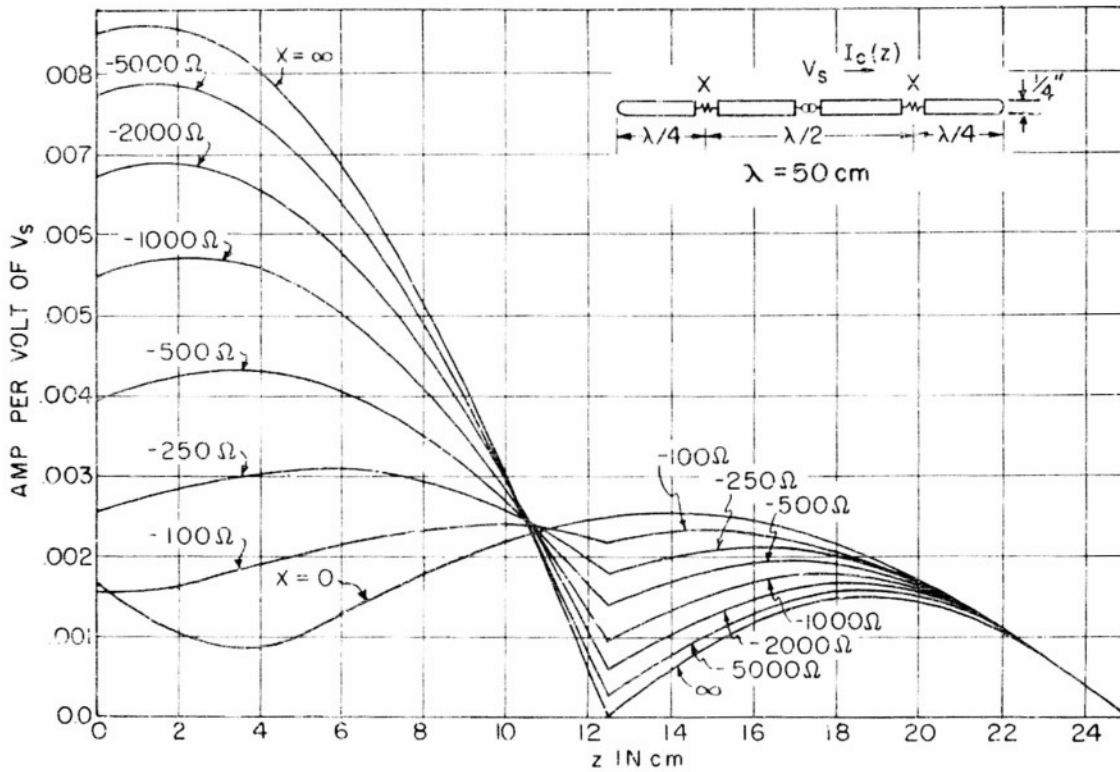


FIG. 25 THEORETICAL CURRENT DISTRIBUTION ON COLLINEAR ARRAY AS A FUNCTION OF LOADING REACTANCE

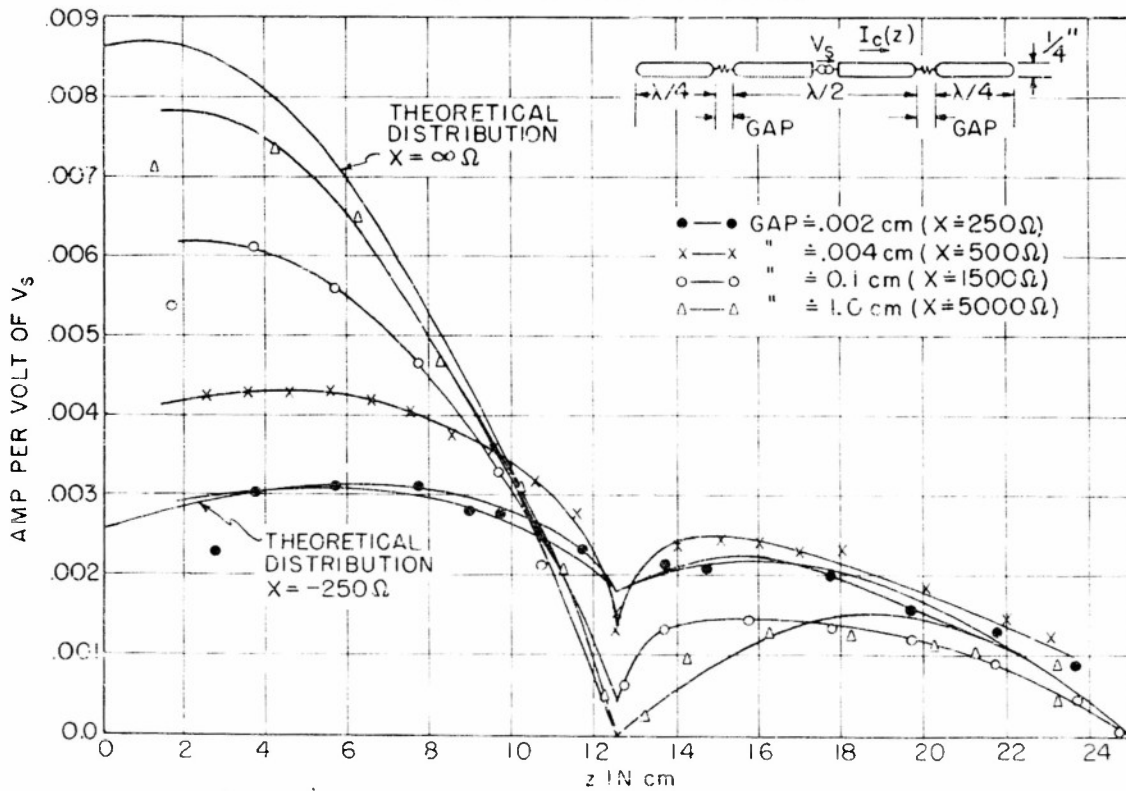


FIG. 26 MEASURED CURRENT DISTRIBUTION ON COLLINEAR ARRAY AS A FUNCTION OF GAP SIZE

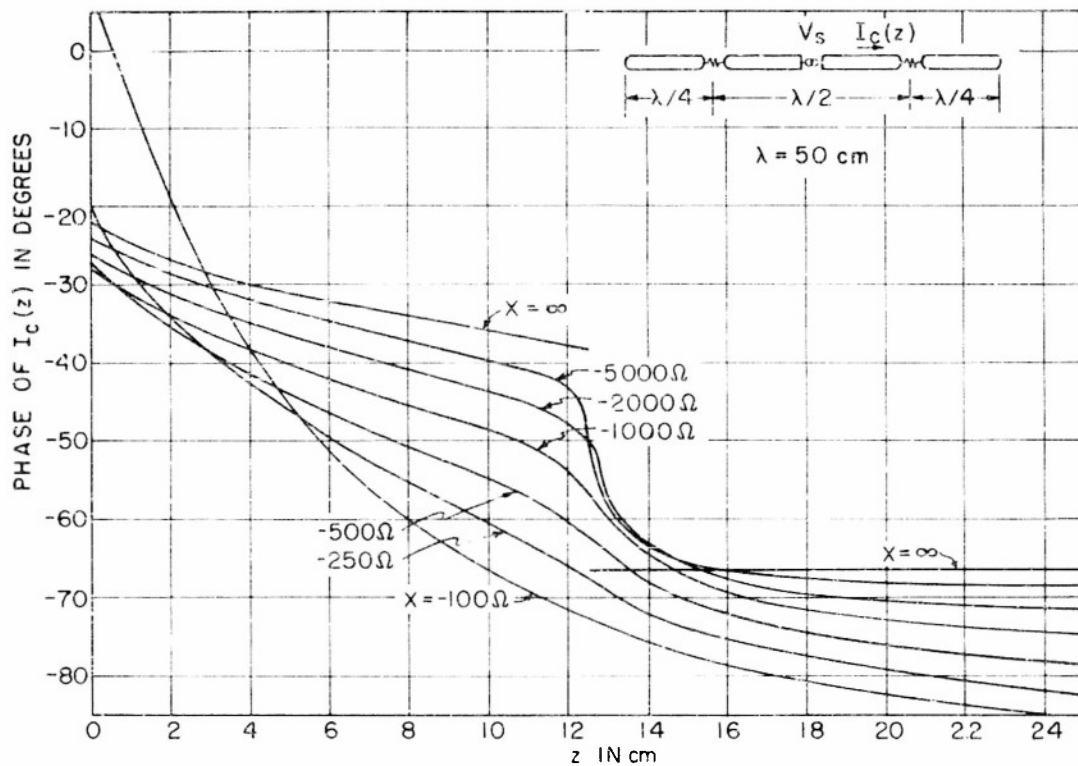


FIG. 27 PHASE OF THEORETICAL CURRENT DISTRIBUTION ON COLLINEAR ARRAY

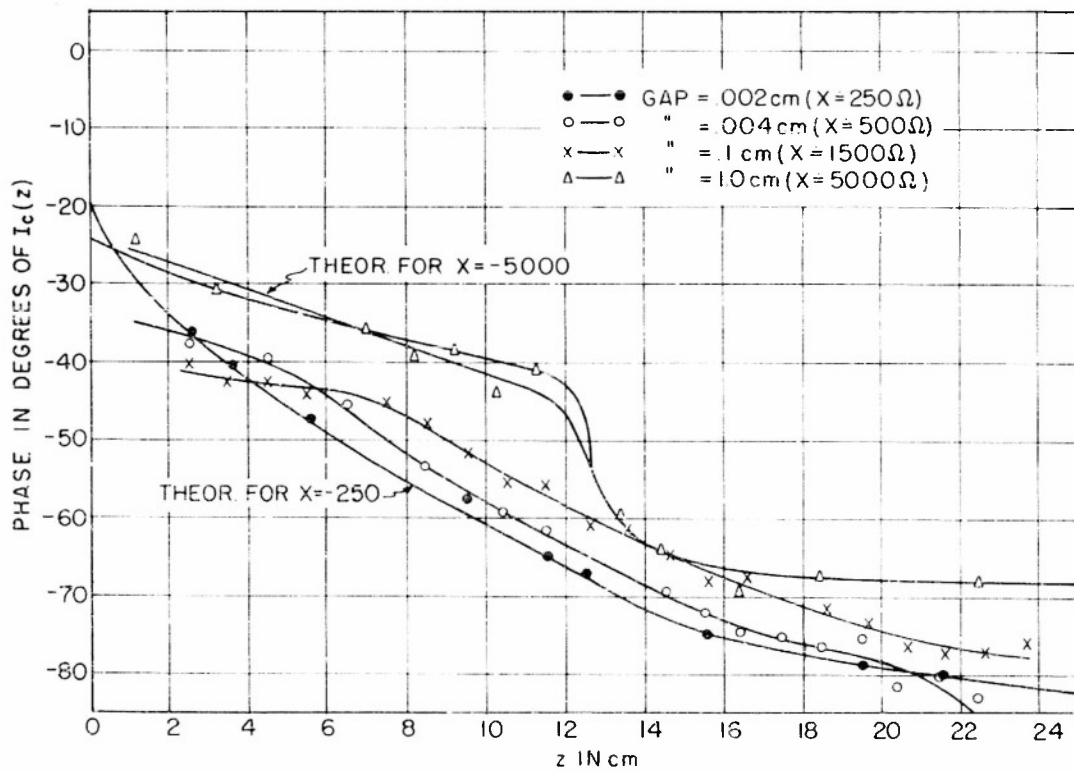


FIG. 28 MEASURED PHASE OF CURRENT DISTRIBUTION ON COLLINEAR ARRAY

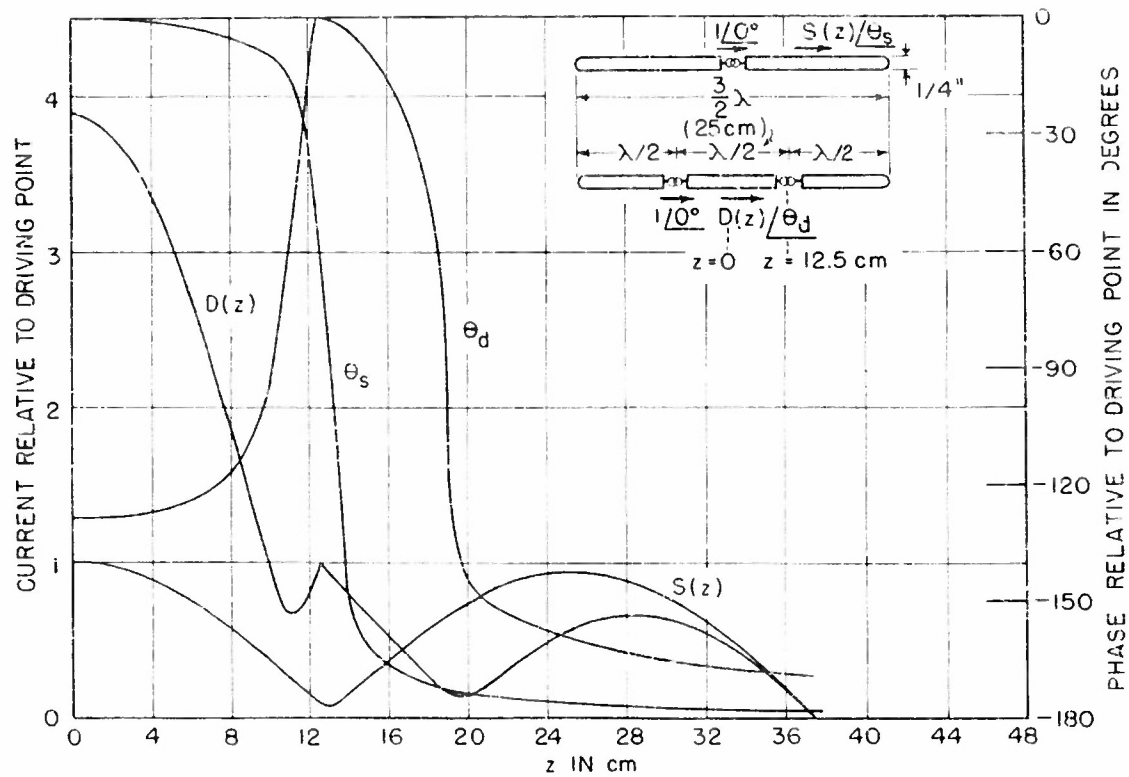


FIG. 29 THEORETICAL CURRENT DISTRIBUTION ON SINGLY AND DOUBLY DRIVEN DIPOLES

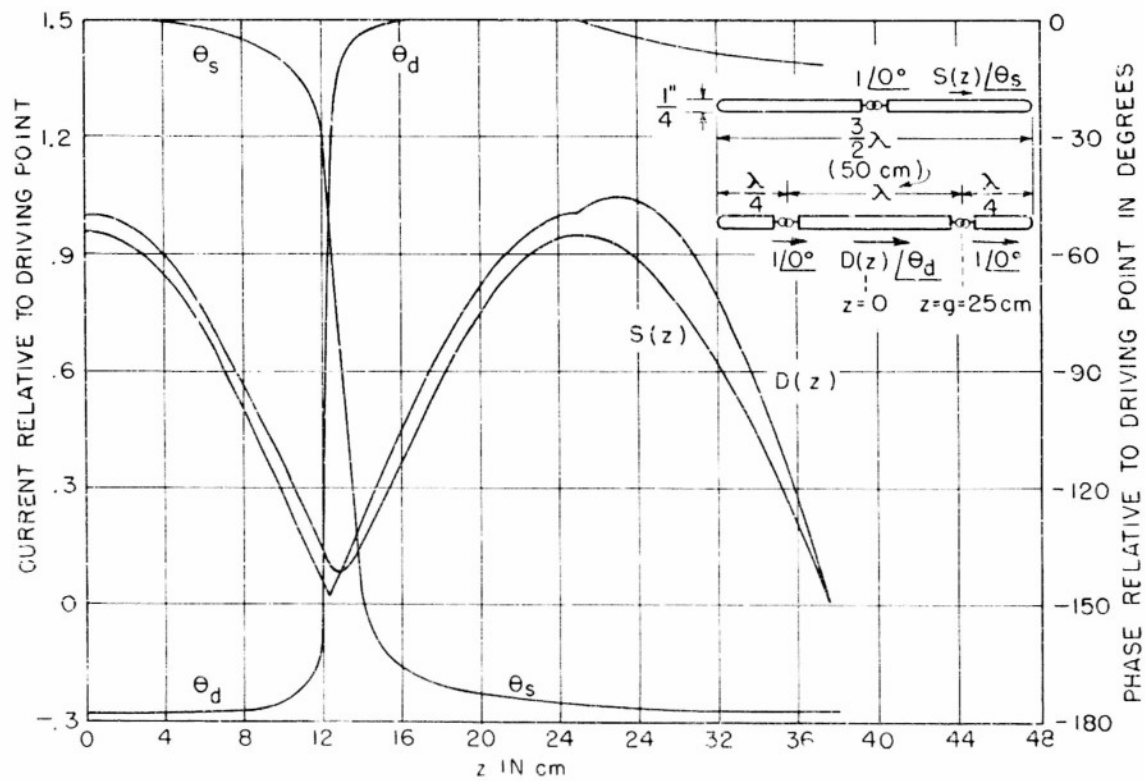


FIG. 30 THEORETICAL CURRENT DISTRIBUTION ON SINGLY AND DOUBLY DRIVEN DIPOLES

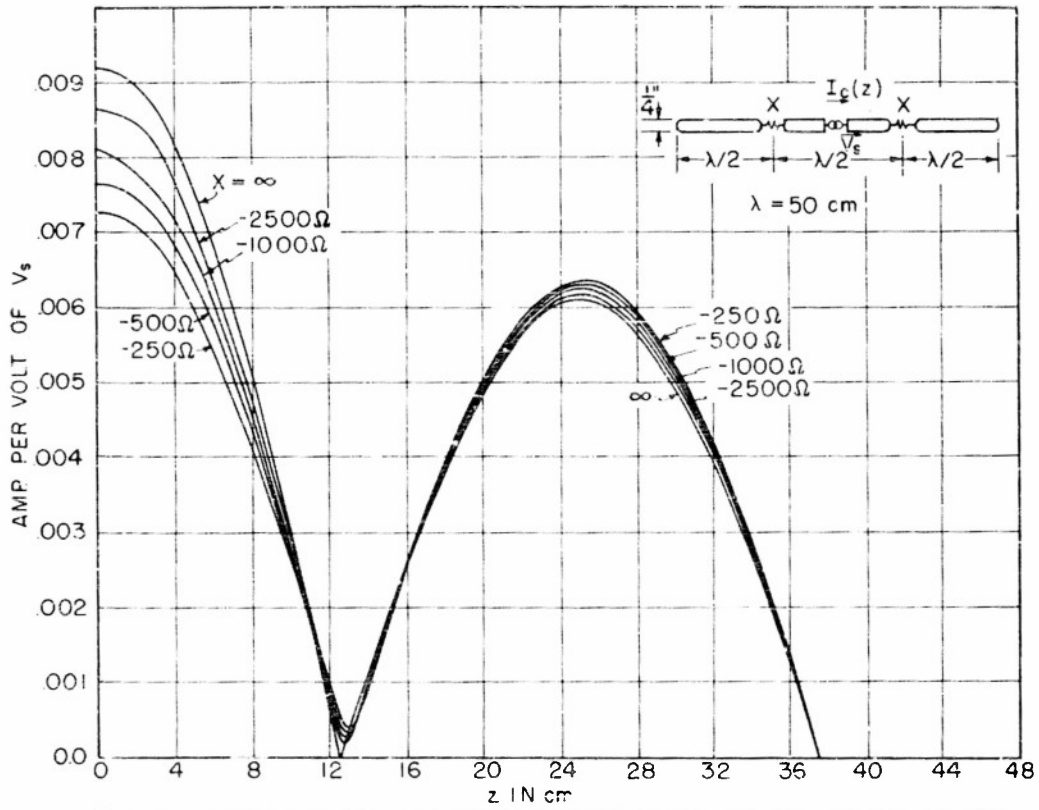


FIG. 31 THEORETICAL CURRENT DISTRIBUTION ON COLLINEAR ARRAY AS A FUNCTION OF LOADING REACTANCE

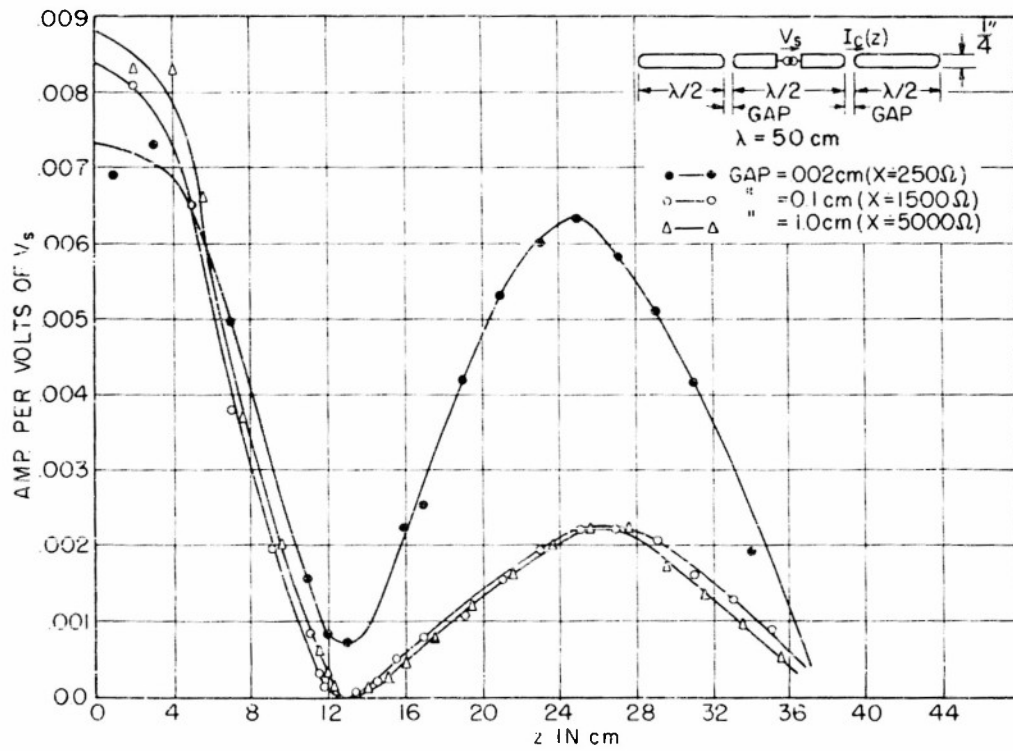


FIG. 32 MEASURED CURRENT DISTRIBUTION ON COLLINEAR ARRAY AS A FUNCTION OF GAP SIZE

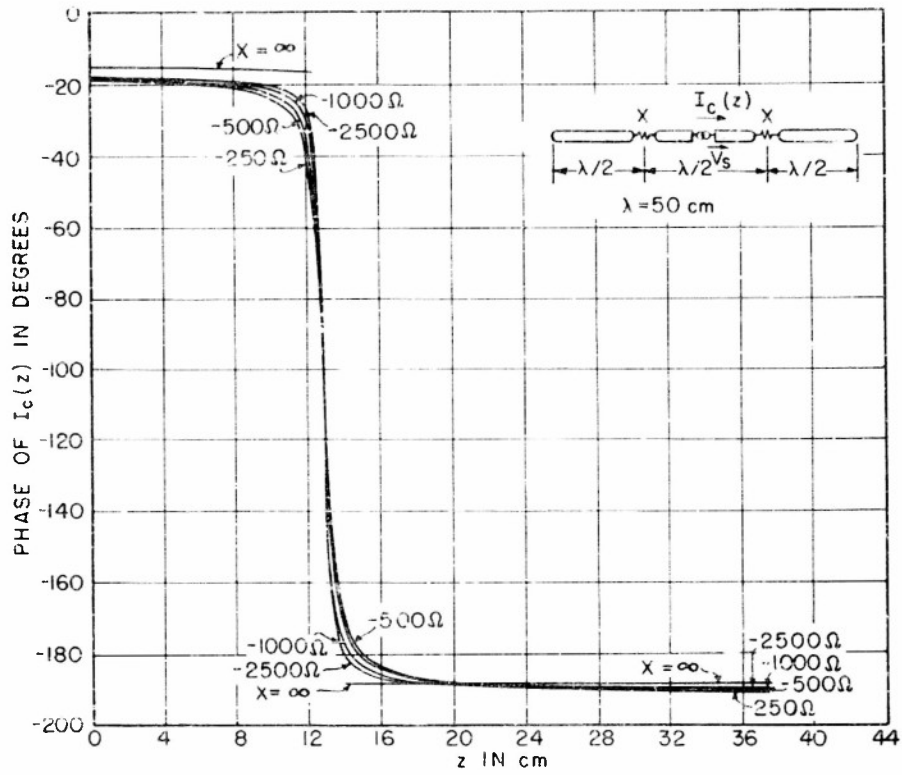


FIG. 33 PHASE OF THEORETICAL CURRENT DISTRIBUTION ON COLLINEAR ARRAY

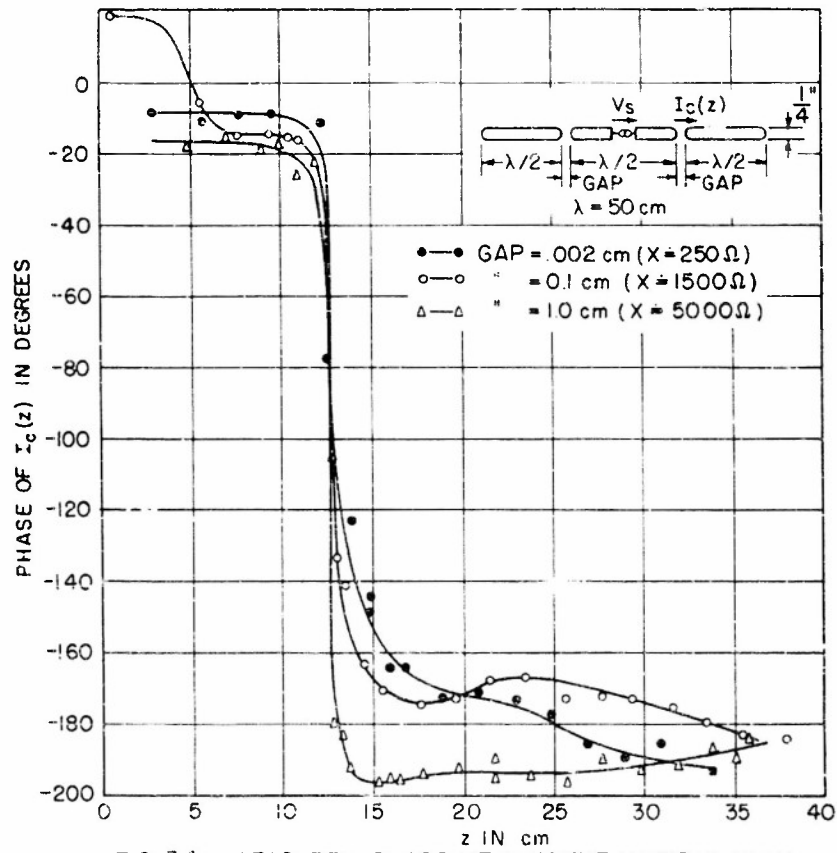


FIG. 34 MEASURED PHASE OF CURRENT DISTRIBUTION ON COLLINEAR ARRAY

are zero in the expressions for the γ 's used in the impedance expression. The trigonometric functions contained therein are zero for combinations of h and g equal to multiples of a quarter wavelength. The other important aspect is to choose a series of lengths that will check the theory over at least its expected range of usefulness. As described in section IV 1 such lengths are for g up to $\lambda/2$ and $h-g$ up to $3\lambda/4$. Such a series of combinations are listed in the table on page 34. In addition are listed the end-point dipoles into which the array degenerates for gaps equal to zero and infinity; the pertinent figures are also given. Figure 39 is a plot of the measured half-dipole impedances on the line with a few of the array impedance spirals.

The current distribution for a particular configuration is computed using Eq. (2-3) after first evaluating (2-26) and (2-23) for $I_d(z)$; $I_s(z)$ is obtained using the equations on p. 24. The phase and amplitude of the current distribution have been plotted as listed on page 34. The experimental data have been plotted by adjusting the experimental amplitude at the peaks to be the same as for the theoretical curves with the exception of Fig. 41 which has been plotted so the amplitude at $z = 0$ corresponds to the measured driving-point impedance for this case. The position of the current relative to the distance scale has been occasionally adjusted to account for errors in knowing the position of the auxiliary probe on the polyfoam column supporting the array.

Equation (2-4) for the theoretical array impedance requires the use of the current distribution at $z = 0$ and at $z = g$. The impedance Z is the apparent reactance X of the gap. Z_c may be computed directly, but there is occasionally some additional information which may be either directly incorporated into the computations or merely used as a check on the infinite gap. The value of Z_c for the infinite gap point is occasionally known from another computation; for example, for configuration 4 of the table $Z_c(\text{gap} = \infty)$ is that for a dipole of half height equal to $\lambda/2$. This impedance is known since it is a necessary part of the computation of Z_c for configuration 2. It may be used as follows. Equation (2-4) is

$$Z_c = Z_s(h) / \left[1 - \frac{D(0)S(g)}{1 + Z_d/Z} \right]$$

LIST OF FIGURES AND IMPEDANCE END-POINTS

Configura- tion	Driving Antenna half- length	Parasite full- length	Zero-gap dipole half- height	infinite gap dipole half- height	impedance comparison for theory and experiment	Distribution comparisons theory and experiment		doubly driven and singly driven dipole currents
						amplitude	phase	
1	.2λ	.3λ	.5λ	.2λ	Fig. 15	Figs. 21 and 22	Figs. 23 and 24	Fig. 19
2	.25λ	.25λ	.5λ	.25λ	Fig. 16	Figs. 25 and 26	Figs. 27 and 28	Fig. 20
3	.25λ	.5λ	.75λ	.25λ	Fig. 18	Figs. 31 and 32	Figs. 33 and 34	Fig. 29
4	.5λ	.25λ	.75λ	.5λ	Fig. 17	Figs. 35 and 36	Figs. 37 and 38	Fig. 30

Evaluating this for the experimentally infinite gap point or for $Z = \infty$ in (2-4) there results

$$Z_c(\text{gap} = \infty) = Z_s(h) / \left[1 - D(0)S(g) \right] \quad (4-1)$$

However this $Z_c(\text{gap} = \infty)$ is that of a singly driven dipole of half height equal to the gap position g ; that is,

$$Z_c(\text{gap} = \infty) = Z_s(\text{half height} = g) \quad (4-2)$$

The symbol $Z_s(\text{half-height} = g)$ is used to avoid any confusion resulting from using the letter h in a description of this dipole. Substituting (4-2) in (4-1) yields

$$D(0)S(g) = 1 - \frac{Z_s(h)}{Z_s(\text{half height} = g)} \quad (4-3)$$

Equation (4-3) was used in the computation for Fig. 17 and considerably improved the theoretical agreement with experiment. It was also used in Fig. 16 and Fig. 18 but had very little effect since the agreement was already quite good. It was not used in Fig. 15. Note that $Z_s(\text{half-height} = g)$ is obtained theoretically by evaluation of 2-29 for the height of interest.

4. Conclusions

The agreement between theoretical computations and experimental measurements is as considered in Section IV-1. When $g < (h-g)$ and both are short, the measurements are in best agreement. The agreement is generally good for configuration 1 (see table on page 34) for a $.2\lambda$ driving element and a $.3\lambda$ parasite. It is less so for configuration 2 in which both elements are $\lambda/4$ long, and it is least good for the 4th case. The impedances generally agree quite well for all except configuration 4 for which the conditions on the trial current distributions are not met. This is to be expected since the variational principle technique allows the use of a rather poor current approximation in obtaining comparatively good impedance values. Note that the agreement (see Fig. 18) of the theory of King is good for large spacings if the theoretical curve were displaced such that the infinite gap point was superimposed onto a better end-point impedance than that obtained in his zero-order theory. The

discrepancy for small spacings is to be expected since his theory is based entirely on varying the coupling between the cylindrical surfaces of the antenna elements and will be in error when the end-cap coupling is appreciable.

On the Smith Chart of Fig. 39 is plotted a curve for the measured half-dipole impedance and a few of the impedance arcs for collinear arrays. This makes the relation of the end-point impedance of the array to those of the half dipole quite obvious. It also makes it possible to guess roughly where an impedance would fall for some other configurations than those considered here.

In conclusion, a theory for the close-spaced collinear array has been formulated on the basis that the array is the superposition of a doubly and a singly driven dipole. The theory has been evaluated for a series of specific configurations that are typical of the applicable range of the theory. These same configurations have been investigated experimentally as a check on the basic assumptions in the theory and also as a check that the region of usefulness of the theory has been properly estimated.

5. A Two-Wire Line as a Coupling Reactance between Elements

This type of coupling has been very briefly considered experimentally. The devices pictured in Fig. 40 have been used to couple the ends of the driven element and the parasitic elements. These permit the coupling reactance between the elements to be varied without changing their spacing. The experimental setup is similar to that used elsewhere except small two-wire line is used at the gap. It has a characteristic impedance of 135 ohms and a spacing of 0.2 inches. Two arrangements were used. One of these is a line whose overall length is constant and upon which a shorting bar is moved. The other is one the overall length of which is varied. Both are needed for a complete study of the problem. The first will have a constant length for the unbalanced mode on the open-wire line; the other will present a variable length to the unbalanced mode. Plots are given in the last figure showing the measured driving-point impedance using both of the line types. The points labeled constant-overall-length line are those for the line using the shorting bar.

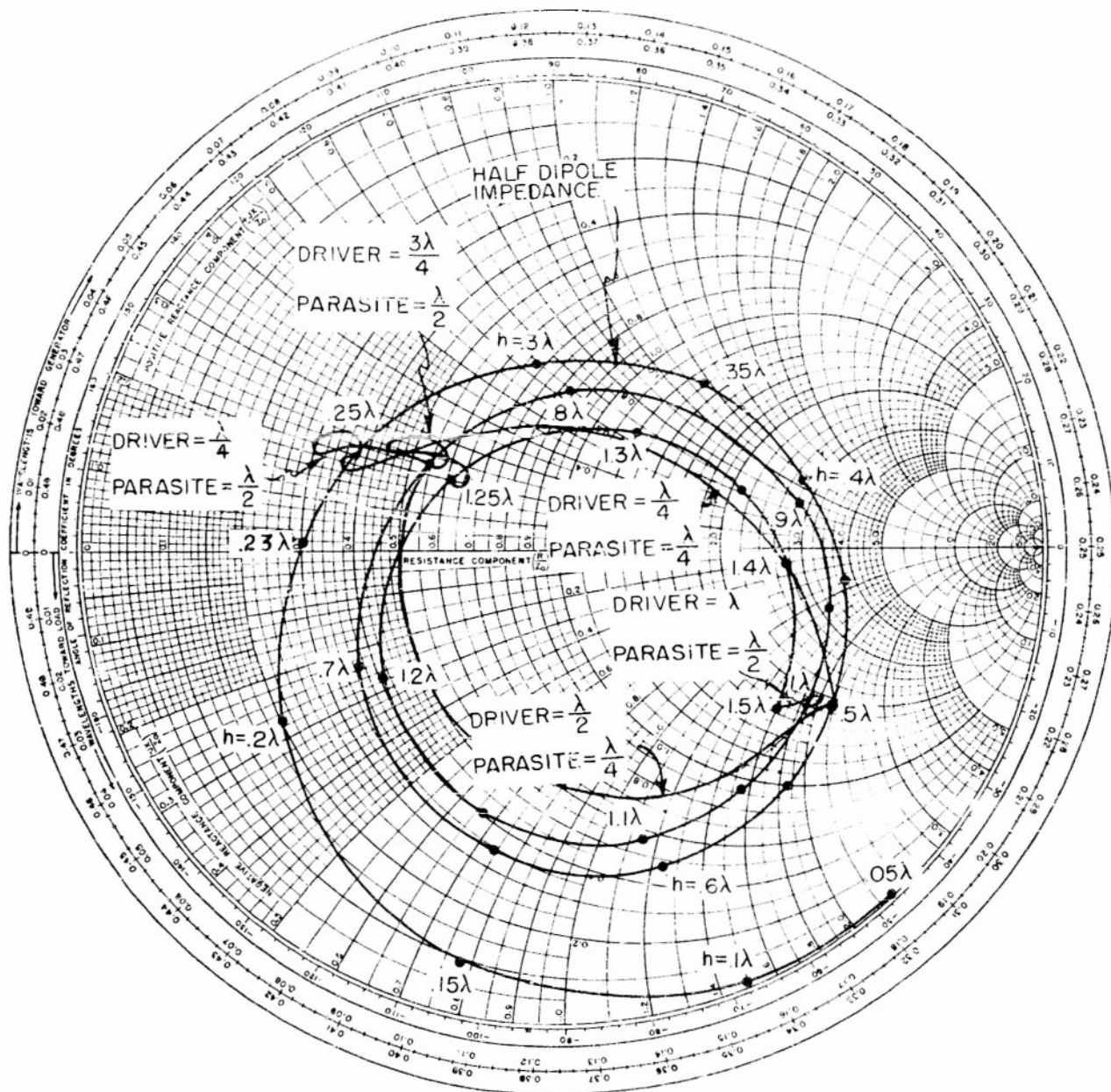
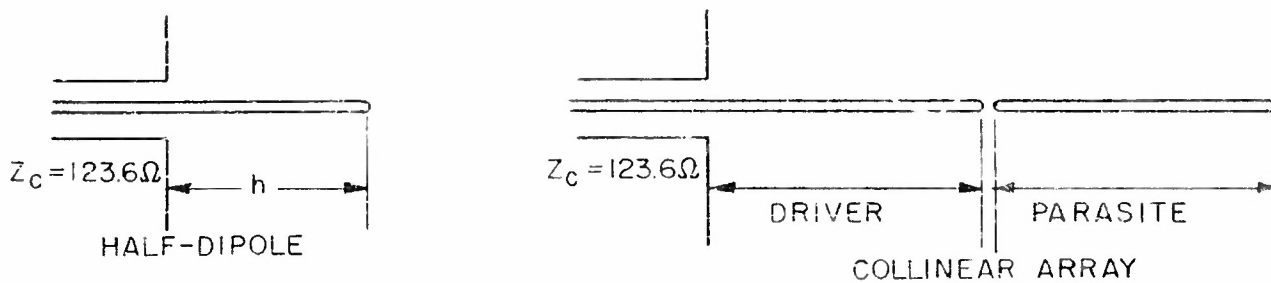


FIG. 39 COMPARISON OF MEASURED HALF-DIPOLE IMPEDANCE WITH MEASURED ARRAY IMPEDANCES

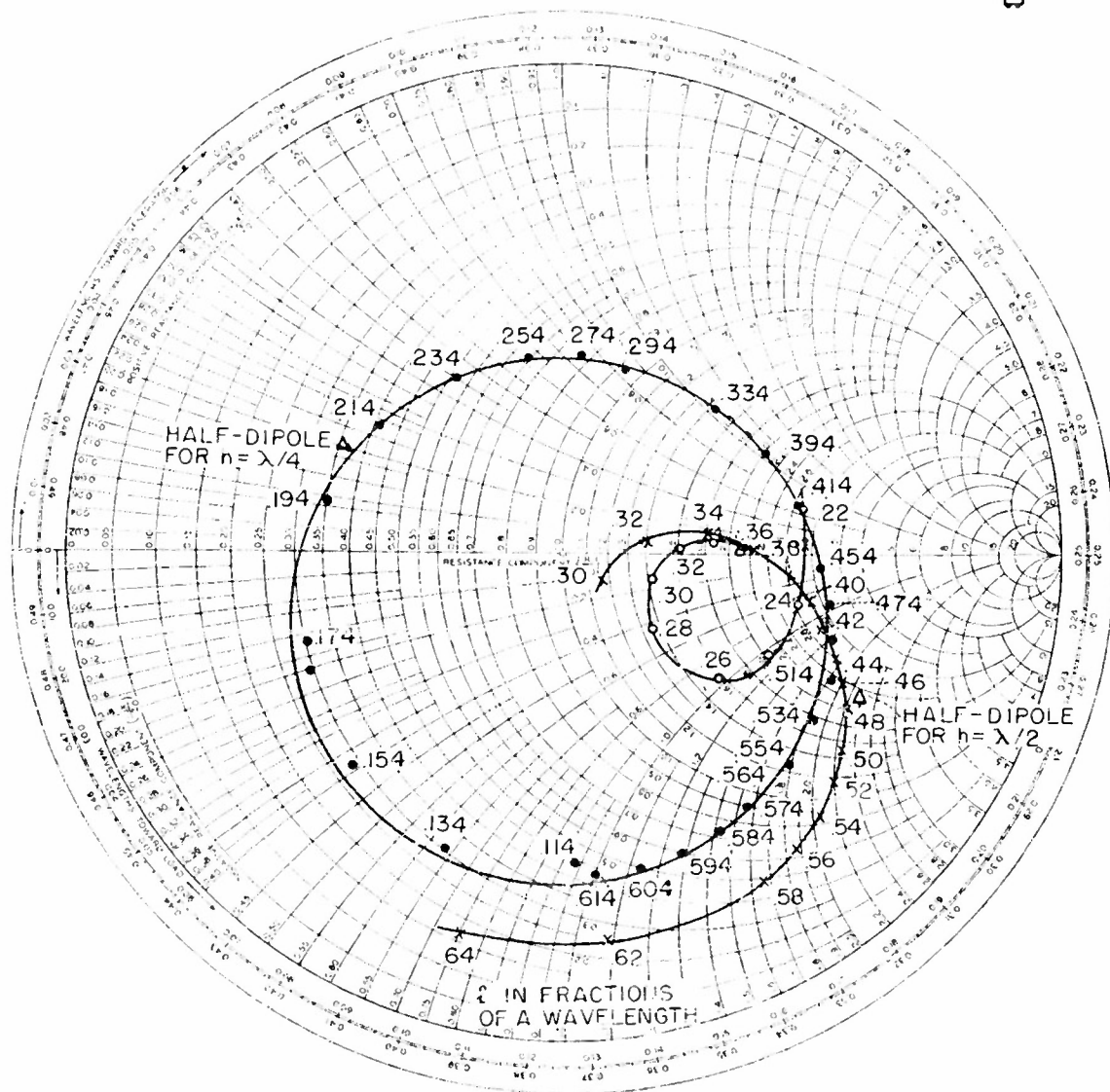
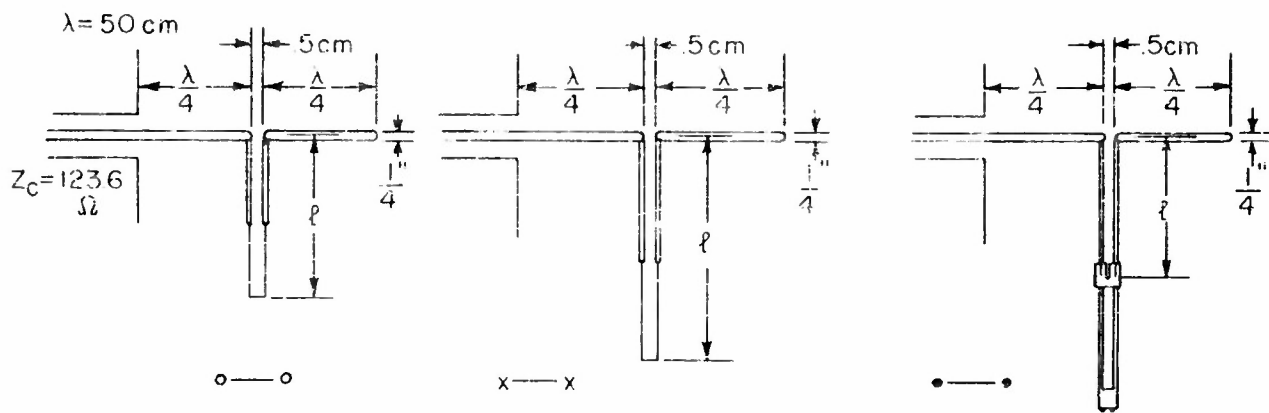


FIG. 40 MEASURED IMPEDANCE USING TWO-WIRE LINE COUPLING BETWEEN ELEMENTS

Appendix A

EVALUATION OF THE γ -INTEGRALS

The substitution of (2-26) and (2-27) into (2-25) yields*

$$\begin{aligned}
 Z_d = \frac{-\mu}{4\pi} & \left\{ -j\omega(1+aC) \int_0^g dz [1+C(a+\cos\beta z)] \int_0^g [K(z,z') + K(z,-z')] dz' \right. \\
 & + \int_0^g dz [1+C(a+\cos\beta z)] \int_{g-}^{g+} [K(z,z') + K(z,-z')] L(z') I_d(z') dz' \\
 & - j\omega(\delta + \epsilon D) \int_0^g dz [1+C(a+\cos\beta z)] \int_g^h [K(z,z') + K(z,-z')] dz' \\
 & \left. - j\omega(1+aC) \int_g^h dz \left[\delta \left\{ 1 - \cos\beta(h-z) \right\} + D(\sin\beta(h-z) + \epsilon \left\{ 1 - \cos\beta(h-z) \right\}) \right] \right. \\
 & \quad \int_0^g [K(z,z') + K(z,-z')] dz' \\
 & \left. + \int_g^h dz \left[\delta \left\{ 1 - \cos\beta(h-z) \right\} + D(\sin\beta(h-z) + \epsilon \left\{ 1 - \cos\beta(h-z) \right\}) \right] \right. \\
 & \quad \left. \int_{g-}^{g+} [K(z,z') + K(z,-z')] L(z') I_d(z') dz' \right\}
 \end{aligned}$$

*Most of the following expressions are taken from reference 6.

$$\begin{aligned}
& -j\omega(\delta + \epsilon D) \int_g^h dz \left[\delta \{1 - \cos \beta(h-z)\} + D(\sin \beta(h-z) + \epsilon \{1 - \cos \beta(h-z)\}) \right] \\
& \int_g^h [K(z, z') + K(z, -z')] dz' \\
& - \frac{j\omega}{\beta} D \int_0^g [1 + C(\alpha + \cos \beta z)] [K(z, h) + K(z, -h)] dz \\
& - \frac{j\omega}{\beta} D \int_g^h \left[\delta \{1 - \cos \beta(h-z)\} + D(\sin \beta(h-z) + \epsilon \{1 - \cos \beta(h-z)\}) \right] \\
& \quad [K(z, h) + K(z, -h)] dz \Big\} . \tag{A-1}
\end{aligned}$$

Note that the integral in the variable z' may be simplified by

$$\begin{aligned}
& \int_{g^-}^{g^+} [K(z, z') + K(z, -z')] L(z') I_d(z') dz' = \\
& - \frac{j\omega}{\beta} [K(z, g) + K(z, -g)] \int_{g^-}^{g^+} \frac{d^2}{dz'^2} (I_d(z')) dz' = \\
& - \frac{j\omega}{\beta} [K(z, g) + K(z, -g)] [\epsilon + D + C \sin \beta g]
\end{aligned}$$

Using this in (A-1) yields

$$Z_d = \frac{j\zeta}{4\pi} [\gamma_0 + \gamma_C C + \gamma_D D + \gamma_{CD} CD + \gamma_{CC} C^2 + \gamma_{DD} D^2]$$

where

$$\gamma_0 = \beta \int_0^g dz \int_0^g [K(z, z') + K(z, -z')] dz'$$

$$\begin{aligned}
& + \epsilon \int_0^g [K(z, g) + K(z, -g)] dz \\
& + \beta \delta \int_0^g dz \int_g^h [K(z, z') + K(z, -z')] dz' \\
& + \beta \delta \int_g^h dz \{1 - \cos \beta(h-z)\} \int_0^g [K(z, z') + K(z, -z')] dz' \\
& + \delta \epsilon \int_g^h \{1 - \cos \beta(h-z)\} [K(z, g) + K(z, -g)] dz \\
& + \beta \delta^2 \int_g^h dz \{1 - \cos \beta(h-z)\} \int_g^h [K(z, z') + K(z, -z')] dz' \\
\gamma_C = & \beta \int_0^g dz (2a + \cos \beta z) \int_0^g [K(z, z') + K(z, -z')] dz' \\
& + \epsilon \int_0^g (a + \cos \beta z) [K(z, g) + K(z, -g)] dz \\
& + \sin \beta g \int_0^g [K(z, g) + K(z, -g)] dz \\
& + \beta \delta \int_0^g dz (a + \cos \beta z) \int_g^h [K(z, z') + K(z, -z')] dz' \\
& + a \beta \delta \int_g^h dz \{1 - \cos \beta(h-z)\} \int_0^g [K(z, z') + K(z, -z')] dz' \\
& + \delta \sin \beta g \int_g^h \{1 - \cos \beta(h-z)\} [K(z, g) + K(z, -g)] dz
\end{aligned}$$

$$\begin{aligned}
\gamma_{CD} = & \int_0^g (a + \cos \beta z) [K(z, g) + K(z, -g)] dz \\
& + \epsilon \beta \int_0^g dz (a + \cos \beta z) \int_g^h [K(z, z') + K(z, -z')] dz' \\
& + \alpha \beta \int_g^h dz \sin \beta (h-z) \int_0^g [K(z, z') + K(z, -z')] dz' \\
& + \alpha \epsilon \beta \int_g^h dz \{1 - \cos \beta (h-z)\} \int_0^g [K(z, z') + K(z, -z')] dz' \\
& + \sin \beta g \int_g^h \sin \beta (h-z) [K(z, g) + K(z, -g)] dz \\
& + \epsilon \sin \beta g \int_g^h \{1 - \cos \beta (h-z)\} [K(z, g) + K(z, -g)] dz \\
& + \int_0^g (a + \cos \beta z) [K(z, h) + K(z, -h)] dz
\end{aligned}$$

$$\begin{aligned}
\gamma_{CC} = & \alpha \beta \int_0^g dz (a + \cos \beta z) \int_0^g [K(z, z') + K(z, -z')] dz' \\
& + \sin \beta g \int_0^g (a + \cos \beta z) [K(z, -g) + K(z, g)] dz
\end{aligned}$$

$$\begin{aligned}
\gamma_D = & \int_0^g [K(z, g) + K(z, -g)] dz + \int_0^h [K(z, h) + K(z, -h)] dz \\
& + \epsilon \beta \int_g^h dz \{2 - \cos \beta (h-z)\} \int_0^g [K(z, z') + K(z, -z')] dz'
\end{aligned}$$

$$\begin{aligned}
& + \beta \int_g^h dz \sin \beta(h-z) \int_0^g [K(z, z') + K(z, -z')] dz' \\
& + \epsilon \int_g^h \sin \beta(h-z) [K(z, g) + K(z, -g)] dz \\
& + (\delta + \epsilon^2) \int_g^h \{1 - \cos \beta(h-z)\} [K(z, g) + K(z, -g)] dz \\
& + \delta \beta \int_g^h dz \sin \beta(h-z) \int_g^h [K(z, z') + K(z, -z')] dz' \\
& + 2\delta\epsilon\beta \int_g^h dz \{1 - \cos \beta(h-z)\} \int_g^h [K(z, z') + K(z, -z')] dz' \\
& + \delta \int_g^h \{1 - \cos \beta(h-z)\} [K(z, h) + K(z, -h)] dz \\
\gamma_{DD} = & \int_g^h \sin \beta(h-z) [K(z, g) + K(z, -g)] dz \\
& + \epsilon \int_g^h \{1 - \cos \beta(h-z)\} [K(z, g) + K(z, -g)] dz \\
& + \epsilon \beta \int_g^h dz \sin \beta(h-z) \int_g^h [K(z, z') + K(z, -z')] dz' \\
& + \epsilon^2 \beta \int_g^h dz \{1 - \cos \beta(h-z)\} \int_g^h [K(z, z') + K(z, -z')] dz' \\
& + \int_g^h \sin \beta(h-z) [K(z, h) + K(z, -h)] dz
\end{aligned}$$

$$+ \epsilon \int_g^h \{1 - \cos \beta(h-z)\} [K(z,h) + K(z,-h)] dz$$

The above γ expressions contain integrals of six different forms. Three may be evaluated as follows:

$$F(b,c,f,g) = \beta \int_b^c dz \int_f^g K(z,z') dz' = \beta \int_b^c dz \int_f^g \frac{e^{-j\beta \sqrt{(z-z')^2 + a^2}}}{\sqrt{(z-z')^2 + a^2}} dz'$$

Since

$$\frac{\partial}{\partial z} K(z,z') = - \frac{\partial}{\partial z'} K(z,z')$$

an integration by parts yields

$$\begin{aligned} F(b,c,f,g) &= \beta c \int_f^g K(c,z') dz' - \beta b \int_f^g K(b,z') dz' \\ &+ \beta g \int_b^c K(z,g) dz - \beta f \int_b^c K(z,f) dz \\ &+ \int_b^c \beta(z-g) \frac{e^{-j\beta \sqrt{(z-g)^2 + a^2}}}{\sqrt{(z-g)^2 + a^2}} dz - \int_b^c \beta(z-f) \frac{e^{-j\beta \sqrt{(z-f)^2 + a^2}}}{\sqrt{(z-f)^2 + a^2}} dz \end{aligned}$$

$$F(b,c,f,g) = \beta(f-c)\overline{C}(\beta a, \beta(f-c)) - \beta(g-c)\overline{C}(\beta a, \beta(g-c))$$

$$- \beta(f-b)\overline{C}(\beta a, \beta(f-b)) + \beta(g-b)\overline{C}(\beta a, \beta(g-b))$$

$$+ \sin \beta \sqrt{(g-c)^2 + a^2} - \sin \beta \sqrt{(g-b)^2 + a^2}$$

$$- \sin \beta \sqrt{(f-c)^2 + a^2} + \sin \beta \sqrt{(f-b)^2 + a^2}$$

$$- j(\beta(f-c)S(\beta a, \beta(f-c)) - \beta(g-c)S(\beta a, \beta(g-c)))$$

$$- \beta(f-b)S(\beta a, \beta(f-b)) + \beta(g-b)S(\beta a, \beta(g-b))$$

$$- \cos \beta \sqrt{(g-c)^2 + a^2} + \cos \beta \sqrt{(g-b)^2 + a^2}$$

$$+ \cos \beta \sqrt{(f-c)^2 + a^2} - \cos \beta \sqrt{(f-b)^2 + a^2}$$

Another form is

$$G(b,c,f,g) = \beta \int_b^c dz \sin \beta z \int_f^g K(z,z') dz'$$

and an integration by parts yields

$$G(b,c,f,g) = \cos \beta b \int_f^g K(b,z') dz' - \cos \beta c \int_f^g K(c,z') dz' \\ - \int_b^c \cos \beta z K(z,g) dz + \int_b^c \cos \beta z K(z,f) dz$$

$$G(b,c,f,g) = \cos \beta b [\bar{C}(\beta a, \beta(g-b)) - \bar{C}(\beta a, \beta(f-b))] \\ - \cos \beta c [\bar{C}(\beta a, \beta(g-c)) - \bar{C}(\beta a, \beta(f-c))] \\ - \cos \beta g [\bar{C}_c(\beta a, \beta(c-g)) - \bar{C}_c(\beta a, \beta(b-g))] \\ + \sin \beta g [C_g(\beta a, \beta(c-g)) - C_g(\beta a, \beta(b-g))] \\ + \cos \beta f [\bar{C}_c(\beta a, \beta(c-f)) - \bar{C}_c(\beta a, \beta(b-f))] \\ - \sin \beta f [C_g(\beta a, \beta(c-f)) - C_g(\beta a, \beta(b-f))] \\ - j \left\{ \begin{aligned} & \cos \beta b [S(\beta a, \beta(g-b)) - S(\beta a, \beta(f-b))] \\ & - \cos \beta c [S(\beta a, \beta(g-c)) - S(\beta a, \beta(f-c))] \\ & - \cos \beta g [S_c(\beta a, \beta(c-g)) - S_c(\beta a, \beta(b-g))] \\ & + \sin \beta g [S_a(\beta a, \beta(c-g)) - S_g(\beta a, \beta(b-g))] \\ & + \cos \beta f [S_c(\beta a, \beta(c-f)) - S_c(\beta a, \beta(b-f))] \\ & - \sin \beta f [S_g(\beta a, \beta(c-f)) - S_g(\beta a, \beta(b-f))] \end{aligned} \right\}$$

By a similar process

$$H(b,c,f,g) = \beta \int_b^c dz \cos \beta z \int_f^g K(z,z') dz$$

$$\begin{aligned}
H(b,c,f,g) = & \sin \beta c [\overline{C}(\beta a, \beta(g-c)) - \overline{C}(\beta a, \beta(f-c))] \\
& - \sin \beta b [\overline{C}(\beta a, \beta(g-b)) - \overline{C}(\beta a, \beta(f-b))] \\
& + \cos \beta g [C_g(\beta a, \beta(c-g)) - C_g(\beta a, \beta(b-g))] \\
& + \sin \beta g [\overline{C}_c(\beta a, \beta(c-g)) - \overline{C}_c(\beta a, \beta(b-g))] \\
& - \cos \beta f [C_g(\beta a, \beta(c-f)) - C_g(\beta a, \beta(b-f))] \\
& - \sin \beta f [\overline{C}_c(\beta a, \beta(c-f)) - \overline{C}_c(\beta a, \beta(b-f))] \\
-j \{ & \sin \beta c [S(\beta a, \beta(g-c)) - S(\beta a, \beta(f-c))] \\
& - \sin \beta b [S(\beta a, \beta(g-b)) - S(\beta a, \beta(f-b))] \\
& + \cos \beta g [S_g(\beta a, \beta(c-g)) - S_g(\beta a, \beta(b-g))] \\
& + \sin \beta g [S_c(\beta a, \beta(c-g)) - S_c(\beta a, \beta(b-g))] \\
& - \cos \beta f [S_g(\beta a, \beta(c-f)) - S_g(\beta a, \beta(b-f))] \\
& - \sin \beta f [S_c(\beta a, \beta(c-f)) - S_c(\beta a, \beta(b-f))] \}
\end{aligned}$$

Three single integrals are immediately expressible in terms of the tabulated functions. These integrals are

$$\begin{aligned}
I(b,c,g) &= \int_b^c \cos \beta z K(z,g) dz \\
&= \cos \beta g [\overline{C}_c(\beta a, \beta(c-g)) - \overline{C}_c(\beta a, \beta(b-g))] \\
&\quad - \sin \beta g [C_g(\beta a, \beta(c-g)) - C_g(\beta a, \beta(b-g))] \\
-j \{ & \cos \beta g [S_c(\beta a, \beta(c-g)) - S_c(\beta a, \beta(b-g))] \\
& - \sin \beta g [S_g(\beta a, \beta(c-g)) - S_g(\beta a, \beta(b-g))] \}
\end{aligned}$$

$$\begin{aligned}
 J(b,c,g) &= \int_b^c \sin \beta g K(z,g) dz \\
 &= \cos \beta g [C_g(\beta a, \beta(c-g)) - C_g(\beta a, \beta(b-g))] \\
 &\quad + \sin \beta g [\bar{C}_c(\beta a, \beta(c-g)) - \bar{C}_c(\beta a, \beta(b-g))] \\
 &\quad - j \left\{ \cos \beta g [S_g(\beta a, \beta(c-g)) - S_g(\beta a, \beta(b-g))] \right. \\
 &\quad \left. + \sin \beta g [S_c(\beta a, \beta(c-g)) - S_c(\beta a, \beta(b-g))] \right\}
 \end{aligned}$$

$$\begin{aligned}
 M(b,c,g) &= \int_b^c K(z,g) dz \\
 &= \bar{C}(\beta a, \beta(c-g)) - \bar{C}(\beta a, \beta(b-g)) \\
 &\quad - j \{ S(\beta a, \beta(c-g)) - S(\beta a, \beta(b-g)) \}
 \end{aligned}$$

The following symmetries are applicable throughout

$$\beta \int_b^c dz \int_f^g K(z, -z') dz' = -F(b,c, -f, -g)$$

$$\beta \int_b^c dz \sin \beta z \int_f^g K(z, -z') dz' = -G(b,c, -f, -g)$$

$$\beta \int_b^c dz \cos \beta z \int_f^g K(z, -z') dz' = -H(b,c, -f, -g)$$

The functions S , S_g , S_c , C_g , \bar{C}_c are defined and tabulated very completely in the reference. All are odd about the origin except S_g and C_g .

Note that in evaluating the various integrals that there is a definite relationship between the tabulated functions appearing in real parts of F, G , etc. and those that appear in the imaginary parts of the integrals. One of these for example, is

$$H = f [C_g(w), \bar{C}_c(x), C(y), \sin z] - jf [S_g(w), S_c(x), S(y), -\cos z]$$

The real parts of the integrals contain only C_s , C_c , C , and sine functions while the imaginary parts contain an identical arrangement of S_s , S_c , S , and minus cosine functions.

References

1. P. S. Carter, "Circuit Relations in Radiating Systems and Application to Antenna Problems," Proc. I.R.E. 20, 1004-1041, (June 1932).
2. C. W. Harrison, Jr., "Mutual and Self-Impedances for Collinear Antennas," Proc. I.R.E. 33, 398-408 (June 1945).
3. Ronold King, "Theory of Collinear Antennas," Jour. Appl. Phys. 21, 1232-1251 (December 1951).
4. Kosmo Affahasieu, "Simplifications in the Consideration of Mutual Effects between Half-Wave Dipoles in Collinear and Parallel Orientations," Proc. I.R.E. 34, 635-638 (September 1946), Proc. I.R.E. 34, 863 (November 1946).
5. Erik Hallén, "Theoretical Investigations into the Transmitting and Receiving Qualities of Antennae," Nova Acta Regiae Societates Scientiarum Upsaliensis 11, No. 4, November 11, 1938.
6. John Taylor, "The Sleeve Antenna," Cruft Laboratory Technical Report No. 128, Harvard University, April 20, 1951.
7. James E. Storer, "Variational Solution to the Problem of the Symmetrical Cylindrical Antenna," Cruft Laboratory Technical Report No. 101, Harvard University, February 10, 1950.
8. Ronold King, "Asymmetrically Driven Antennas and the Sleeve Dipole," Proc. I.R.E. 38, 1154-1164 (October 1950).
9. C. T. Tai, "A Variational Solution to the Problem of Cylindrical Antennas," Technical Report No. 12, Stanford Research Institute, August 1950.
10. Ronold King and David Middleton, "The Cylindrical Antenna, Current and Impedance," Quart. of Appl. Math. 3, 302-335, (January 1946).
11. S. A. Schelkunoff, "Theory of Antennas of Arbitrary Size and Shape," Proc. I.R.E., September 1941.
12. Ronold King, Electromagnetic Engineering Vol. I, p. 239-243, McGraw-Hill, 1945.
13. O. Zinke, Archiv fur Elektrotechnik 35, p. 67 (1941).

14. C. W. Oseen, Archiv fur Elektrotechnik Mat. Astron. och. Fys. 9, Nos. 12, 28, 30 (1913).
15. R. W. P. King, "Transmission-Line Theory and its Applications," J. Appl. Phys. 14, 577 (1943).
16. D. D. King, Measurements at Centimeter Wavelength, D. Van Nostrand Co., Inc., 1952, p. 196.
17. E. O. Hartig, "Circular Apertures and their Effects on Half-Dipole Impedances," Cruft Laboratory Technical Report No. 107, June 15, 1950, pp. 40-49.
18. J. R. Whinnery, "The Effect of Input Configuration on Antenna Impedances," U. S. Navy Electronics Research Report No. 142, University of California.
19. G. W. Zeoli, "Impedance of Antennas with Various Input Configurations," U. S. Navy Electronics Research Report No. 157, University of California.
20. P. A. Kennedy and R. W. P. King, "Experimental and Theoretical Impedances and Admittances of Center Driven Antennas," Cruft Laboratory Technical Report No. 155, Table X, 1953.
21. R. W. P. King, Theory of Linear Antennas, Harvard University Press, to be published.
22. Sir James Jeans, The Mathematical Theory of Electricity and Magnetism, Cambridge University Press, Cambridge, England, 1948.

Antennas

DISTRIBUTION

2	Office of Naval Research (427) Navy Department Washington 25, D. C.
1	Office of Naval Research (460) Navy Department Washington, 25, D. C.
1	Chief, Bureau of Ordnance (Re4f) Navy Department Washington 25, D. C.
1	Chief, Bureau of Ships (816) Navy Department Washington 25, D. C.
1	Chief, Bureau of Ships (833) Navy Department Washington 25, D. C.
1	Chief, Bureau of Aeronautics (EL-51) Navy Department Washington 25, D. C.
1	Chief of Naval Operations (Op-413) Navy Department Washington 25, D. C.
1	Chief of Naval Operations (Op-20) Navy Department Washington 25, D. C.
1	Chief of Naval Operations (Op-32) Navy Department Washington 25, D. C.
9	Naval Research Laboratory (2027) Bellevue D. C.
1	Naval Research Laboratory (2020) Bellevue D. C.
1	Naval Research Laboratory (3480) Bellevue D. C.
1	Naval Ordnance Laboratory White Oak Maryland

Antennas

-2-

DISTRIBUTION

2 U. S. Naval Electronics Laboratory
San Diego 52
California

1 Naval Air Development Center (AAEL)
Johnsville
Pennsylvania

1 U. S. Navy Underwater Sound Laboratory
New London
Connecticut

U. S. Navy Office of Naval Research
Branch Offices:

2 Boston
1 New York
1 Chicago
1 San Francisco
1 Pasadena

3 U. S. Navy Office of Naval Research
U. S. Navy 100, Fleet Post Office
New York, N. Y.

1 Librarian
U. S. Naval Post Graduate School
Monterey, California

1 U. S. Coast Guard (EEE)
1300 E Street, N. W.
Washington, D. C.

1 Research and Development Board
Pentagon Building
Washington, D. C.

1 National Bureau of Standards
Department of Commerce
Washington, D. C.
Attention: Dr. N. Smith

1 Naval Ordnance Development Unit
Johns Hopkins University
Radiation Laboratory
Homewood Campus
Baltimore 18, Maryland
Attention: Dr. C. R. Larkin

Antennas

-3-

DISTRIBUTION

1 Applied Physics Laboratory
Johns Hopkins University
8621 Georgia Avenue
Silver Spring, Maryland

6 Library of Congress
Navy Research Section
Washington, D. C.

1 Massachusetts Institute of Technology
Research Laboratory of Electronics
Cambridge 39, Massachusetts
Attention: Professor L. J. Chu

1 Stanford University
Stanford, California
Attention: Professor K. Spangenberg

1 University of Illinois
Urbana, Illinois
Attention: Professor E. C. Jordan

1 Ohio State University
Columbus, Ohio
Attention: Dr. V. H. Rumsey

1 Cornell University
Ithaca, New York
Attention: Professor C. R. Burrows

1 University of California
Berkeley, California
Attention: Electrical Engineering Department

1 Oregon State College
Corvallis, Oregon
Attention: Professor J. J. Brady

1 University of Texas
Austin, Texas
Attention: Electrical Engineering Department

2 Librarian
National Bureau of Standards
Washington 25, D. C.

1 Librarian
Radio Corporation of America
RCA Laboratories
Princeton, New Jersey

DISTRIBUTION

- 1 Exchange and Gift Division
Library of Congress
Washington 25, D. C.
Attn: Exchange Division
American and British
- 1 Ballistic Research Laboratories
White Sands Proving Ground
Las Cruces, New Mexico
- 1 Professor Morris Kline
Mathematics Research Group
New York University
45 Astor Place
New York, N. Y.
- 1 Technical Library
Bell Telephone Laboratories
Murray Hill Laboratory
Murray Hill, New Jersey
- 1 Technical Library
Federal Telecommunications Laboratories Inc.
500 Washington Avenue
Nutley 10, New Jersey
- 1 Library
Philco Corporation
Philadelphia 34, Pennsylvania
- 1 Library of the College of Engineering
University Heights Library
New York University
New York 53, N. Y.
- 1 Library
Central Radio Propagation Laboratory
National Bureau of Standards
Washington 25, D. C.
- 1 Dr. John V. N. Granger
Stanford Research Institute
Stanford, California
- 1 Document and Research
Raytheon Manufacturing Company
Equipment Engineering Division
Newton 53, Massachusetts

DISTRIBUTION

1 Dr. A. G. Hill
Lincoln Laboratory
Massachusetts Institute of Technology
Cambridge 38, Massachusetts

1 Professor H. G. Booker
Department of Electrical Engineering
Cornell University
Ithaca, New York

50 Signal Corps, Transportation Officer
Asbury Park
New Jersey

50 Chief, Administration Section
Electronics Research Division
Air Force Cambridge Research Center
Cambridge, Massachusetts

1 Signal Corps Liaison Office
Massachusetts Institute of Technology
Attention: Mr. R. E. Campbell

1 Document Room
Research Laboratory of Electronics
Massachusetts Institute of Technology
Attention: Mr. Hewitt

1 Library
Watson Laboratories, AMC
Red Bank, New Jersey
(ENAGS1)